In-situ Calibration of DU-2

Principles and Results after one Month of Data-taking

Karel Melis

Nikhef

February 16, 2016

Abstract

The aim of the methods described in this document is to calibrate the first KM3NeT detection unit (DU) purely in-situ, with at least dependence on Monte Carlo information as possible. In this note, the results and procedures of the first month of data-taking with the first deployed KM3NeT DU will be reviewed. During the analysis, plots in this document will be updated and distributed via my website:
http://www.nikhef.nl/∼kmelis/notes/InsituCalibration_DU2_KMelis.pdf.

Contents

1 Introduction

The procedure followed for the in-situ calibration can be summarised as follows: First a set of runs with non-corrupted data is selected (section 2). Using this set of runs, the PMTs of each DOM are calibrated using the ^{40}K-background (section 3). After this step, the inter-DOM calibration is performed using the light from atmospheric muons, first by analysing the coincidence rate of L1 hits on each DOM pair (section 4), and in order to get an even more precise calibration by using the hit time residual plots of reconstructed tracks (section5).

2 Run selection

During the first period of data taking, several issues were noticed in the written data. The most relevant issue for this analysis is the fact that during a run the data of a DOM can become corrupted, leading to a loss of data of that DOM until the end of the run.

In order to distill a workable set of runs, only runs with at least one DOM producing non-corrupted data all the time are selected. In these runs, only the data written from DOMs giving non-corrupted data for at least 95% of the total run duration has been considered. In figure 1 the resulting data-set is displayed.

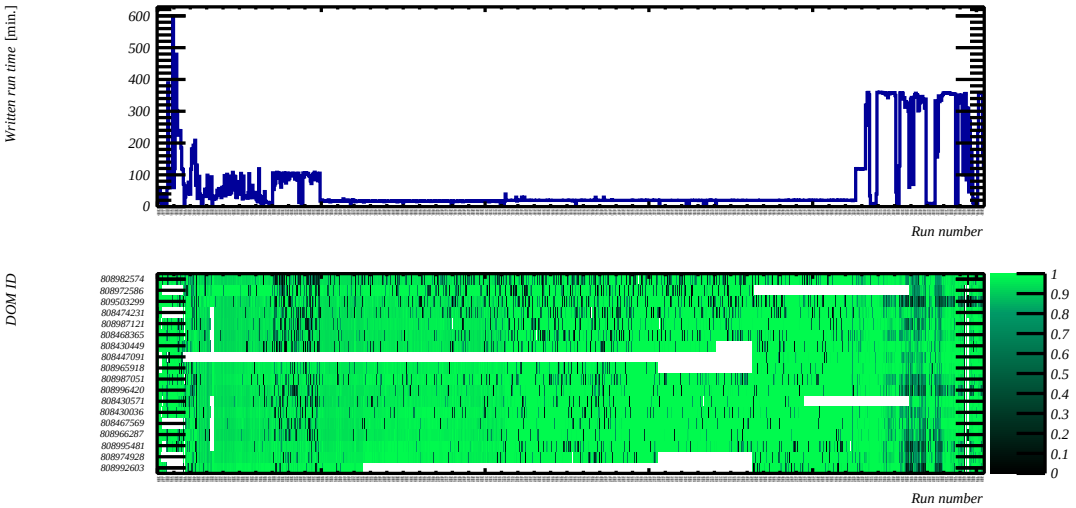

Figure 1: All runs of the first month of data-taking used for this work. The upper plot gives the recorded length of each run. The bottom plot shows which DOMs produced data used in this analysis.

3 Trigger rates

Triggrerrate:

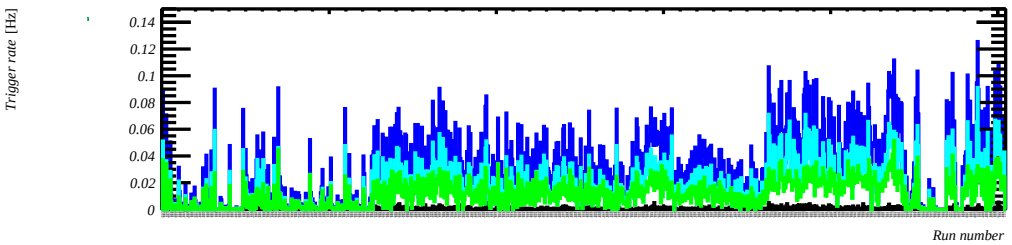

Figure 2: Rate of triggered events as function run number. Shower trigger in green, muon trigger in black, both triggers for the same event: cyan and total trigger rate in blue.

4 Inter-PMT calibration

4.1 Principle

The inter-PMT (or intra-DOM) calibration relies on the coincidence rate of hits on PMTs on the same DOM. The method for the inter-PMT calibration has been extensively covered in the note written by Niklas Kitzmann and Robert Bormuth (PPM-DU Intra-DOM Calibration Studies, december 2015) and will therefore not be covered in this document. In summary the PMT time-offsets $t0's$ (closely related to the PMT transit time), PMT relative efficiency and an upper limit on the transit time spread can be determined from the coincidence rate of PMTs.

4.2 Stability

In order to monitor the stability of the fit, figure 3 shows the determined fit parameters of an arbitrarily chosen DOM for all runs. Each coloured dot gives the determined calibration value of a single PMT on that DOM. Please see appendix A for similar plots of all DOMs.

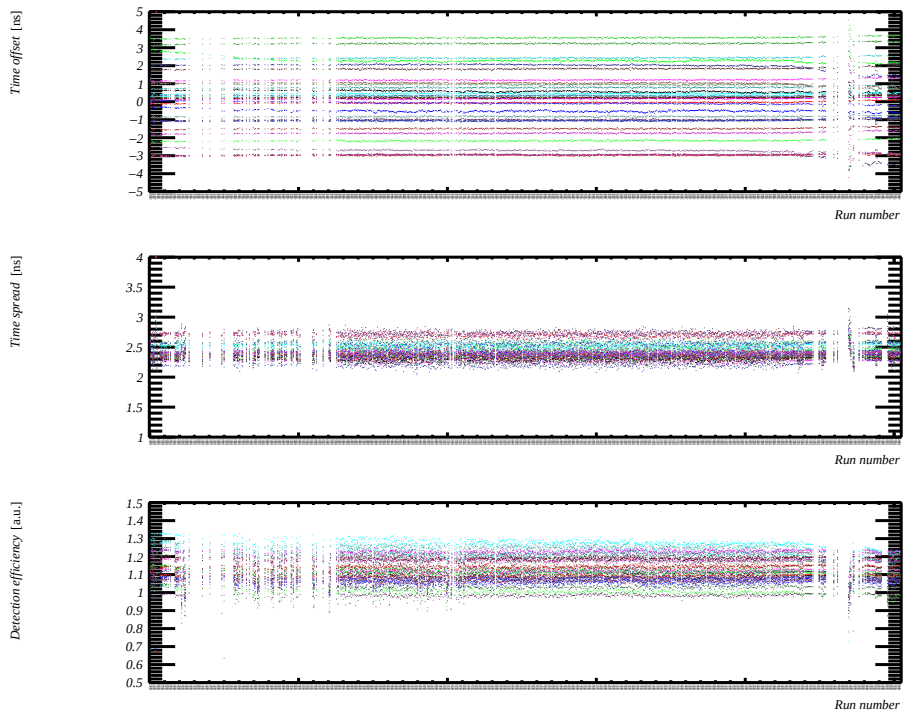

Figure 3: Fitted PMT parameters of the inter-PMT calibration as function of the run number for the DOM with ID 808966287. The upper plot gives the time-offset of all 31 PMTs on this DOM, the middel plot shows the relative detection efficiency and the bottom plot gives the spread in the hit time distributions.

As can be seen, all fitted parameters are very stable long periods, except for a few runs. These runs correspond to nano-beacon calibration runs, also included in this plot.

4.3 Global PMT parameter fit

The stability of the PMT parameters over the complete time-range paves the way for a global fit of the PMT parameters. In figures 4, 5 and 6, the deviation of the fitted PMT parameters of each run with respect to the global fit is plotted for all PMTs of DOM 808966287. All DOMs are covered in appendix A.

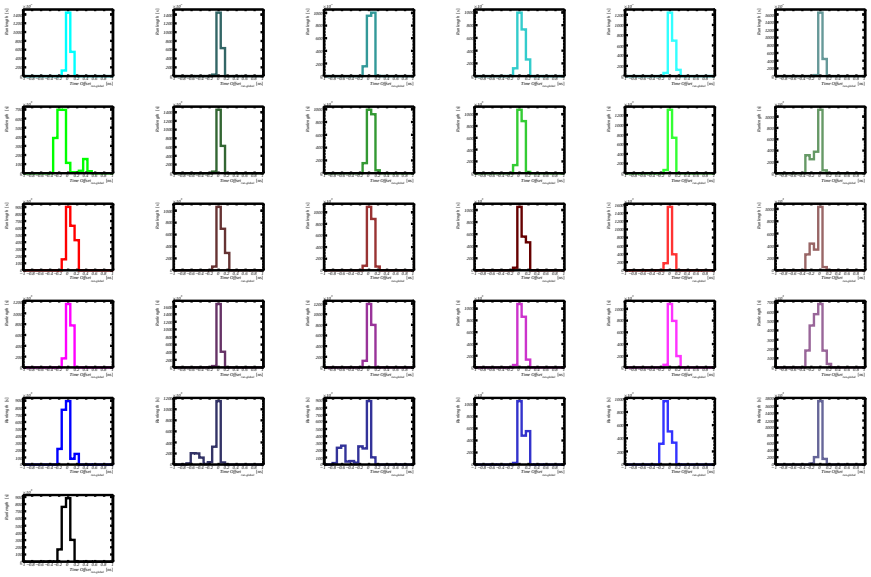

Figure 4: Fitted PMT time offset distribution of each run with respect to the globally fitted PMT time offset. Each row of plots gives the PMTs of one ring (upper row=ring F, lower ring=ring A). The x-axis ranges from -1 to +1 ns.

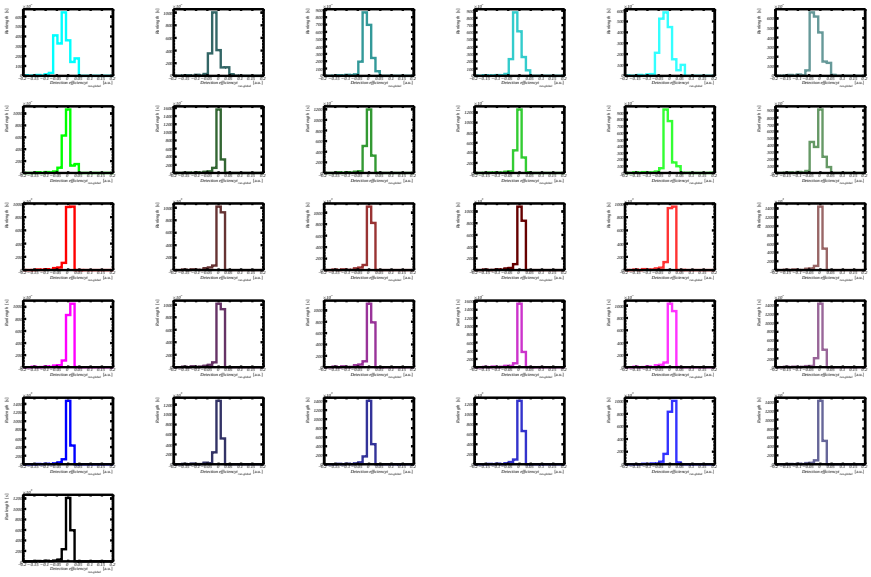

Figure 5: Fitted PMT relative detection efficiency distribution of each run with respect to the globally fitted PMT time offset. Each row of plots gives the PMTs of one ring (upper row=ring F, lower ring=ring A). The x-axis ranges from -0.2 to +0.2

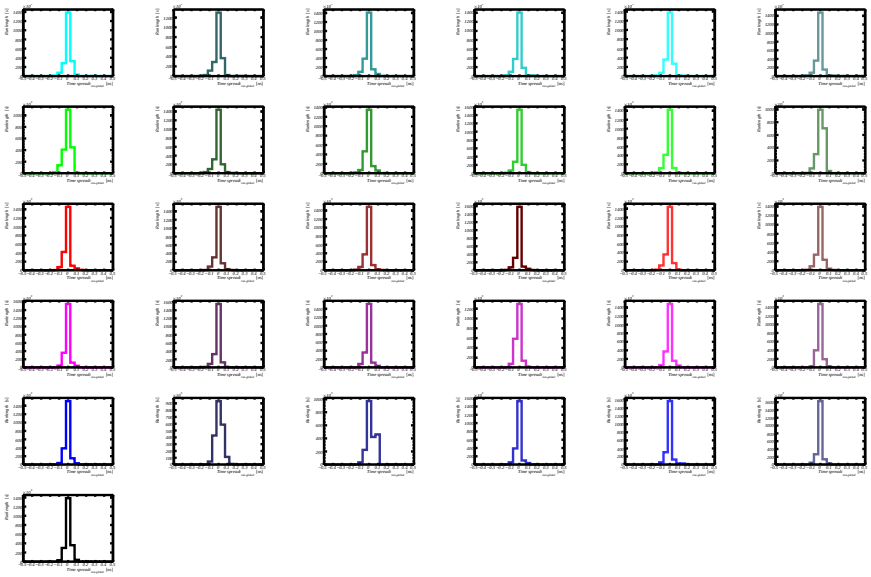

Figure 6: Fitted PMT time spread distribution of each run with respect to the globally fitted PMT time offset. Each row of plots gives the PMTs of one ring (upper row=ring F, lower ring=ring A). The x-axis ranges from -0.5 to +0.5

Fitting the PMT parameters using all selected runs leads to the PMT parameter values presented in table 11 for the arbitrarily chosen DOM. In appendix B, all DOMs are covered.

PMT #	Time offset [ns]	Det. eff. [a.u.]	Time spread [ns]
F1	0.441512	1.2867	2.53557
F2	-1.05814	1.20451	2.5839
F3	0.77084	1.2081	2.43608
F4	2.41605	1.25985	2.38576
F5	0.33084	1.22774	2.54592
F6	-0.832999	1.24774	2.49451
E1	2.37547	1.11077	2.4479
E2	0.241022	1.02755	2.34637
E3	3.22137	1.11621	2.35238
E4	3.53589	1.12525	2.33319
E5	-2.17516	1.00588	2.57899
E6	0.964747	1.17809	2.37787
D1	-0.0696585	1.13821	2.38316
D2	1.81752	1.13593	2.39631
D3	-1.51482	1.06016	2.37424
D4	0.202058	1.18493	2.324
D5	-2.985	1.08761	2.73097
D6	1.02887	1.08918	2.41407
C1	0.146856	1.22298	2.4117
C2	-1.01409	0.981549	2.71784
C3	-2.95956	1.18445	2.73978
C4	-1.75832	1.17386	2.42482
C5	1.19707	1.11649	2.28542
C6	-2.68116	1.21712	2.4206
B1	-0.482218	1.06739	2.42857
B2	-2.96818	1.10718	2.75903
B3	2.02988	1.07614	2.20638
B4	-1.06533	1.07722	2.57285
B5	-0.0586403	1.04312	2.36359
B6	0.322548	1.05726	2.2856
A1	0.580717	1.08486	2.30751

Table 1: Calibrated PMT quantities of DOM 808966287.

4.4 Systematic effects of surrounding material

Systematic behaviour of the fitted PMT parameters can be monitored by plotting the fitted parameters as function of the DOM and PMT. In figure 7, such a plot for the fitted detection efficiency is drawn. To guide the eye, the average over all PMTs resp. DOMs is given in figures:

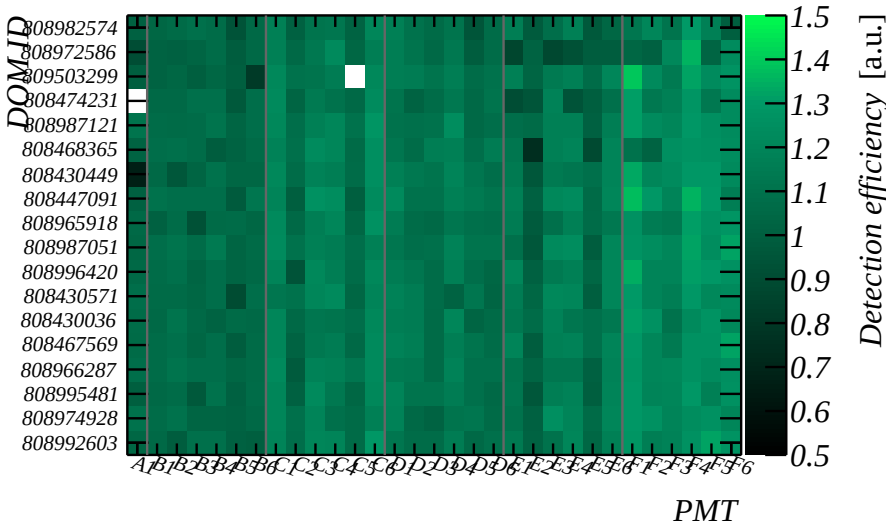

Figure 7: Fitted detection efficiency as function of all PMTs and DOMs.

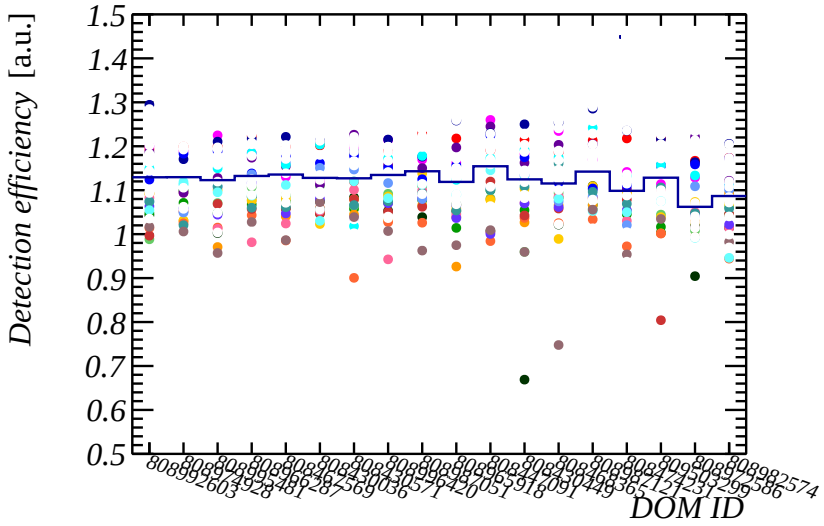

Figure 8: Detection efficiency of all PMTs at the same position in all DOMs versus the DOM index. The average over all DOMs is given by the blue lines.

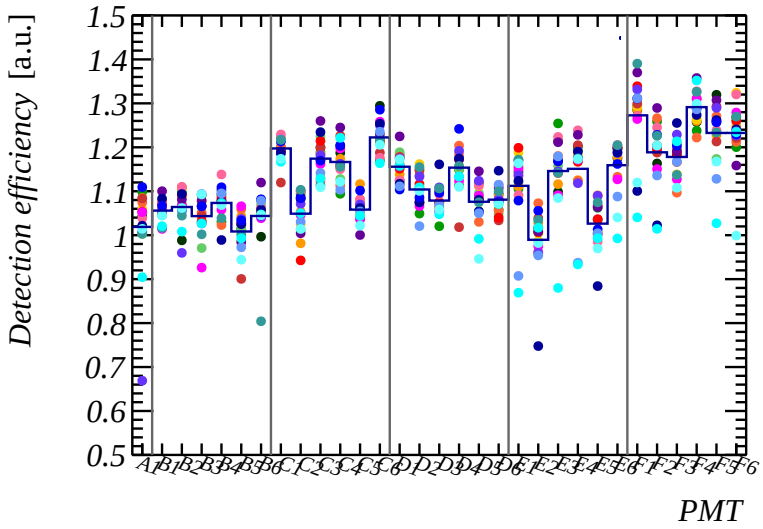

Figure 9: Detection efficiency of all PMTs at the same position in all DOMs versus the PMT index. The average over all PMTs is given by the blue lines.

As is clear from these figures, there is no correlation with the DOM, thus indicating that the influenco of atm. muon light on the fit is negligible. For the different PMTs however there is a clear decrease in efficiency for some of the PMT channels.

These artefacts are convincingly explained by the holding structure surrounding each DOM. The so-called collar shields PMTs C2,C5,2,D3,D5,D6 and E2,E6,F2,F3,F5 and F6 more than the other PMTs. Secondly, the coincidence rate of the upper ring (F) can be increased by the reflecting aluminium surface of the cooling-'mushroom'. In figure 10, the holding structure is schematically drawn.

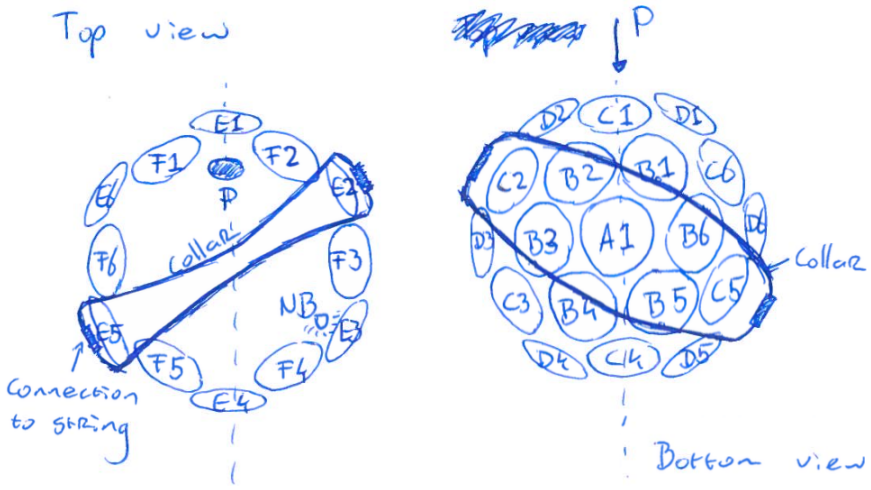

Figure 10: Schematic view on the distribution of the PMTs in the DOM. The holding structure is given by thick lines.

5 Comparison with singles rate

The decreased efficiency of the PMTs close to the holding structure can be explained either by ... In order to measure the singles rate, summary data of each PMT is monitored during the entire data-taking period. In order to show the method used to determine the overall singles rate of a PMT, figure **??**, the distribution of the measured singles rate is plotted for a certain PMT.

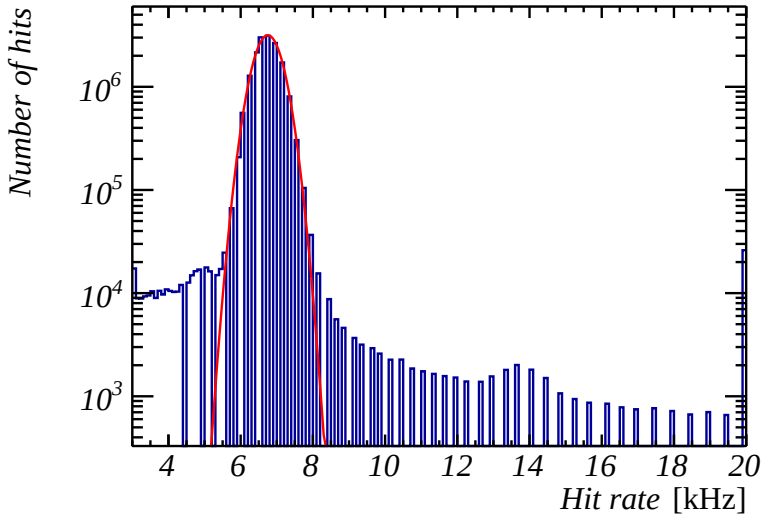

Figure 11: Measured rate distribution of an arbitrarily chosen PMT in DOM 808992603, of which the peak has been fitted with a gaussian distribution.

Plotting the singles rate in similar plots as for the QE leads to:

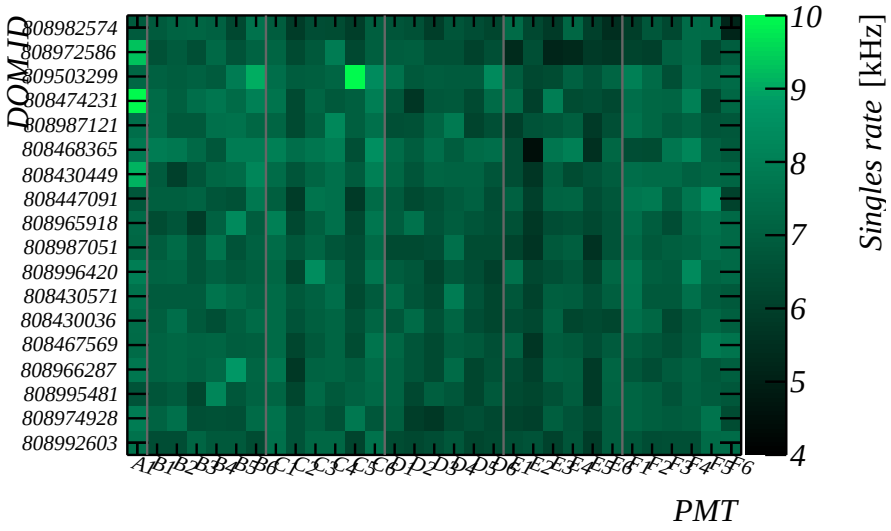

Figure 12: Average singles rate of all PMTs at the same position in all DOMs versus the PMT index.

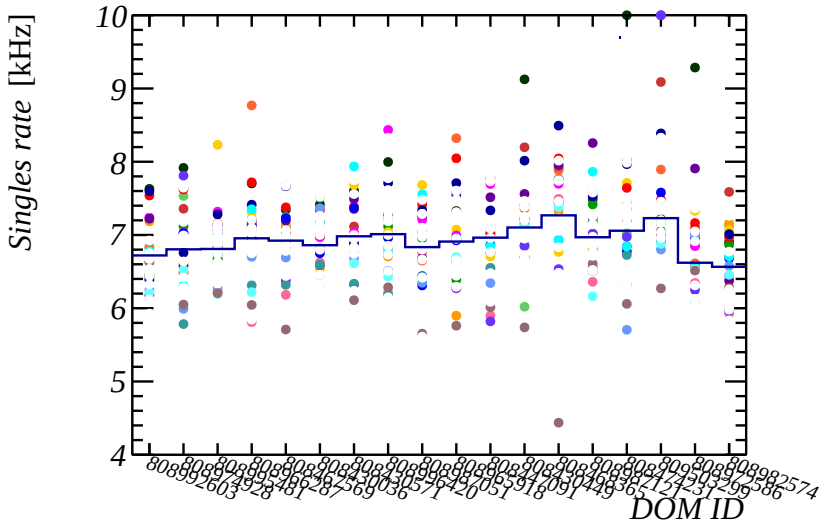

Figure 13: Average singles rate of all PMTs at the same position in all DOMs versus the DOM index.

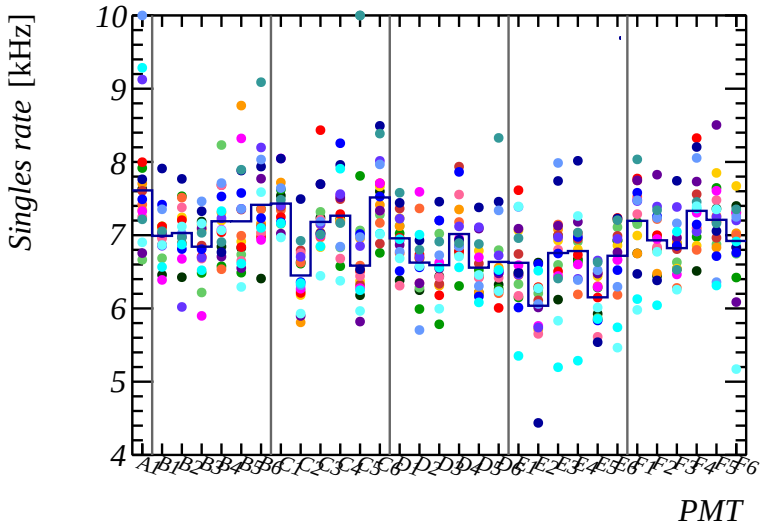

Figure 14: Average singles rate of all PMTs at the same position in all DOMs versus the PMT index. The average over all PMTs is given by the blue lines.

The same systematic decrease in detected hits as shown in figure 9 is also observed in the singles rate (figure 15).

In the following figure, the correlation between the singles rates and the fitted detection efficiency is plotted.

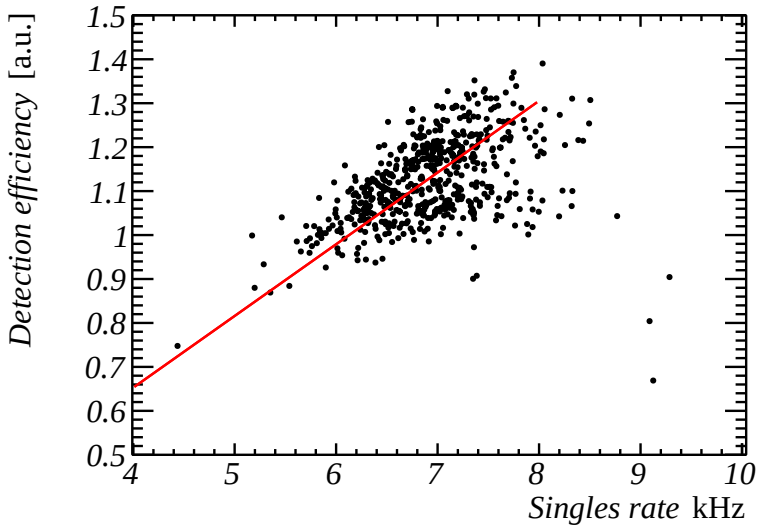

Figure 15: Fitted detection efficiencies of all PMTs plotted versus the average singles rate of the PMT. A linear fit passing through the origin is superimposed.

6 Inter-DOM calibration (1): L1 hit time difference

6.1 Principle

Each local coincidence of recorded hits (L0's) gives a L1 hit. In the used runs, the causality relation is given by at least two L0 hits on the same DOM within 25ns.

As expected from Monte Carlo (MC) simulations, the majority of the triggered events are caused by nearly straight down-going atmospheric muons passing by. As a result of this, a time difference between recorded hits on two neighbouring DOMs in the order of $\frac{36m}{0.3m/ns} \approx 112ns$ can be expected. If this is not the case, then most likely the hit times on one of the two DOMs are determined with respect to a wrong DOM time-offset. In this manner, the hit time differences between all DOM pairs can be used to determine the DOM time-offsets.

To illustrate the method used, the upper plot in figure 16 shows the time difference between all L1 hits (two L0 hits on the same DOM within 25 ns.) recorded on both DOM 808992603 and 808974928 (which are the two lowest neighbouring DOMs).

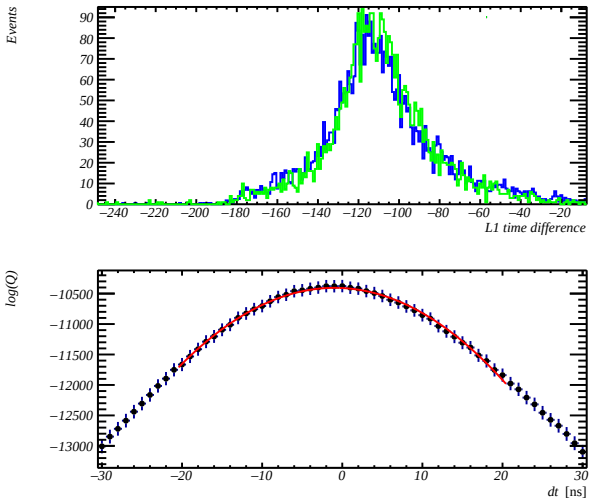

Figure 16: Upper plot: Time difference between coincident L1-hits on arbitrarily chosen DOMs 808474231 and 809503299, both for data (green) and MC simulated data (blue). Both histograms are normalised to match in integral. Bottom plot: The ..., accompanied by a 2nd order polynomial fit (red line) through the top ± 10 ns.

As can be seen, the data and MC are in relatively good agreement. Also, the fitted mean time difference is comparable, indicating that the detector file used for data-taking (based on the inter-DOM dark room calibration) is already using time-offsets close to the true offsets.

An even better agreement between the data and the MC simulations can be obtained by shifting the two distributions by about 3 ns. For each DOM-pair k, l, the relation used to quantify the agreement between the data and MC is given by the multiplied Poisson statistics of all bins:

$$Q_{k,l}(dt) = \prod_{bins} \left[\frac{\widehat{n_i}^{n_{i-di}}}{n_{i-di}!} e^{-\widehat{n_i}} \right] \tag{1}$$

$$di \equiv dt/binwidth \tag{2}$$

Where $\widehat{n_i}$ resp. n_i give the MC predicted resp. detected number of event in bin i. In the bottom plot of figure 16, this function is plotted.

In order to estimate the DOM time offsets, a simultaneous fit of the 18 DOM time-offsets ($t0_i$) is performed, maximising the product of the quality function of all DOM pairs:

$$Q(\vec{t0}) = \prod_{DOMpairs} [Q_{k,l}(t0_l - t0_k)] \tag{3}$$

6.2 Computational implementation

The width of used bins limits the resolution that can be obtained by this procedure (in this case 1 ns). This in combination with the computationally intensive scan over the 18 DOM time offsets lead to an alternative approach.

The peak of the log-quality function of each DOM-pair $\log(Q_{k,l}(dt))$ can be well-approximated by a 2nd order polynomial fit (see figure 16 for such a fit). Maximising 3 is then equivalent to solving:

$$\vec{0} = \frac{\partial}{\partial \vec{t0}} \sum_{DOMpairs} [\log(Q_{k,l}(t0_l - t0_k))] \tag{4}$$

$$= \frac{\partial}{\partial \vec{t0}} \sum_{DOMpairs} \left[a_{k,l} \cdot (t0_l - t0_k)^2 + b_{k,l} \cdot (t0_l - t0_k) + c_{k,l} \right] \tag{5}$$

$$= 2 \cdot \begin{pmatrix} \sum_{i \neq 0} [a_{0,i}] & -a_{0,1} & -a_{0,2} & \cdots \\ -a_{1,0} & \sum_{i \neq 1} [a_{1,i}] & -a_{1,2} & \cdots \\ -a_{2,0} & -a_{2,1} & \sum_{i \neq 2} [a_{2,i}] & \cdots \\ \vdots & \vdots & \vdots & \ddots \end{pmatrix} \cdot \begin{pmatrix} t0_0 \\ t0_1 \\ t0_2 \\ \vdots \end{pmatrix} + \begin{pmatrix} -\sum_{i>0} [b_{0,i}] \\ \sum_{i<1} [b_{i,1}] - \sum_{i>1} [b_{1,i}] \\ \sum_{i<2} [b_{i,2}] - \sum_{i>2} [b_{2,i}] \\ \vdots \end{pmatrix} \tag{6}$$

$$= 2 \cdot A \cdot \vec{t0} + \vec{b} \tag{7}$$

The best fitted DOM time offsets can thus be found using straightforward linear algebra. In the next subsection the results will be discussed.

6.3 Results

Using the method described in the previous subsection, the inter-DOM time offsets have been fitted.

In table 2, the in-situ calibrated time offsets are compared to the values from the dark room calibration (using lasers flashing a reference PMT on each DOM).

DOM ID #	Est. rel. height [m]	Time offset [ns]	Ref. PMT time offset [ns]	D.R. t0 [ns]
808992603	0	737.914	736.578	744.552
808974928	38.02	934.083	933.715	940.866
808995481	75.87	1136.119	1136.679	1142.0
808966287	112.73	1338.628	1338.959	1342.403
808467569	150.23	1534.619	1536.063	1537.943
808430036	187.53	1743.251	1743.878	1745.707
808430571	224.36	1946.038	1945.993	1947.202
808996420	261.98	2140.262	2138.338	2139.405
808987051	299.36	2337.039	2335.887	2337.662
808965918	336.16	2546.570	2548.372	2552.244
808447091	373.48	2744.514	2743.169	2744.736
808430449	410.64	2939.455	2938.977	2940.523
808468365	447.37	3148.068	3148.952	3145.915
808987121	484.81	3348.588	3350.521	3346.5
808474231	522.09	3548.282	3550.163	3543.48
809503299	558.41	3750.956	3751.257	3742.982
808972586	595.37	3949.984	3949.859	3941.35
808982574	632.17	4151.324	4152.034	4143.923

Table 2: DOM time offsets (third column) compared with the dark room calibration (fifth column) using the time offset of a reference PMT on each DOM (fourth column). The DOM heights have been estimated by E. Berbee.

7 Inter-DOM calibration (2): Hit time residuals

The time-difference distributions between coincident L1 hits on different DOMs gives a first handle on the inter-DOM time calibration and can be used to validate the data with minimal Monte Carlo dependence. A better result for the time calibration (though more dependent on MC models) can be achieved by using the hit time residual plots using reconstructed tracks.

7.1 Principle

For the analysis of the first data of DU1, a reconstruction algorithm has been developed based on the maximum likelihood approach using the timing information of the detected L1 hits on DOM-level and the fact wether or not a DOM has been hit. In the KM3NeT analysis elog entry 61 (and **http://www.nikhef.nl/∼kmelis/notes/Likelihood.pdf**), I describe the used likelihood function in more detail.

The reconstruction has been applied to all events with at least five DOMs hit. For each DOM the time-residual distribution of all reconstructed tracks (i.e. one entry per event for

each hit DOM) gives an probe for how well the data matches the reconstructed track. In figure 17, the time-residual distributions for all 18 DOMs of DU2 are given after this initial reconstruction:

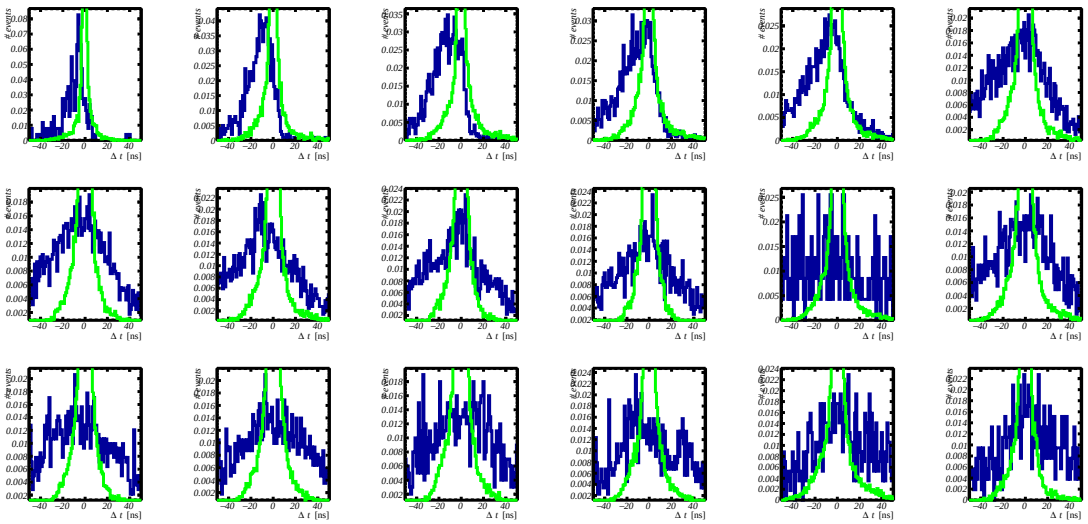

Figure 17: Time residual distributions after all events reconstructed for each DOM (blue) after one iteration. The expected hit time residual distributions from Monte Carlo simulated data are given in green. All histograms are normalised to match in integral.

From this plot, it is clear that there is a disagreement between the data and the Monte Carlo simulated events. This could be caused by the fact that in each data-run several DOMs give corrupted data, and are therefore not used in the reconstruction. This defect is not yet incorporated in the Monte Carlo simulated events (in which all DOMs are constantly working properly). As a results the tracks in the MC simulated data are very well reconstructed compared to the tracks reconstructed in the data. As a result, the resulting width of the MC hit time residual distributions is smaller than the width of the data. I'm currently working to simulate run-by-rum Monte Carlo event incorporating this artefact. Once finished the previous plots will be updated. Nevertheless I will outline the principle in the remainder of this subsection.

For the inter-DOM calibration, the DOM t0's are shifted such that the distributions are centered closer to the MC expected man. In order to suppress oscillations, the shift is made such that the change shifts the mean only halfway. All shift are offsetted such that the average DOM time-offset remains constant.

Since the shift in DOM t0's will also affect the reconstruction, the above procedure is applied several times. In the next subsection, the determined DOM t0's after X iterations are summarised.

7.2 Results

TODO

8 Conclusions and outlook

As shown section 3, the fitted PMT parameters are very stable over time. Using all data taken during the first month of data-taking the PMT time-offsets with respect to the DOM have been determined, paving the way for the inter-DOM calibration using atmospheric muons. Although the statistics are limited, the first results show very good agreement between the in-situ calibration and the dark room calibration. For a precise calibration of the DOM time offsets, dedicated run-by-run Monte Carlo events will be simulated.

9 Appendix A: PMT parameters stability

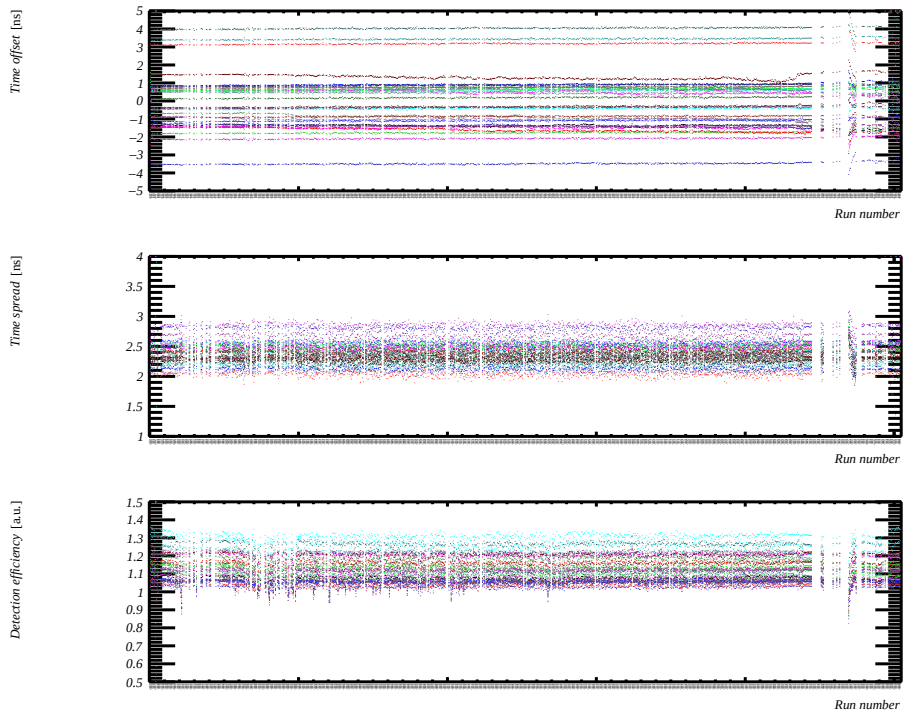

Figure 18: Calibrated PMT parameters of DOM 808430036 for each run in the first month of data-taking

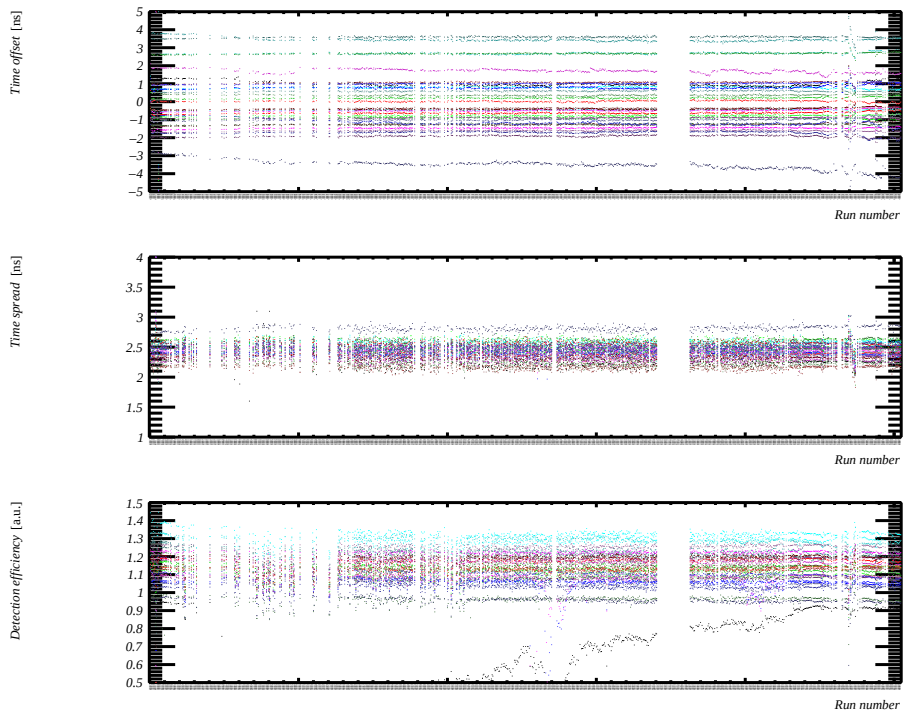

Figure 19: Calibrated PMT parameters of DOM 808430449 for each run in the first month of data-taking

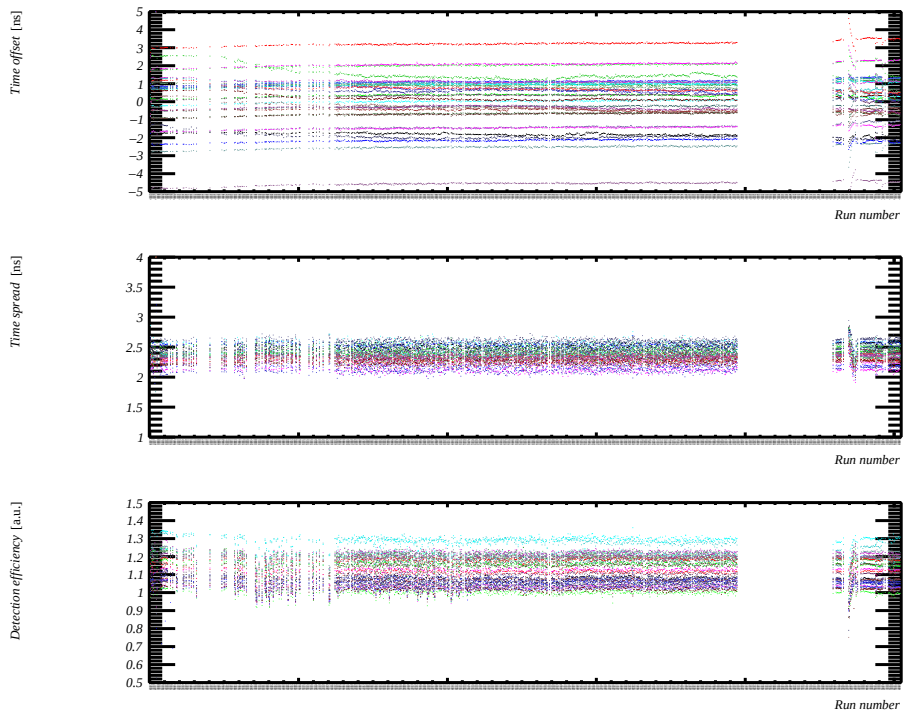

Figure 20: Calibrated PMT parameters of DOM 808430571 for each run in the first month of data-taking

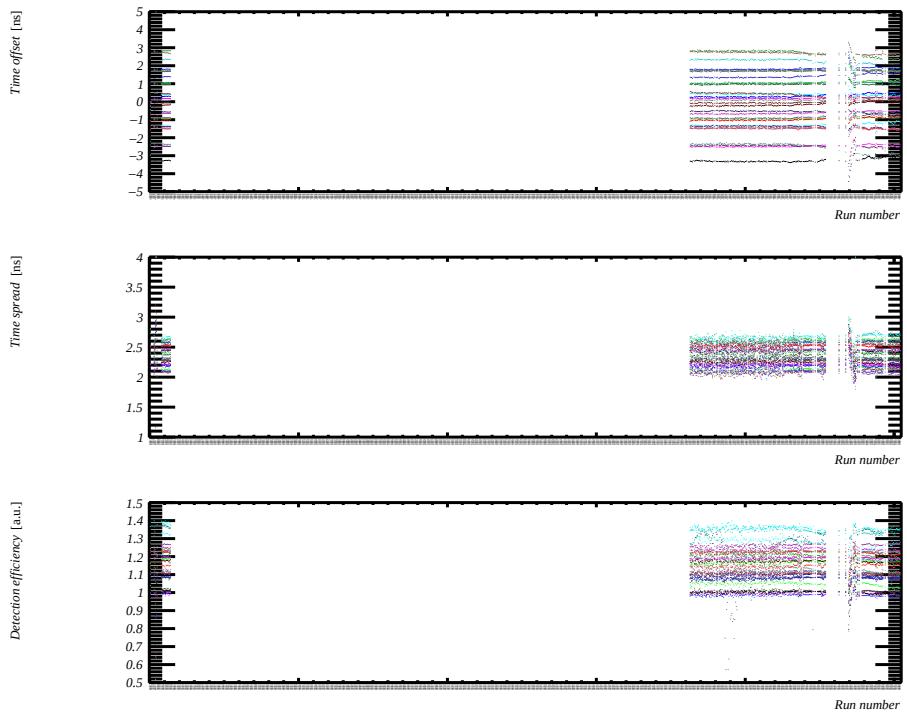

Figure 21: Calibrated PMT parameters of DOM 808447091 for each run in the first month of data-taking

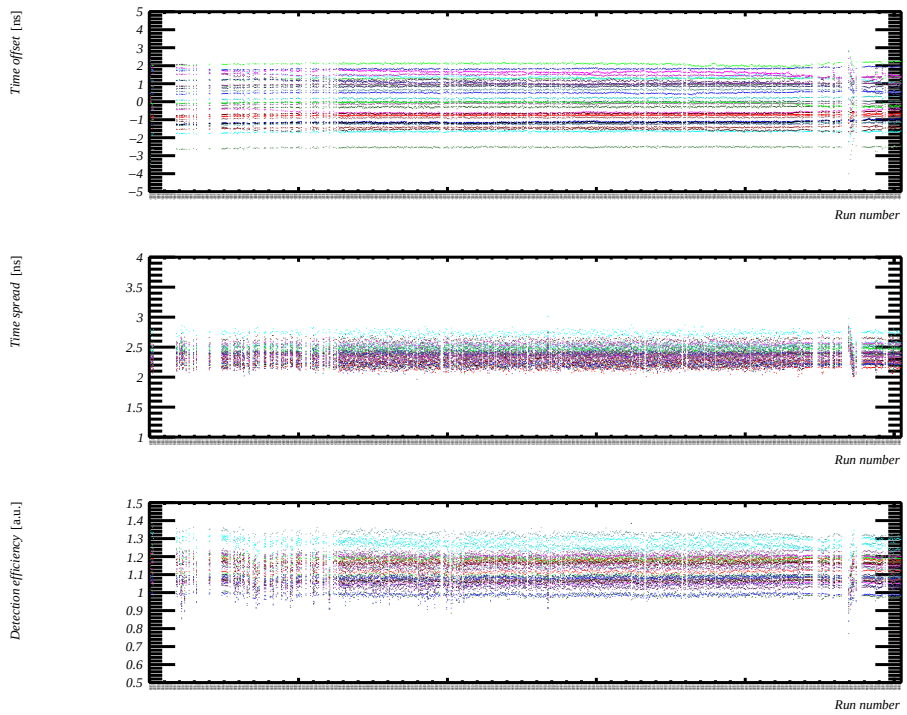

Figure 22: Calibrated PMT parameters of DOM 808467569 for each run in the first month of data-taking

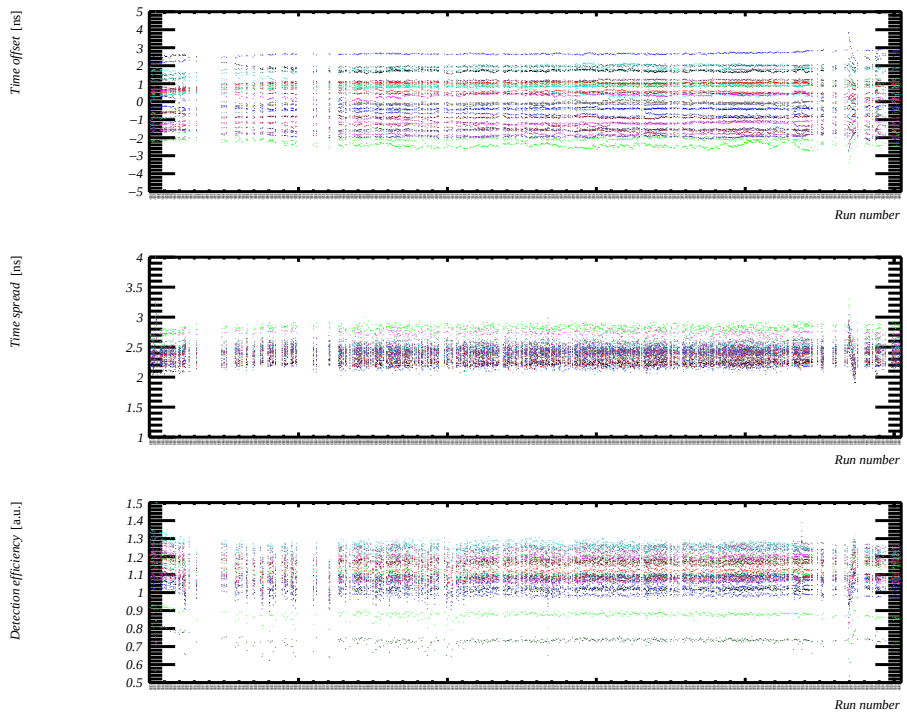

Figure 23: Calibrated PMT parameters of DOM 808468365 for each run in the first month of data-taking

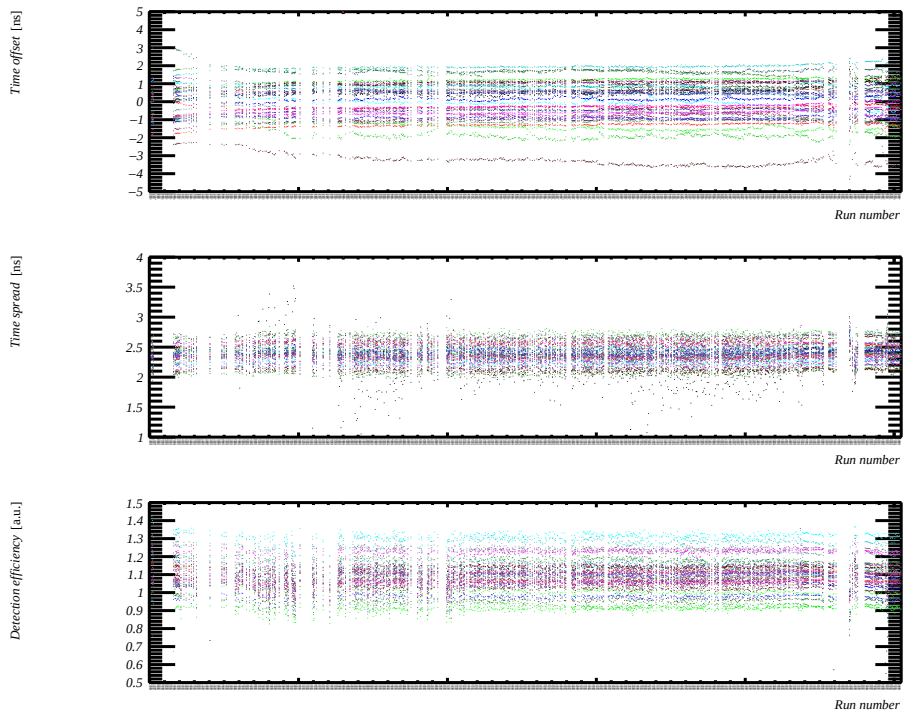

Figure 24: Calibrated PMT parameters of DOM 808474231 for each run in the first month of data-taking

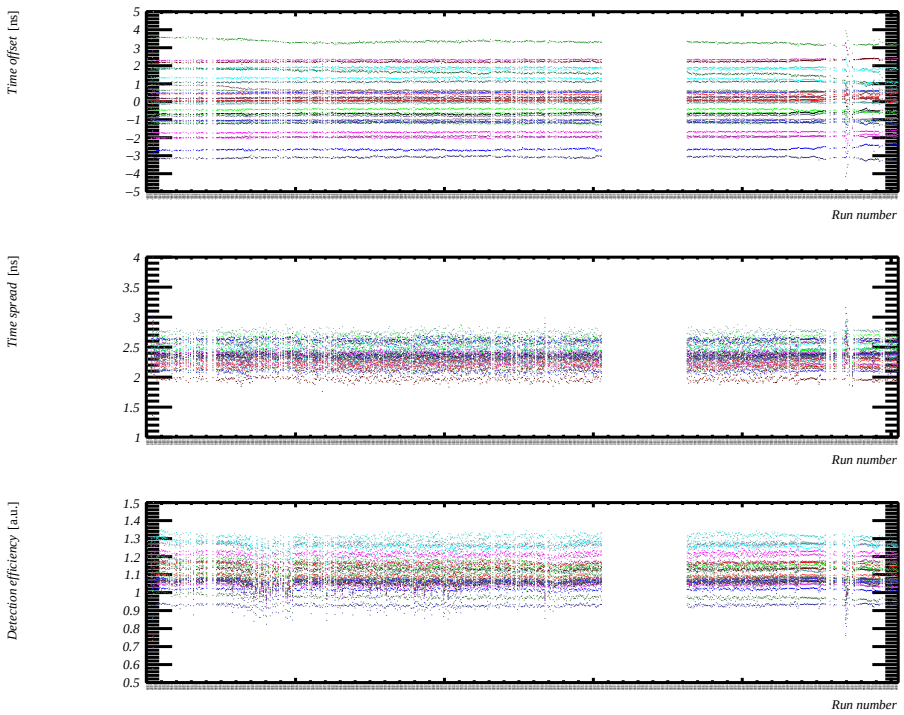

Figure 25: Calibrated PMT parameters of DOM 808965918 for each run in the first month of data-taking

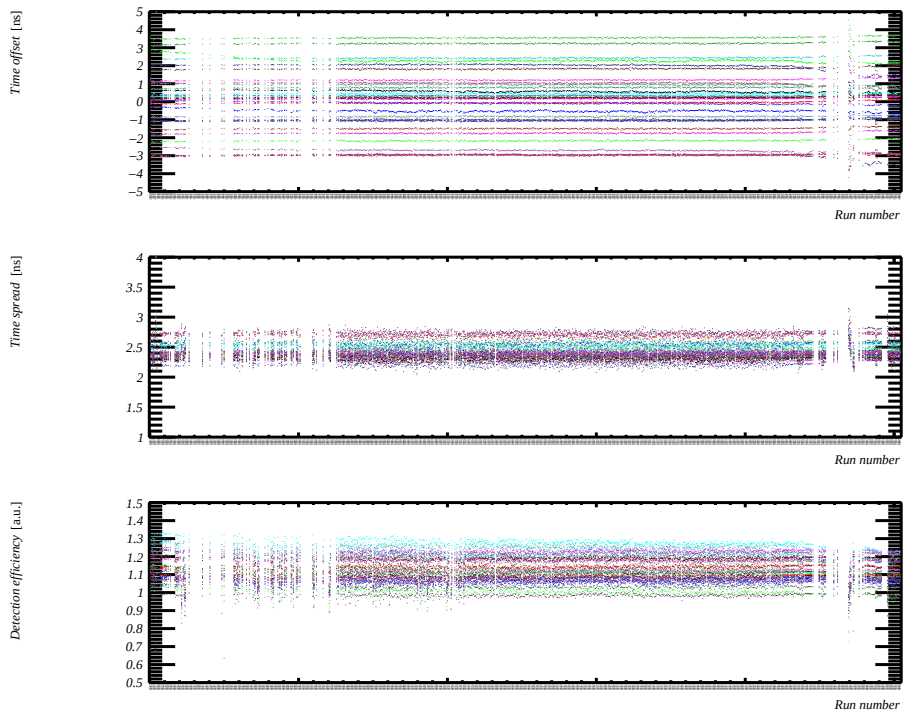

Figure 26: Calibrated PMT parameters of DOM 808966287 for each run in the first month of data-taking

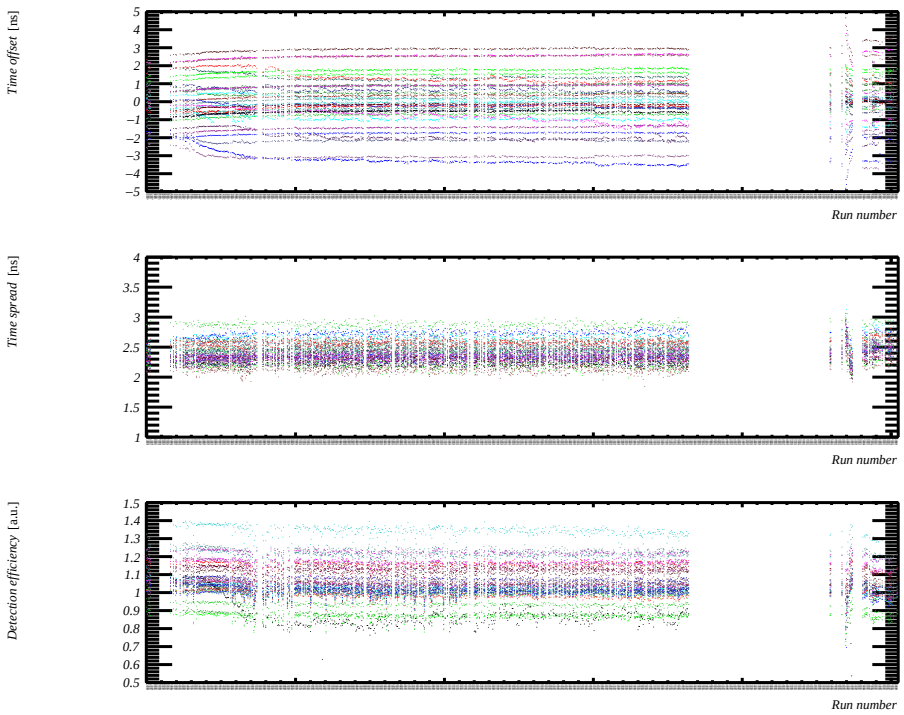

Figure 27: Calibrated PMT parameters of DOM 808972586 for each run in the first month of data-taking

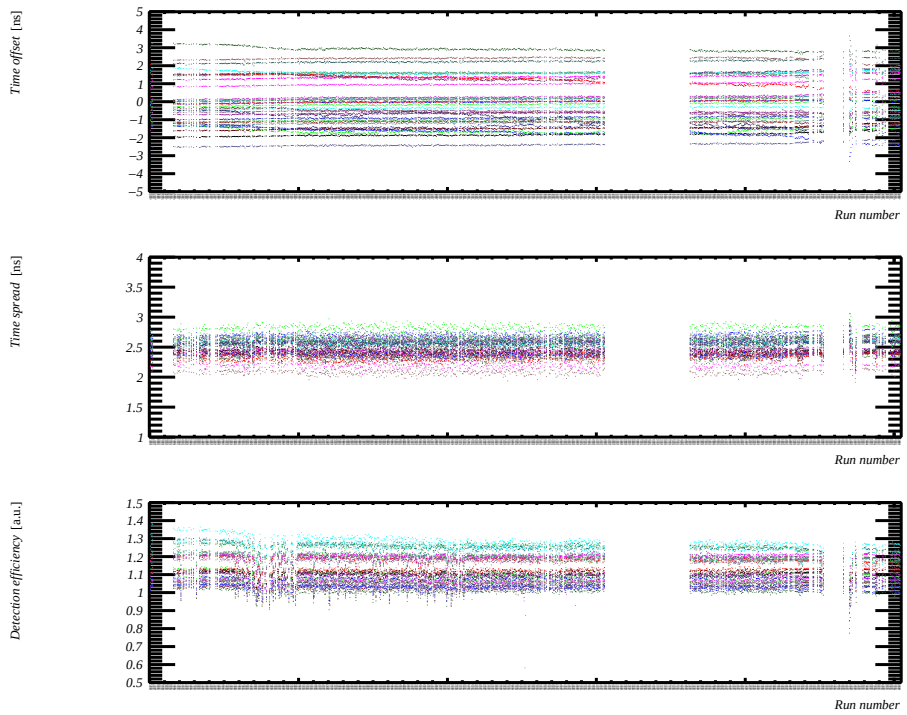

Figure 28: Calibrated PMT parameters of DOM 808974928 for each run in the first month of data-taking

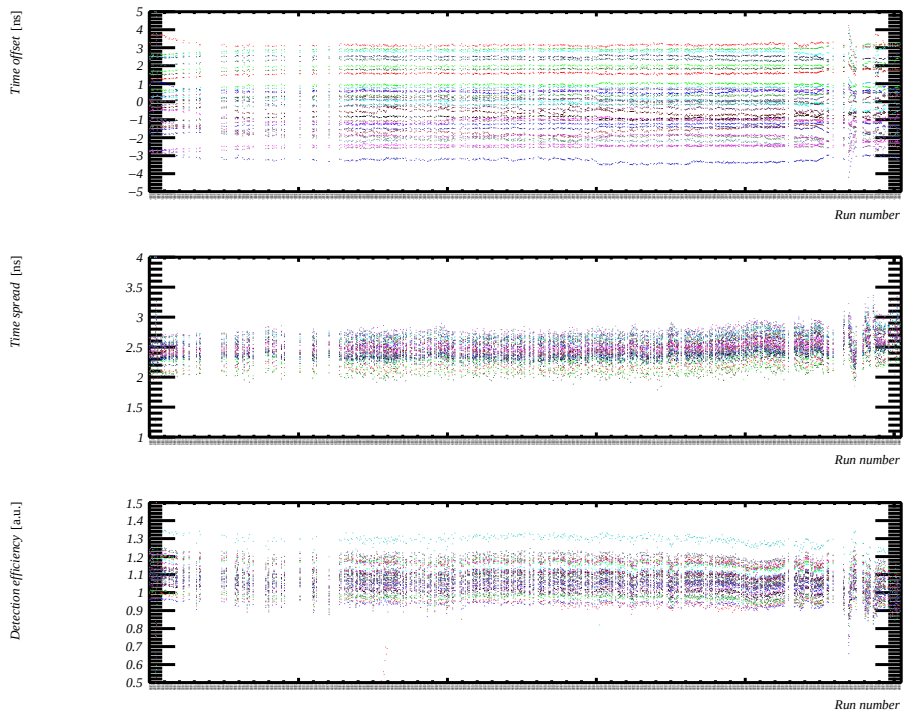

Figure 29: Calibrated PMT parameters of DOM 808982574 for each run in the first month of data-taking

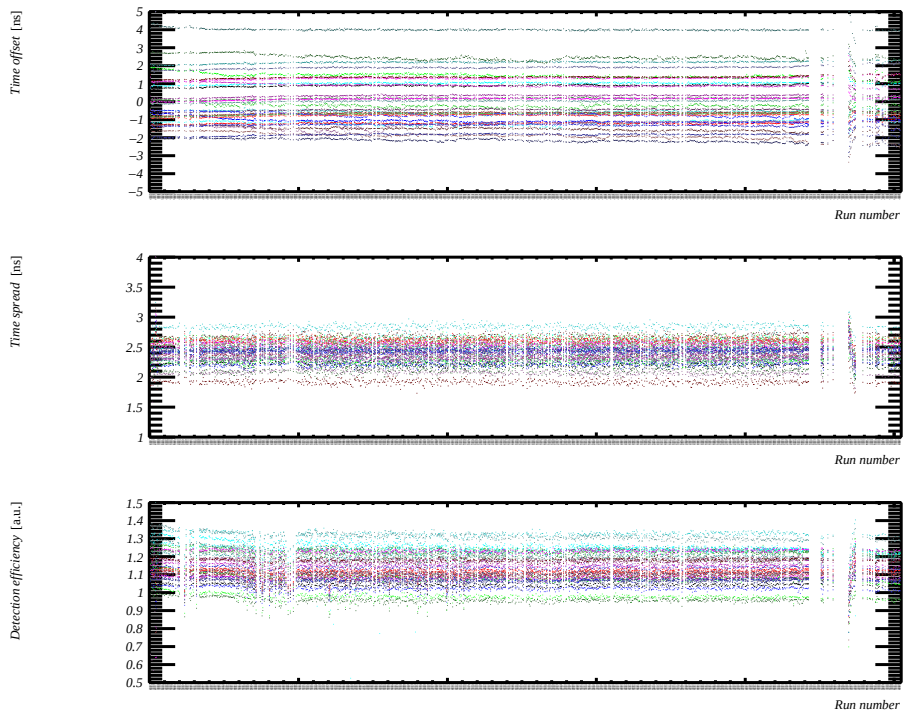

Figure 30: Calibrated PMT parameters of DOM 808987051 for each run in the first month of data-taking

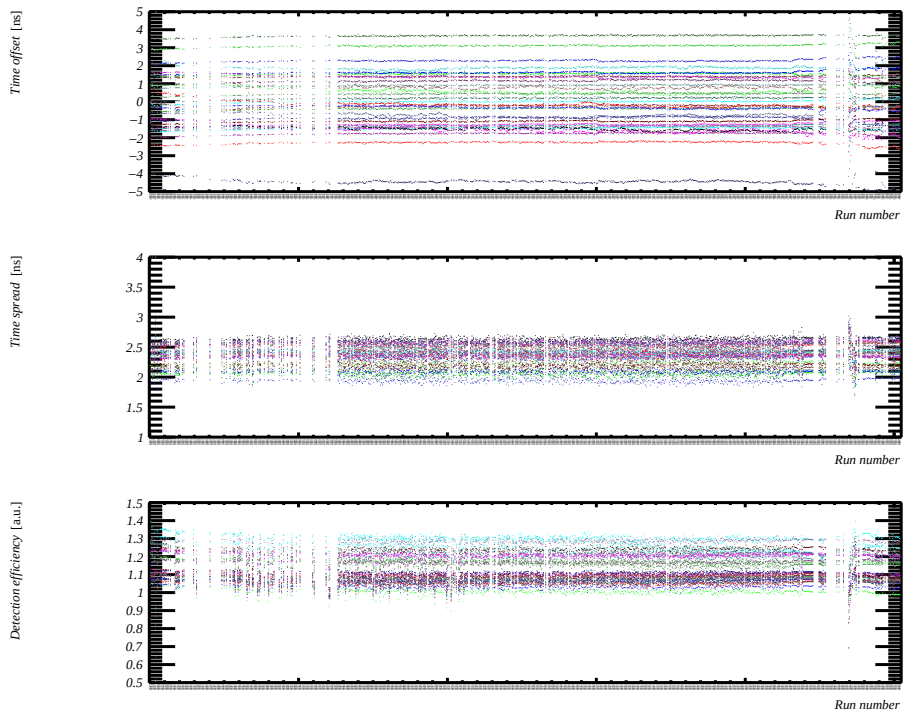

Figure 31: Calibrated PMT parameters of DOM 808987121 for each run in the first month of data-taking

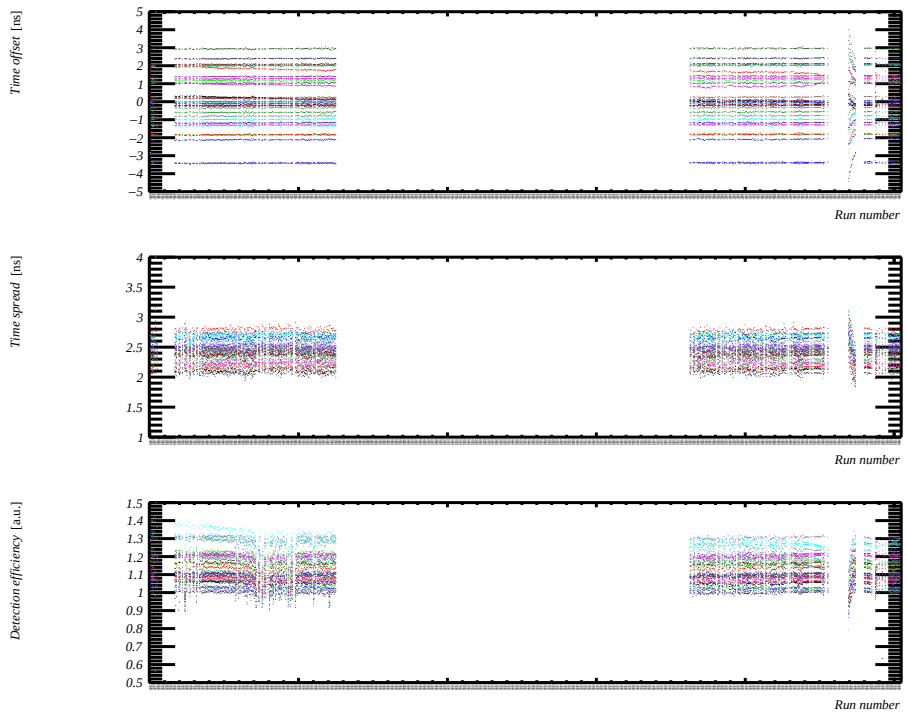

Figure 32: Calibrated PMT parameters of DOM 808992603 for each run in the first month of data-taking

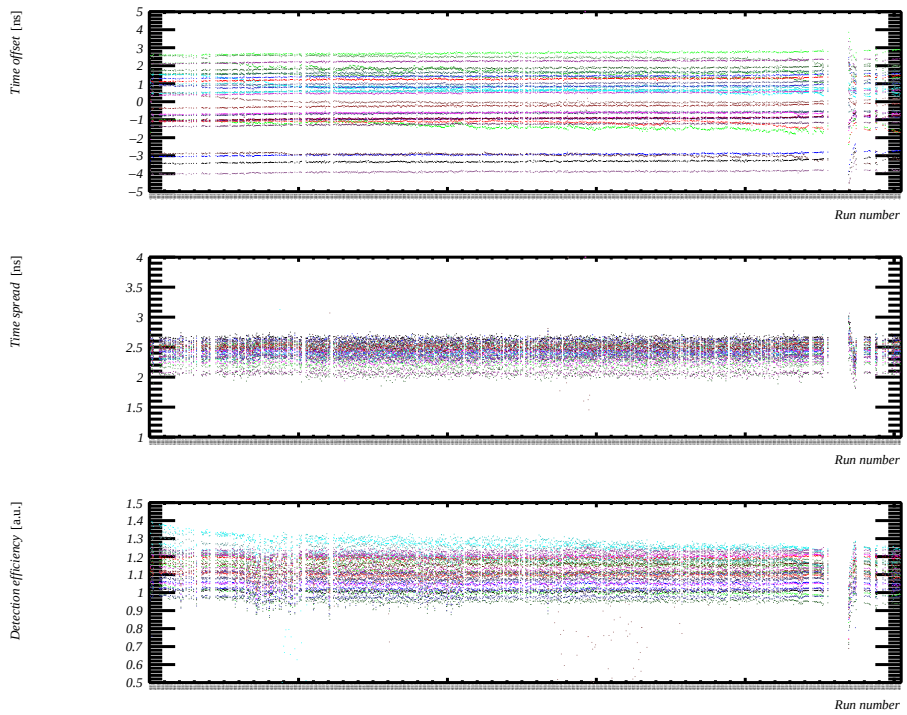

Figure 33: Calibrated PMT parameters of DOM 808995481 for each run in the first month of data-taking

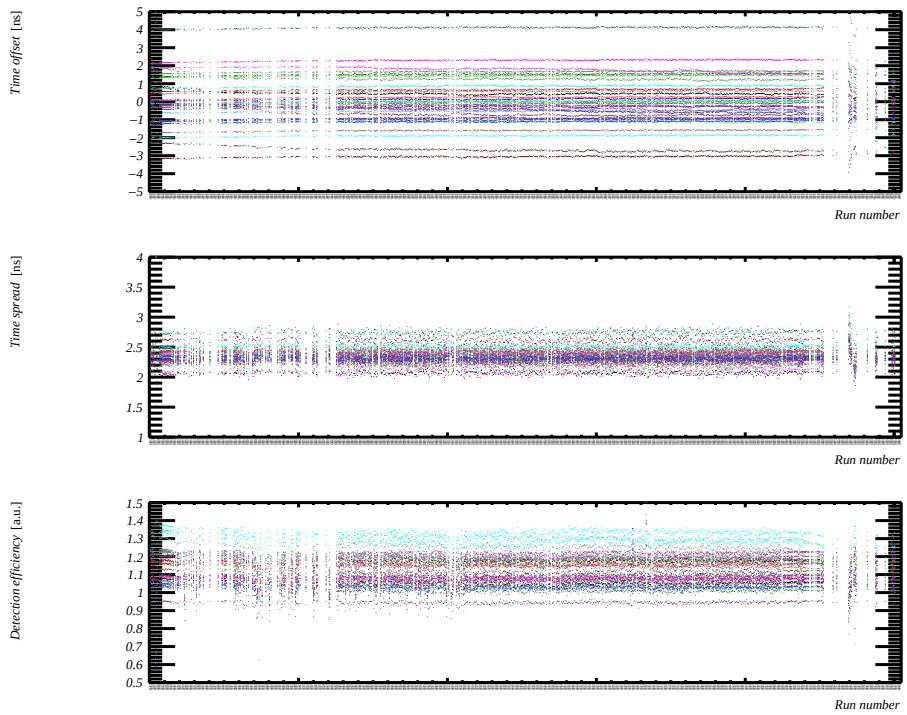

Figure 34: Calibrated PMT parameters of DOM 808996420 for each run in the first month of data-taking

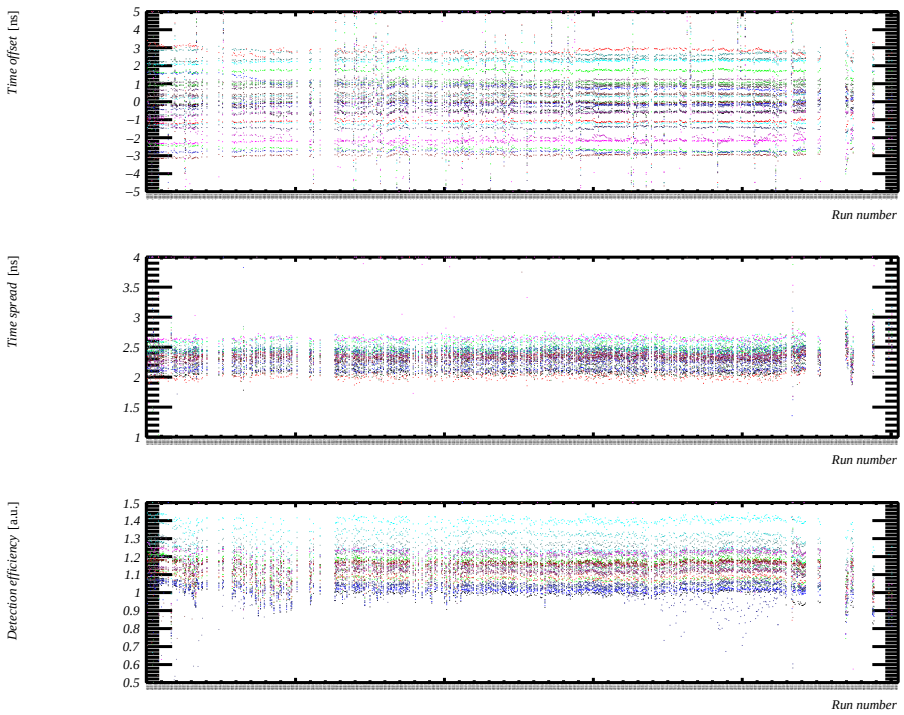

Figure 35: Calibrated PMT parameters of DOM 809503299 for each run in the first month of data-taking

10 Appendix B: PMT time offfset distributions

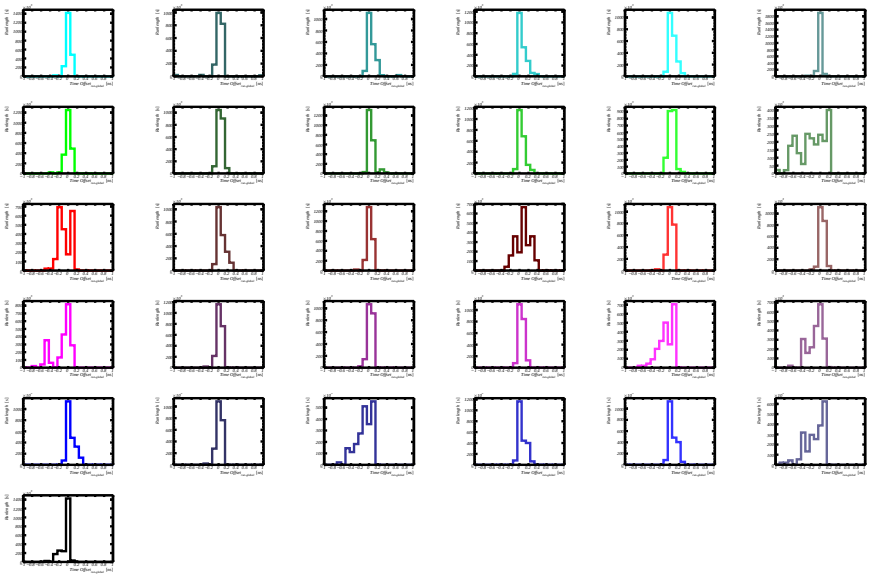

Figure 36: Fitted PMT time offset distribution of each run with respect to the globally fitted PMT time offset. Each row of plots gives the PMTs of one ring (upper row=ring F, lower ring=ring A) of DOM 808430036. The x-axis ranges from -1 to +1 ns.

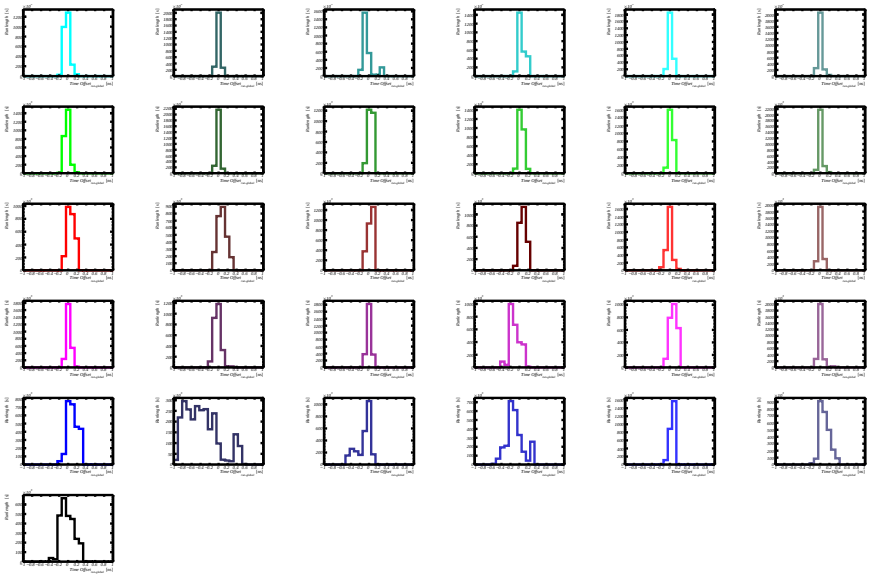

Figure 37: Fitted PMT time offset distribution of each run with respect to the globally fitted PMT time offset. Each row of plots gives the PMTs of one ring (upper row=ring F, lower ring=ring A) of DOM 808430449. The x-axis ranges from -1 to +1 ns.

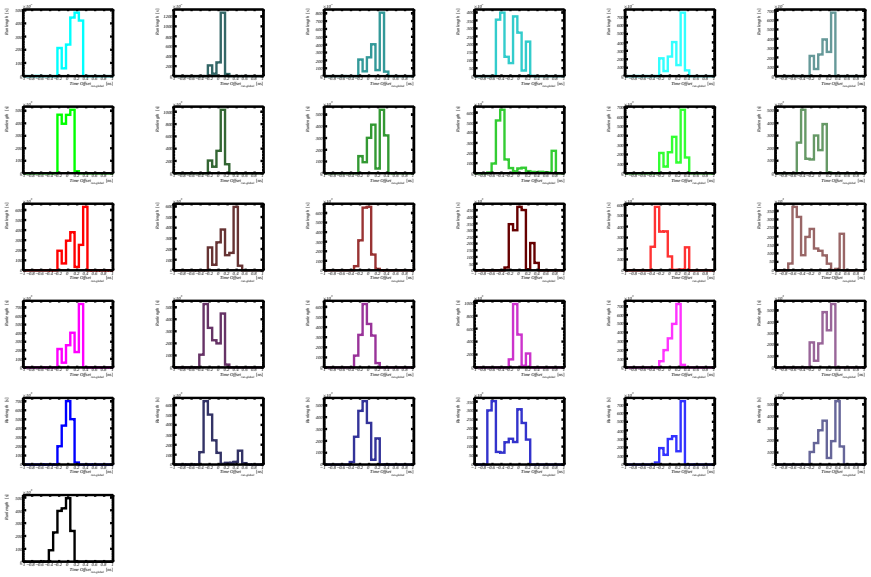

Figure 38: Fitted PMT time offset distribution of each run with respect to the globally fitted PMT time offset. Each row of plots gives the PMTs of one ring (upper row=ring F, lower ring=ring A) of DOM 808430571. The x-axis ranges from -1 to +1 ns.

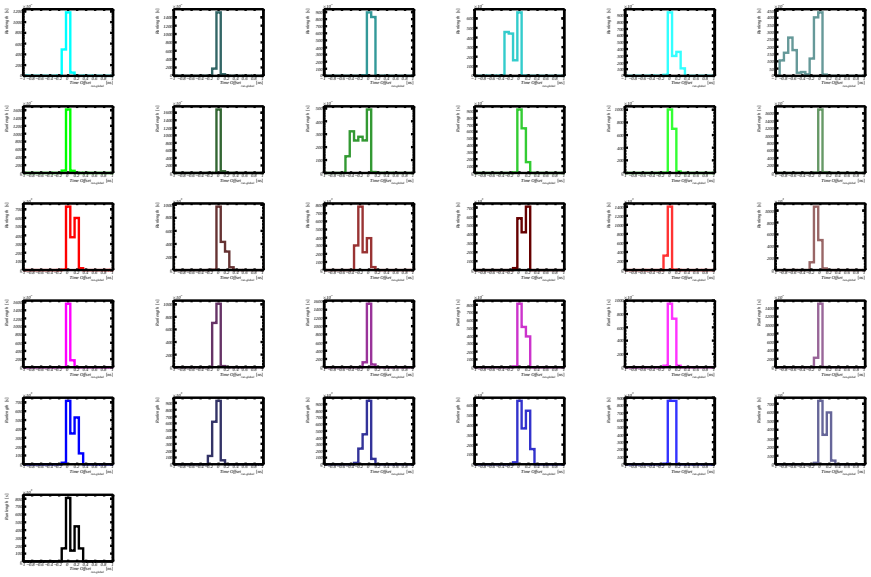

Figure 39: Fitted PMT time offset distribution of each run with respect to the globally fitted PMT time offset. Each row of plots gives the PMTs of one ring (upper row=ring F, lower ring=ring A) of DOM 808447091. The x-axis ranges from -1 to +1 ns.

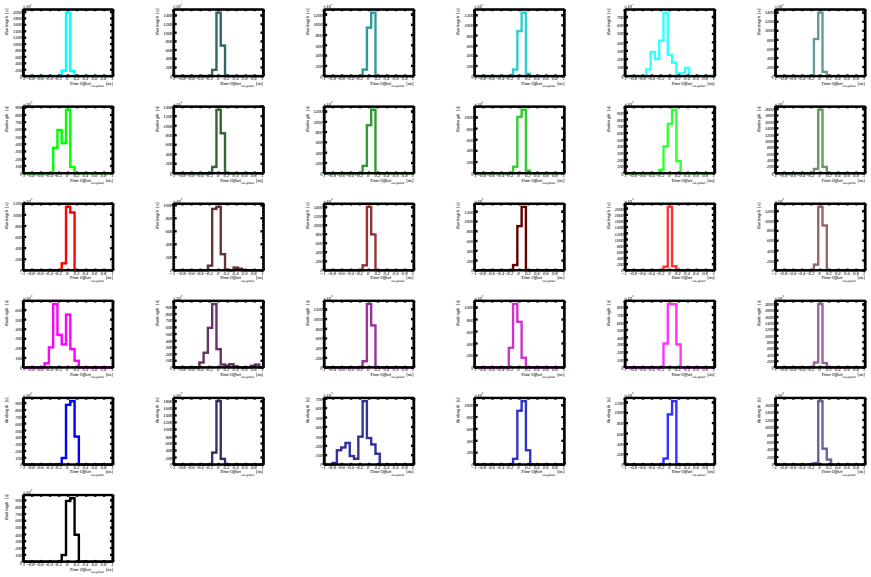

Figure 40: Fitted PMT time offset distribution of each run with respect to the globally fitted PMT time offset. Each row of plots gives the PMTs of one ring (upper row=ring F, lower ring=ring A) of DOM 808467569. The x-axis ranges from -1 to +1 ns.

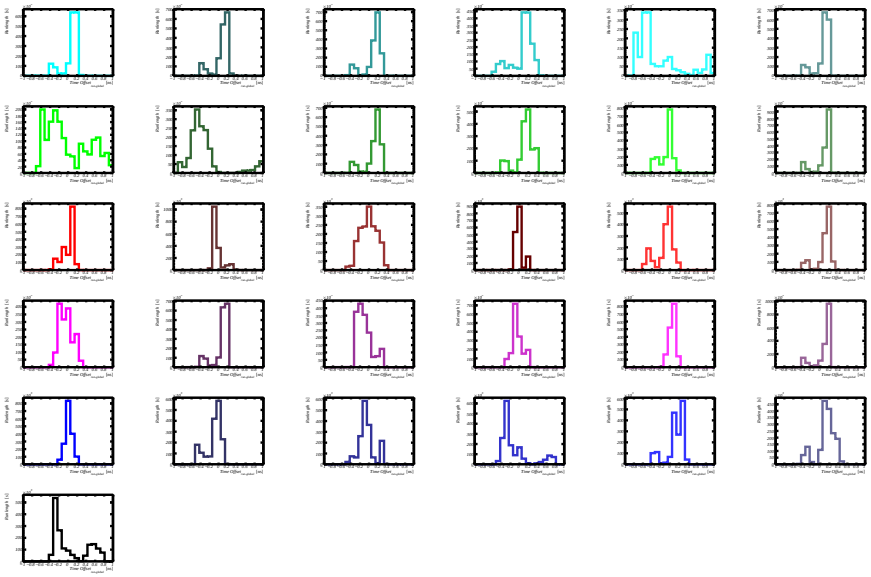

Figure 41: Fitted PMT time offset distribution of each run with respect to the globally fitted PMT time offset. Each row of plots gives the PMTs of one ring (upper row=ring F, lower ring=ring A) of DOM 808468365. The x-axis ranges from -1 to +1 ns.

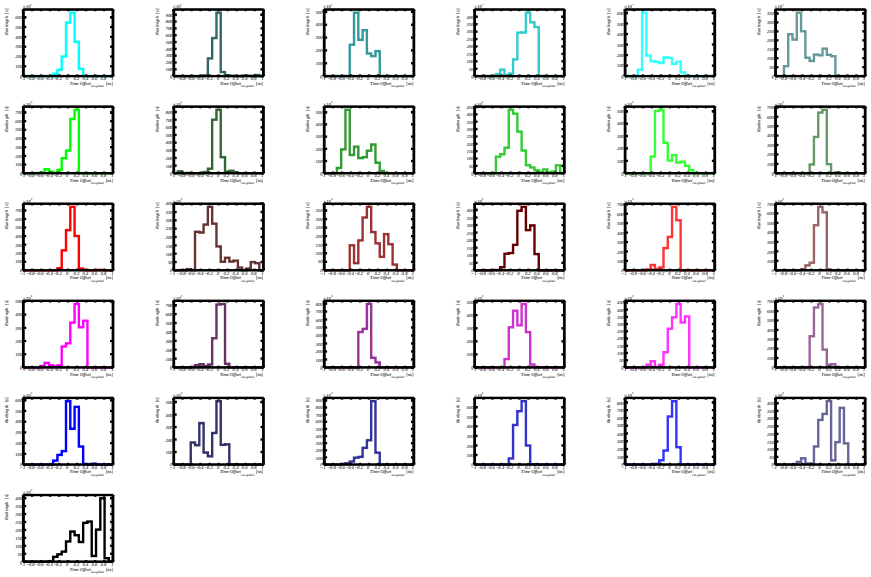

Figure 42: Fitted PMT time offset distribution of each run with respect to the globally fitted PMT time offset. Each row of plots gives the PMTs of one ring (upper row=ring F, lower ring=ring A) of DOM 808474231. The x-axis ranges from -1 to +1 ns.

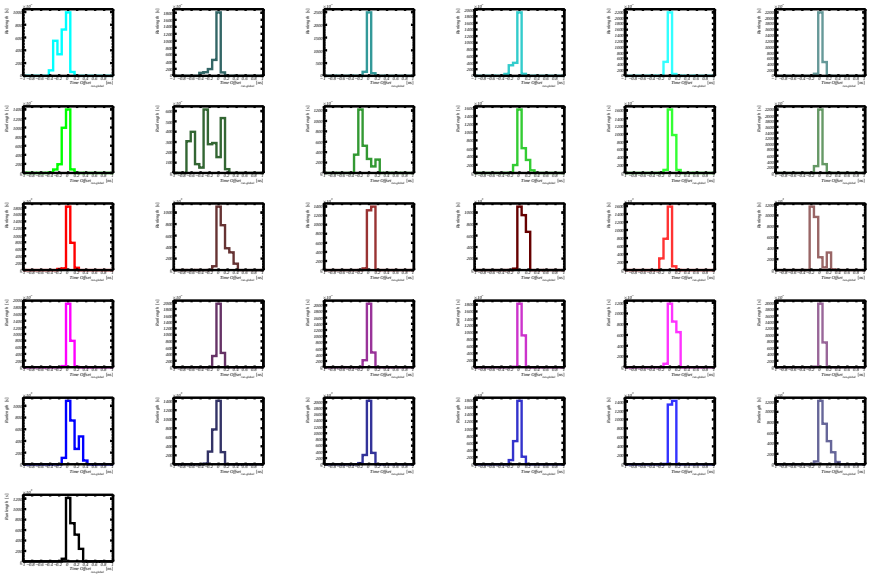

Figure 43: Fitted PMT time offset distribution of each run with respect to the globally fitted PMT time offset. Each row of plots gives the PMTs of one ring (upper row=ring F, lower ring=ring A) of DOM 808965918. The x-axis ranges from -1 to +1 ns.

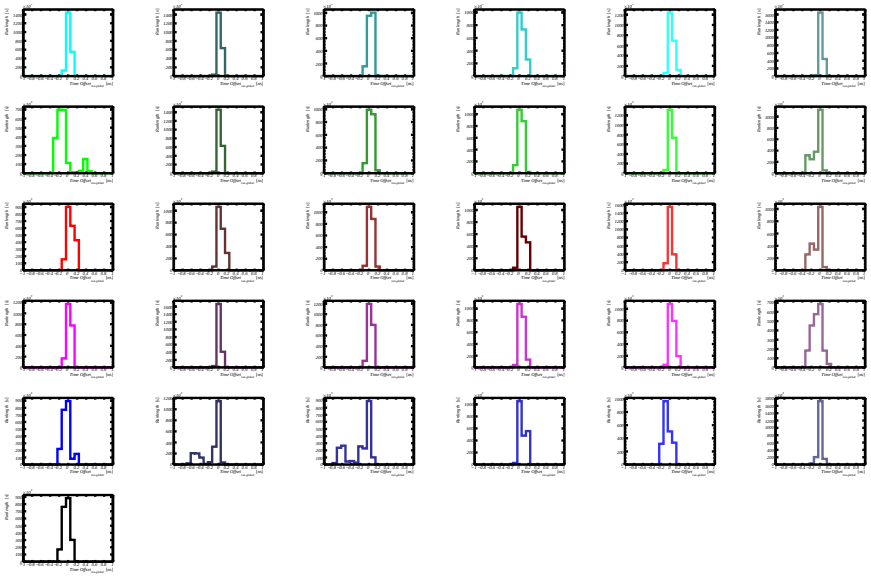

Figure 44: Fitted PMT time offset distribution of each run with respect to the globally fitted PMT time offset. Each row of plots gives the PMTs of one ring (upper row=ring F, lower ring=ring A) of DOM 808966287. The x-axis ranges from -1 to +1 ns.

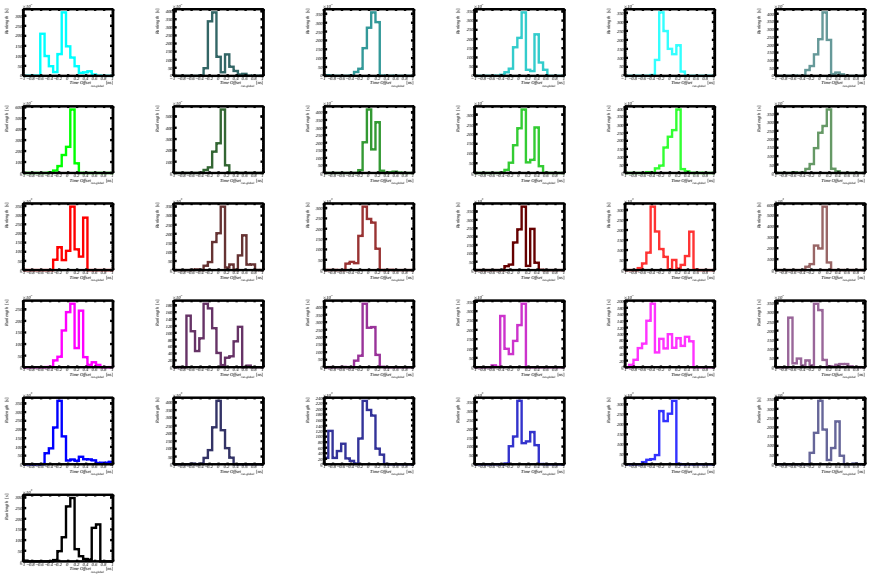

Figure 45: Fitted PMT time offset distribution of each run with respect to the globally fitted PMT time offset. Each row of plots gives the PMTs of one ring (upper row=ring F, lower ring=ring A) of DOM 808972586. The x-axis ranges from -1 to +1 ns.

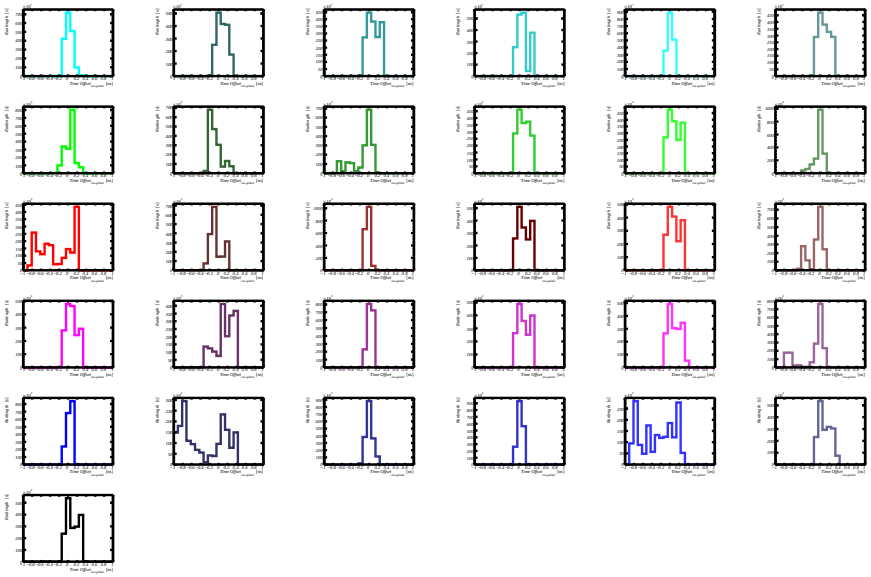

Figure 46: Fitted PMT time offset distribution of each run with respect to the globally fitted PMT time offset. Each row of plots gives the PMTs of one ring (upper row=ring F, lower ring=ring A) of DOM 808974928. The x-axis ranges from -1 to +1 ns.

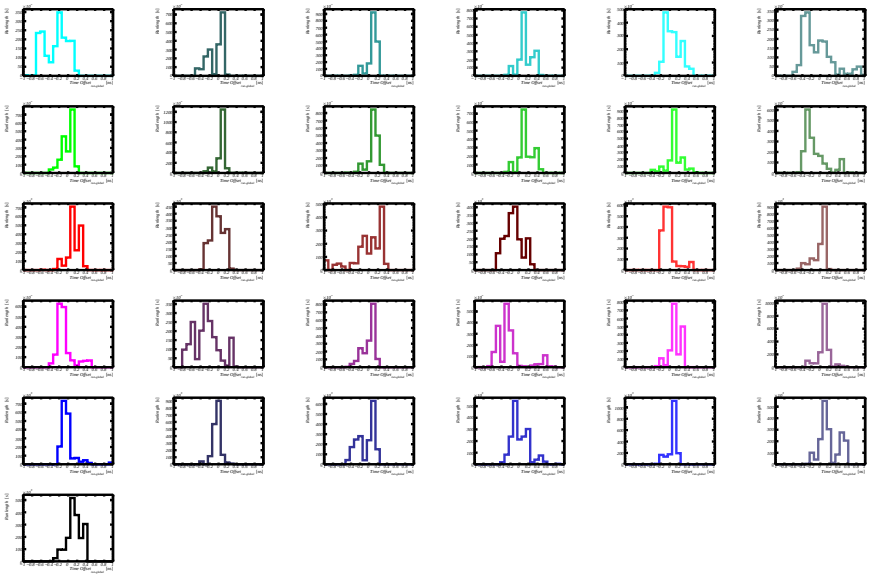

Figure 47: Fitted PMT time offset distribution of each run with respect to the globally fitted PMT time offset. Each row of plots gives the PMTs of one ring (upper row=ring F, lower ring=ring A) of DOM 808982574. The x-axis ranges from -1 to +1 ns.

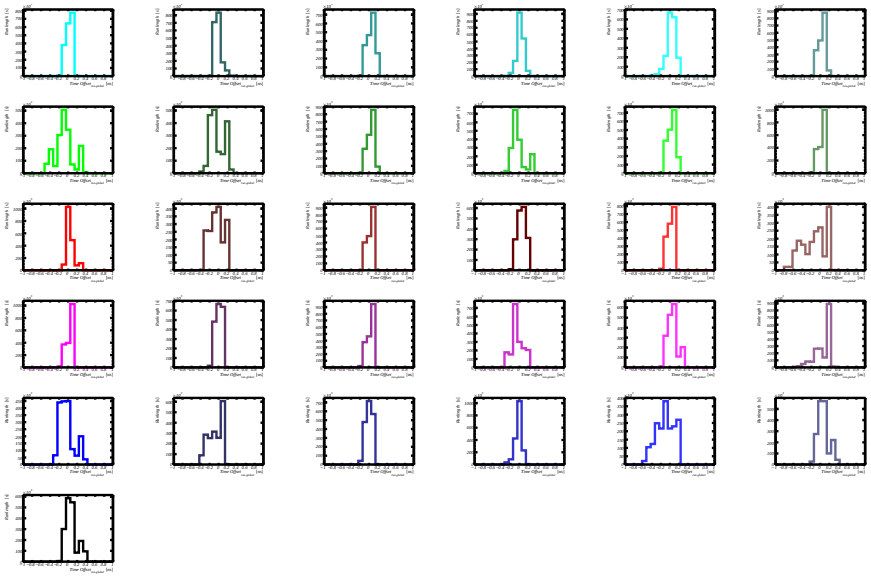

Figure 48: Fitted PMT time offset distribution of each run with respect to the globally fitted PMT time offset. Each row of plots gives the PMTs of one ring (upper row=ring F, lower ring=ring A) of DOM 808987051. The x-axis ranges from -1 to +1 ns.

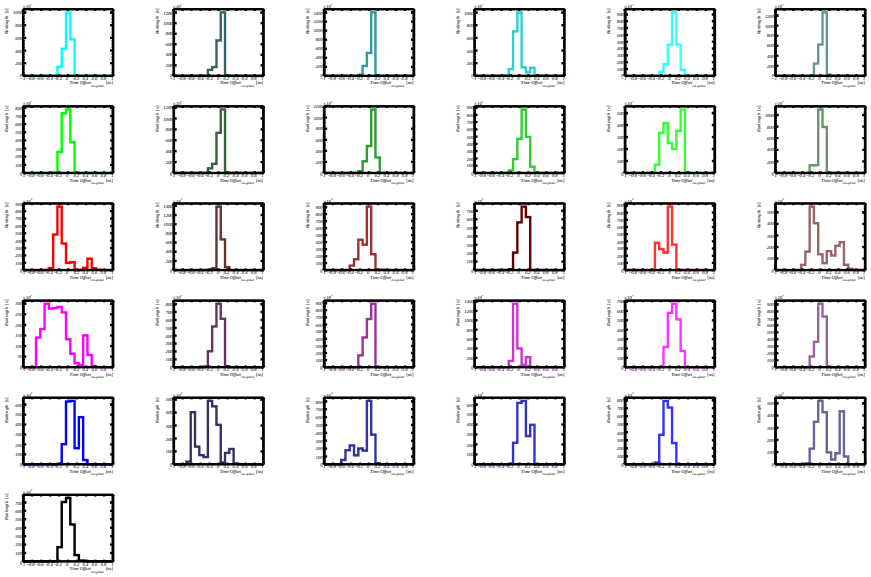

Figure 49: Fitted PMT time offset distribution of each run with respect to the globally fitted PMT time offset. Each row of plots gives the PMTs of one ring (upper row=ring F, lower ring=ring A) of DOM 808987121. The x-axis ranges from -1 to +1 ns.

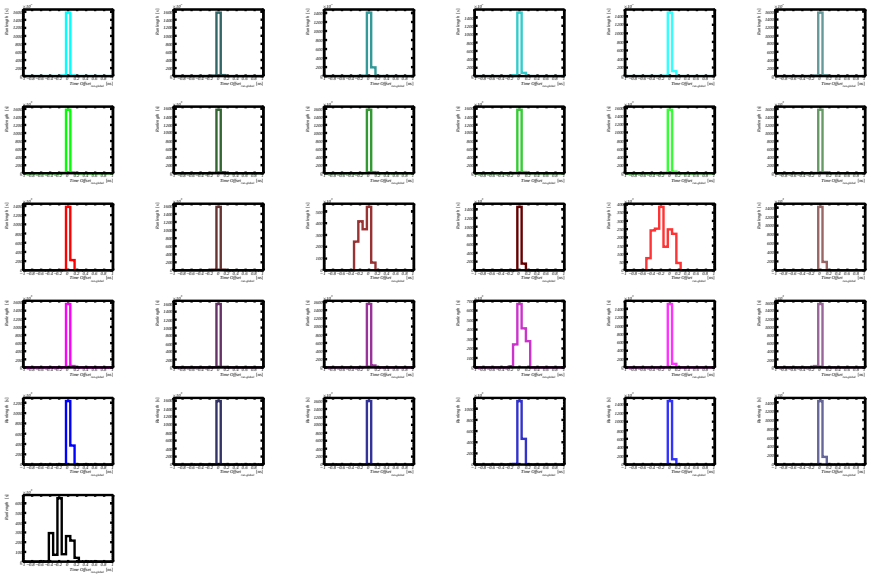

Figure 50: Fitted PMT time offset distribution of each run with respect to the globally fitted PMT time offset. Each row of plots gives the PMTs of one ring (upper row=ring F, lower ring=ring A) of DOM 808992603. The x-axis ranges from -1 to +1 ns.

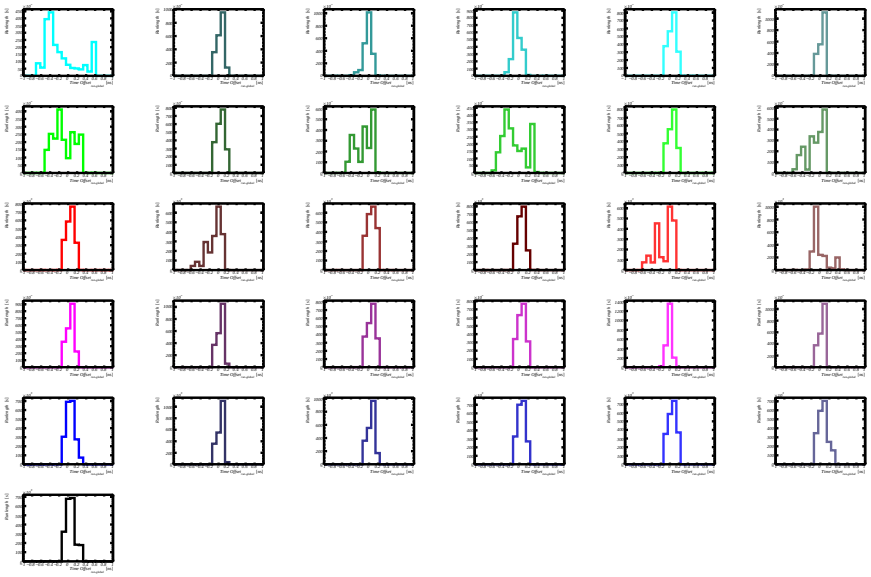

Figure 51: Fitted PMT time offset distribution of each run with respect to the globally fitted PMT time offset. Each row of plots gives the PMTs of one ring (upper row=ring F, lower ring=ring A) of DOM 808995481. The x-axis ranges from -1 to +1 ns.

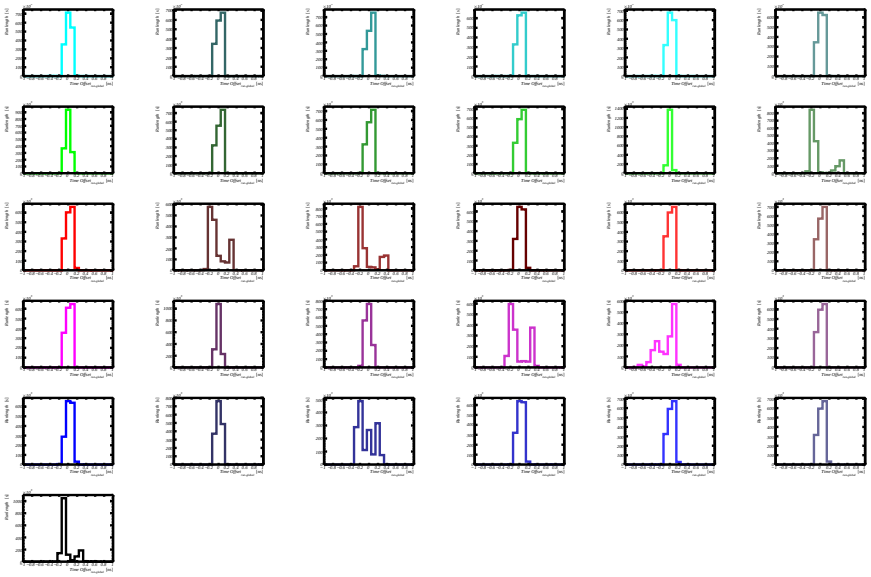

Figure 52: Fitted PMT time offset distribution of each run with respect to the globally fitted PMT time offset. Each row of plots gives the PMTs of one ring (upper row=ring F, lower ring=ring A) of DOM 808996420. The x-axis ranges from -1 to +1 ns.

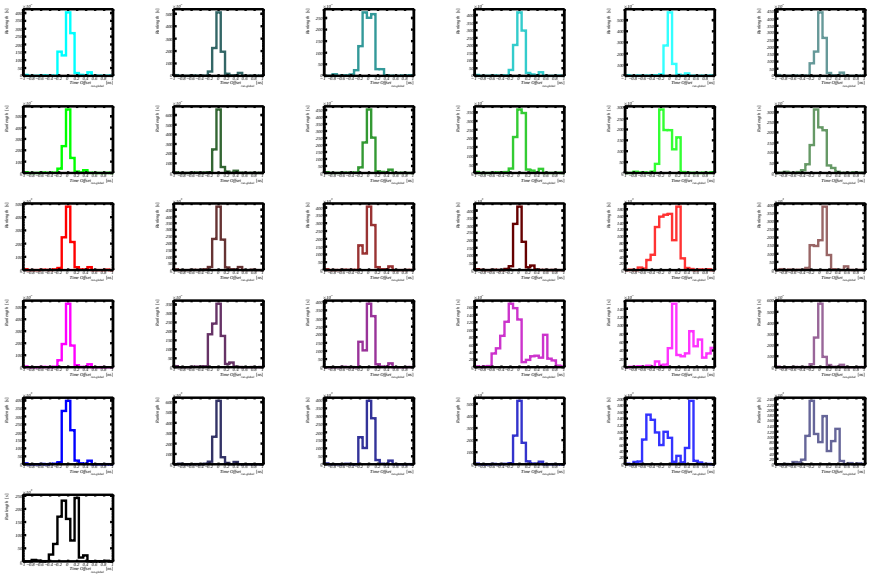

Figure 53: Fitted PMT time offset distribution of each run with respect to the globally fitted PMT time offset. Each row of plots gives the PMTs of one ring (upper row=ring F, lower ring=ring A) of DOM 809503299. The x-axis ranges from -1 to +1 ns.

11 Appendix C: PMT detection efficiency distributions

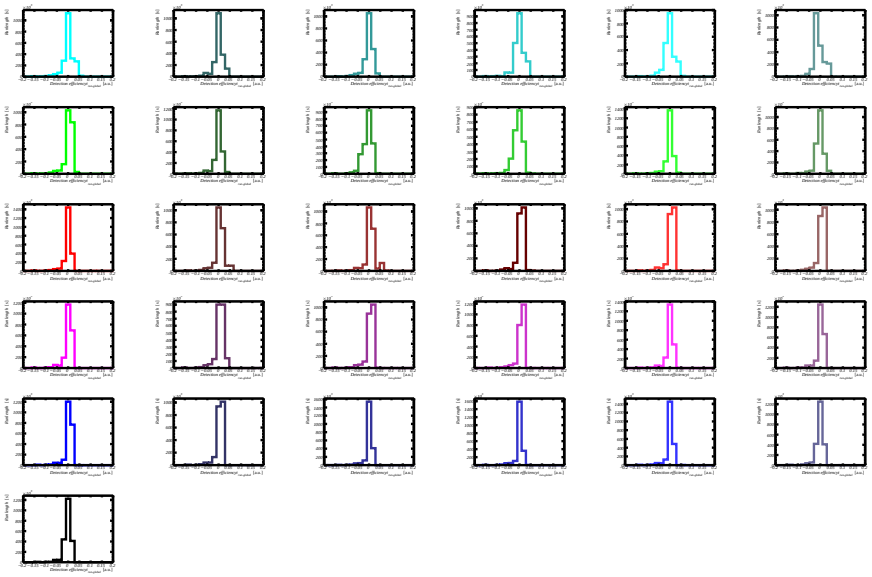

Figure 54: Fitted PMT relative detection efficiency distribution of each run with respect to the globally fitted PMT relative detection efficiency. Each row of plots gives the PMTs of one ring (upper row=ring F, lower ring=ring A) of DOM 808430036. The x-axis ranges from -0.2 to +0.2.

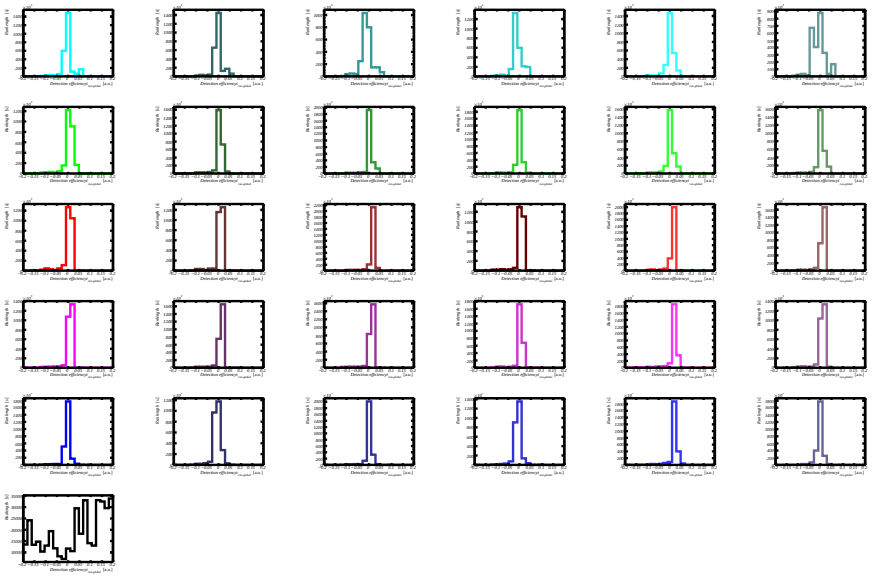

Figure 55: Fitted PMT relative detection efficiency distribution of each run with respect to the globally fitted PMT relative detection efficiency. Each row of plots gives the PMTs of one ring (upper row=ring F, lower ring=ring A) of DOM 808430449. The x-axis ranges from -0.2 to +0.2.

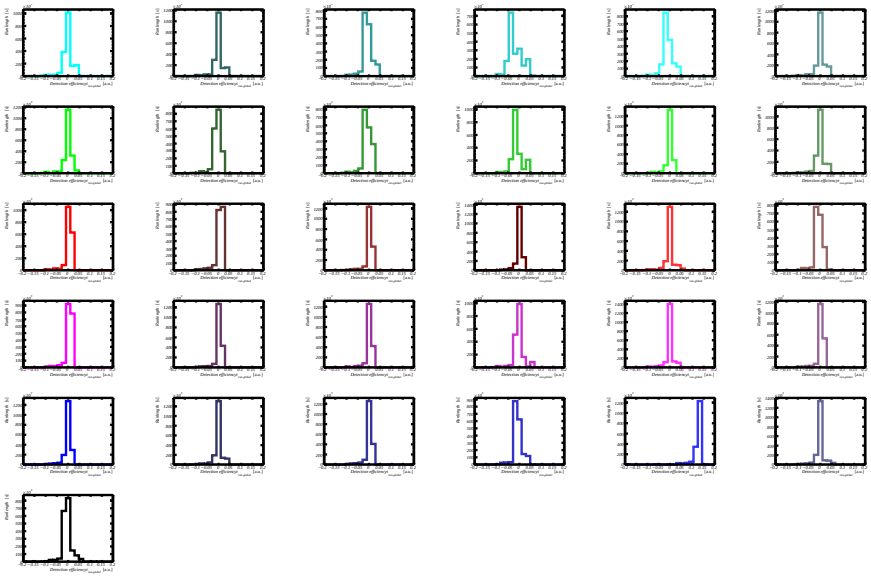

Figure 56: Fitted PMT relative detection efficiency distribution of each run with respect to the globally fitted PMT relative detection efficiency. Each row of plots gives the PMTs of one ring (upper row=ring F, lower ring=ring A) of DOM 808430571. The x-axis ranges from -0.2 to +0.2.

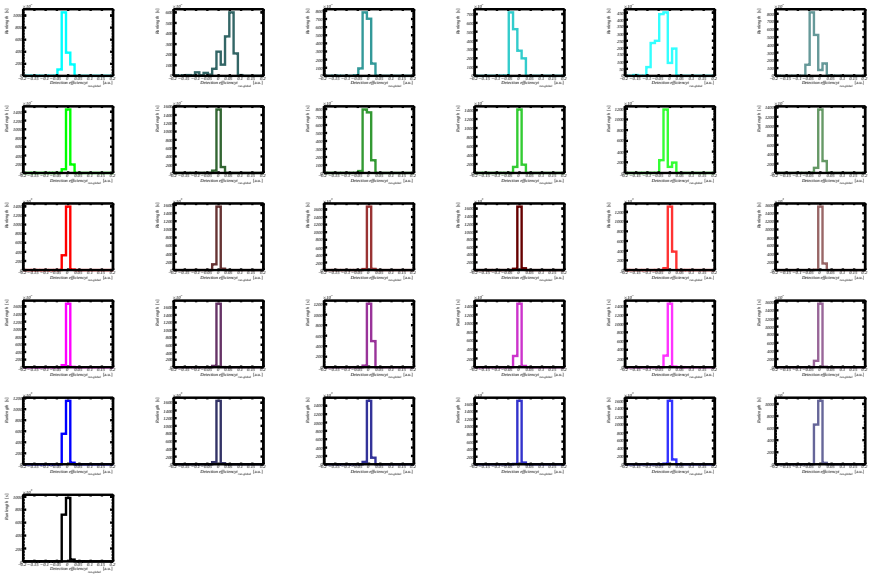

Figure 57: Fitted PMT relative detection efficiency distribution of each run with respect to the globally fitted PMT relative detection efficiency. Each row of plots gives the PMTs of one ring (upper row=ring F, lower ring=ring A) of DOM 808447091. The x-axis ranges from -0.2 to +0.2.

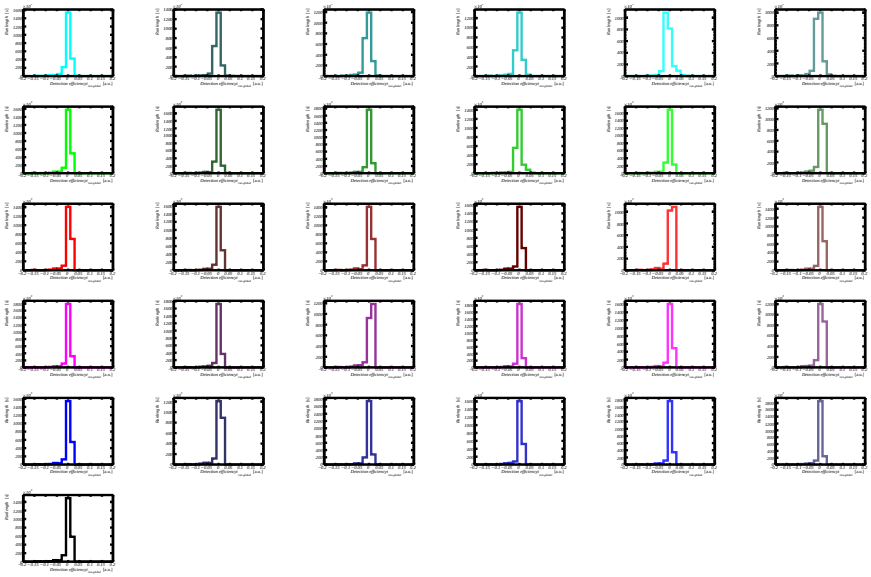

Figure 58: Fitted PMT relative detection efficiency distribution of each run with respect to the globally fitted PMT relative detection efficiency. Each row of plots gives the PMTs of one ring (upper row=ring F, lower ring=ring A) of DOM 808467569. The x-axis ranges from -0.2 to +0.2.

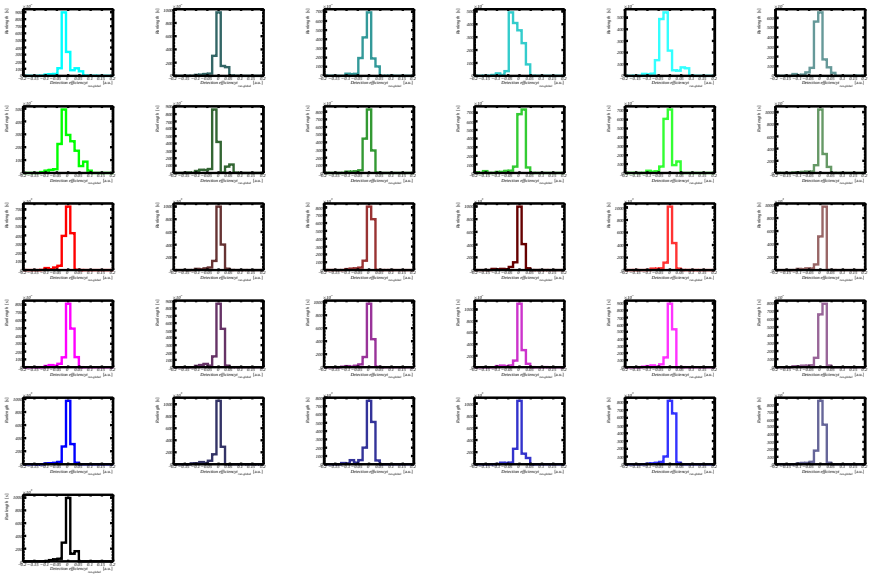

Figure 59: Fitted PMT relative detection efficiency distribution of each run with respect to the globally fitted PMT relative detection efficiency. Each row of plots gives the PMTs of one ring (upper row=ring F, lower ring=ring A) of DOM 808468365. The x-axis ranges from -0.2 to +0.2.

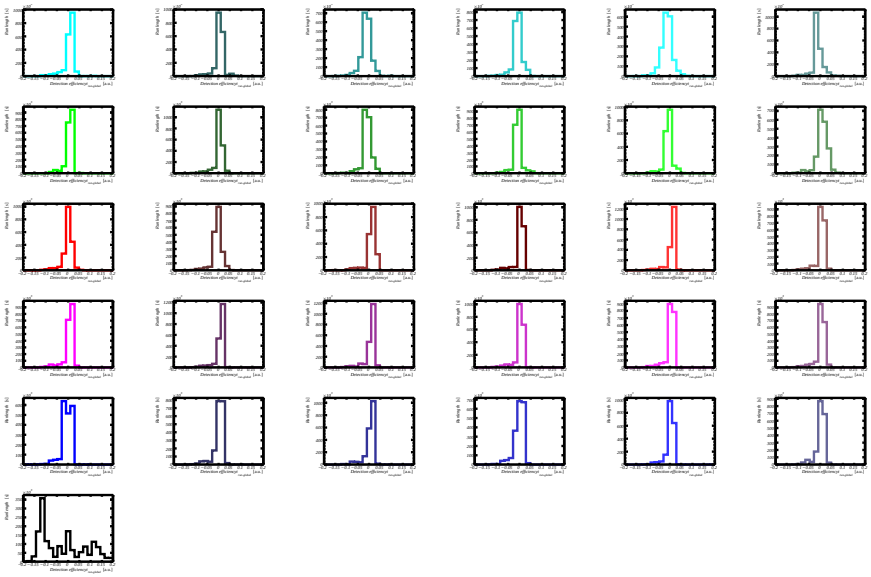

Figure 60: Fitted PMT relative detection efficiency distribution of each run with respect to the globally fitted PMT relative detection efficiency. Each row of plots gives the PMTs of one ring (upper row=ring F, lower ring=ring A) of DOM 808474231. The x-axis ranges from -0.2 to +0.2.

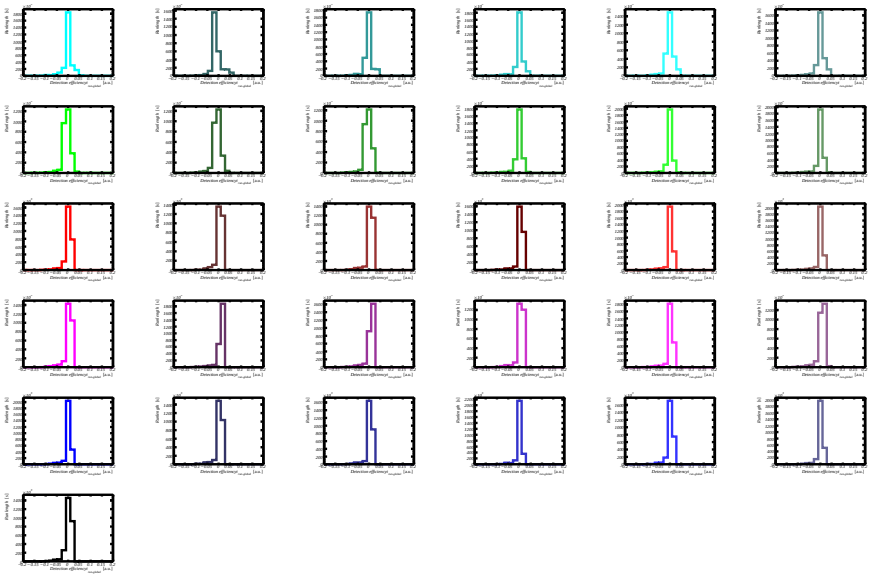

Figure 61: Fitted PMT relative detection efficiency distribution of each run with respect to the globally fitted PMT relative detection efficiency. Each row of plots gives the PMTs of one ring (upper row=ring F, lower ring=ring A) of DOM 808965918. The x-axis ranges from -0.2 to +0.2.

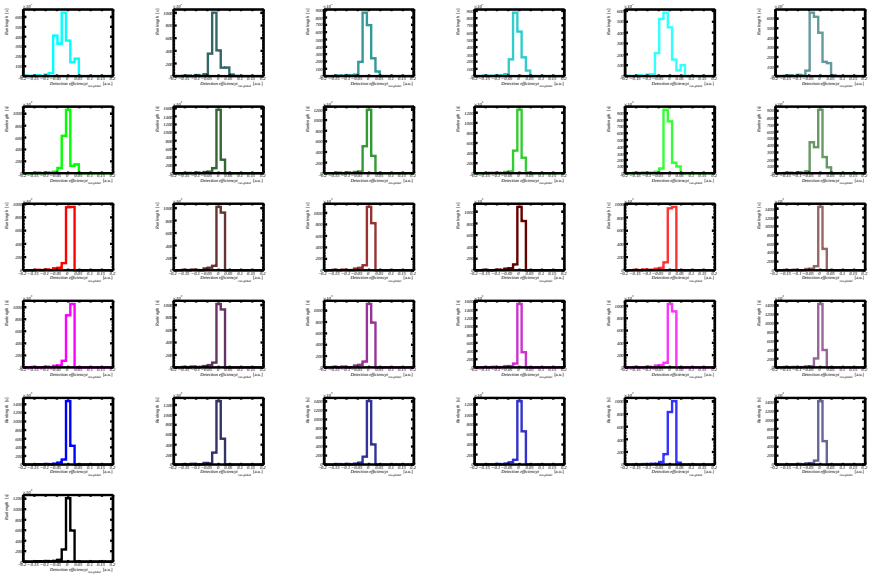

Figure 62: Fitted PMT relative detection efficiency distribution of each run with respect to the globally fitted PMT relative detection efficiency. Each row of plots gives the PMTs of one ring (upper row=ring F, lower ring=ring A) of DOM 808966287. The x-axis ranges from -0.2 to +0.2.

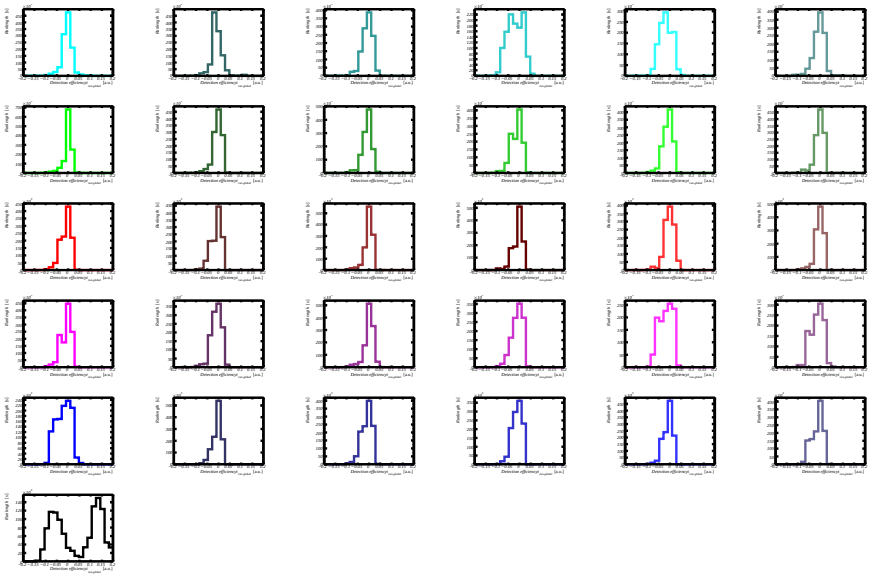

Figure 63: Fitted PMT relative detection efficiency distribution of each run with respect to the globally fitted PMT relative detection efficiency. Each row of plots gives the PMTs of one ring (upper row=ring F, lower ring=ring A) of DOM 808972586. The x-axis ranges from -0.2 to +0.2.

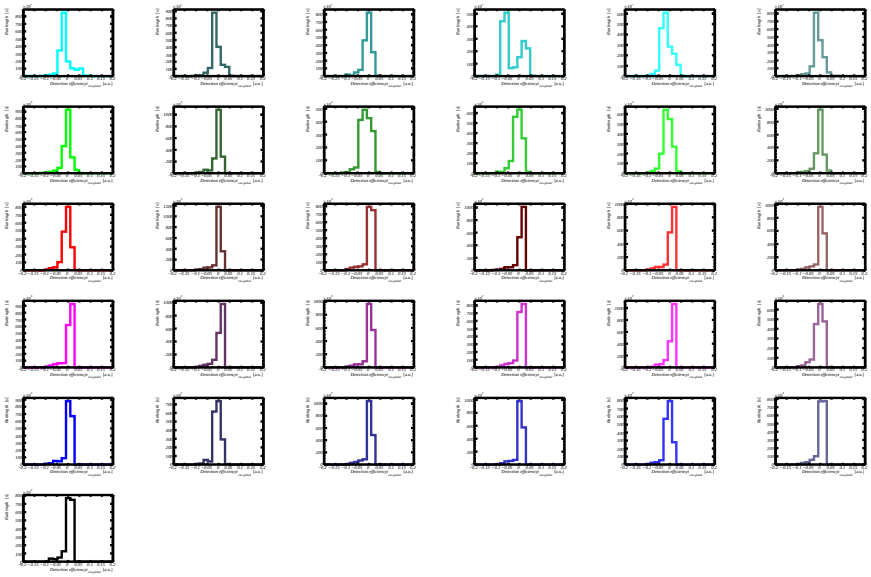

Figure 64: Fitted PMT relative detection efficiency distribution of each run with respect to the globally fitted PMT relative detection efficiency. Each row of plots gives the PMTs of one ring (upper row=ring F, lower ring=ring A) of DOM 808974928. The x-axis ranges from -0.2 to +0.2.

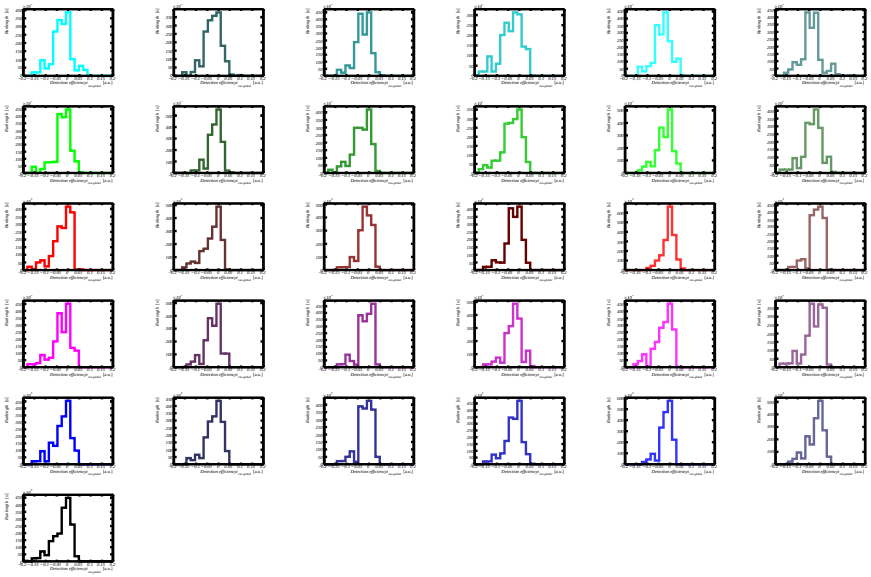

Figure 65: Fitted PMT relative detection efficiency distribution of each run with respect to the globally fitted PMT relative detection efficiency. Each row of plots gives the PMTs of one ring (upper row=ring F, lower ring=ring A) of DOM 808982574. The x-axis ranges from -0.2 to +0.2.

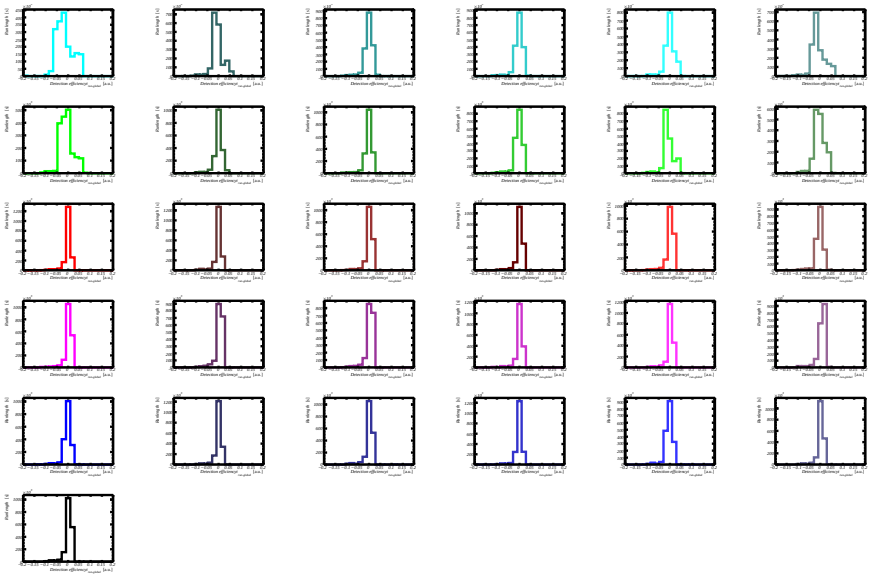

Figure 66: Fitted PMT relative detection efficiency distribution of each run with respect to the globally fitted PMT relative detection efficiency. Each row of plots gives the PMTs of one ring (upper row=ring F, lower ring=ring A) of DOM 808987051. The x-axis ranges from -0.2 to +0.2.

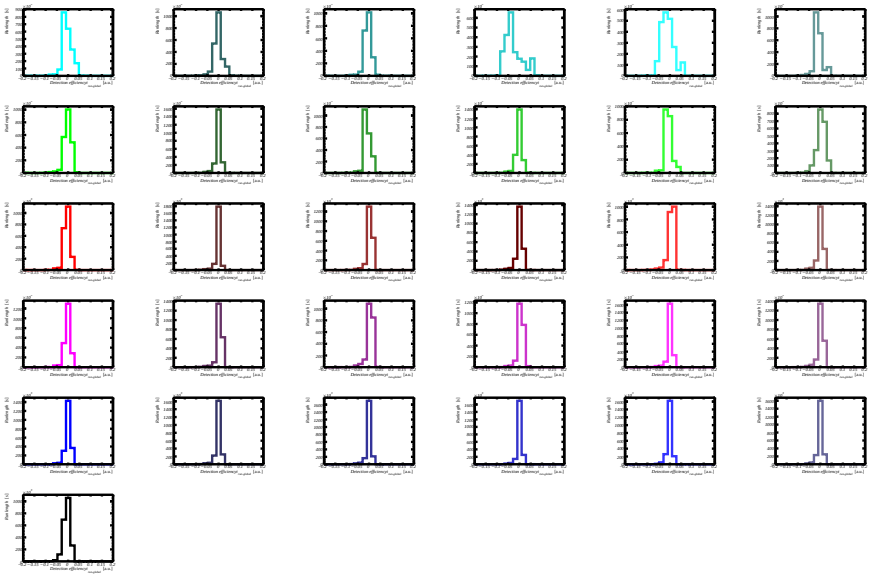

Figure 67: Fitted PMT relative detection efficiency distribution of each run with respect to the globally fitted PMT relative detection efficiency. Each row of plots gives the PMTs of one ring (upper row=ring F, lower ring=ring A) of DOM 808987121. The x-axis ranges from -0.2 to +0.2.

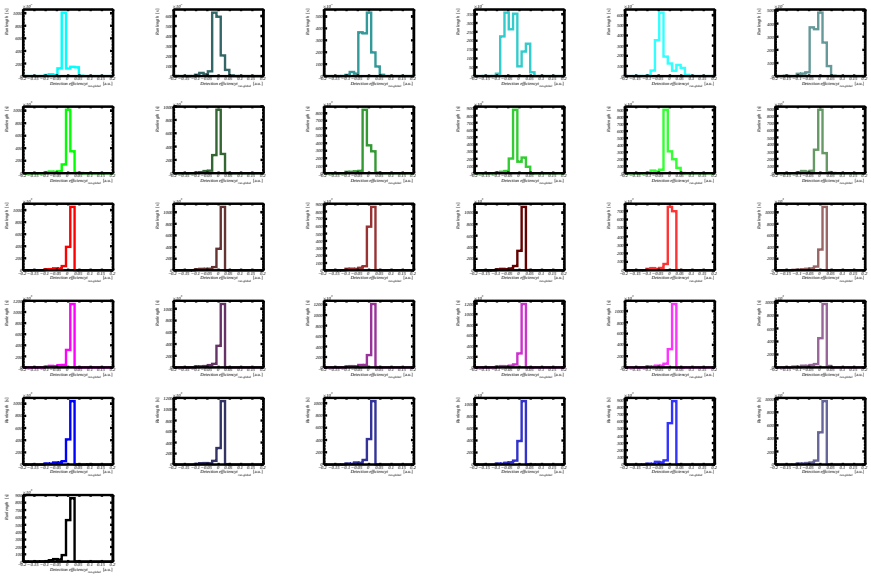

Figure 68: Fitted PMT relative detection efficiency distribution of each run with respect to the globally fitted PMT relative detection efficiency. Each row of plots gives the PMTs of one ring (upper row=ring F, lower ring=ring A) of DOM 808992603. The x-axis ranges from -0.2 to +0.2.

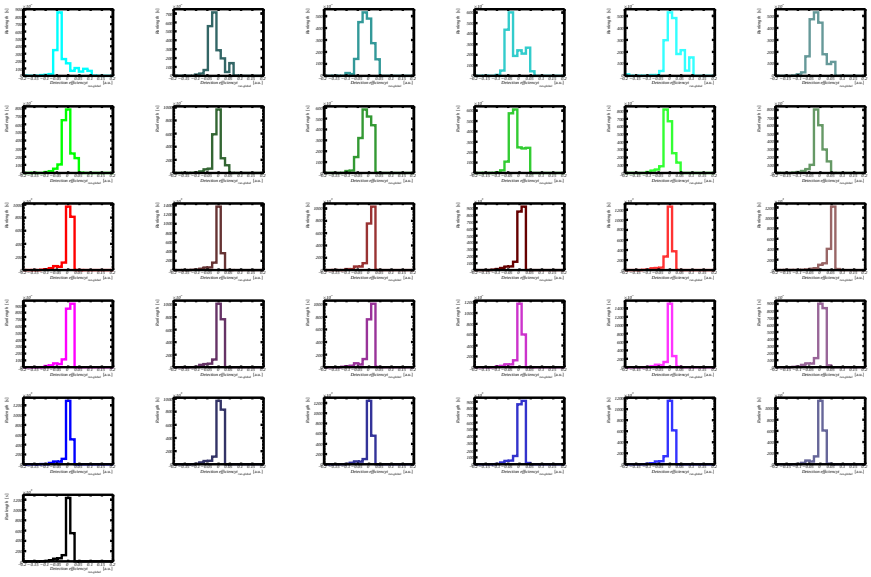

Figure 69: Fitted PMT relative detection efficiency distribution of each run with respect to the globally fitted PMT relative detection efficiency. Each row of plots gives the PMTs of one ring (upper row=ring F, lower ring=ring A) of DOM 808995481. The x-axis ranges from -0.2 to +0.2.

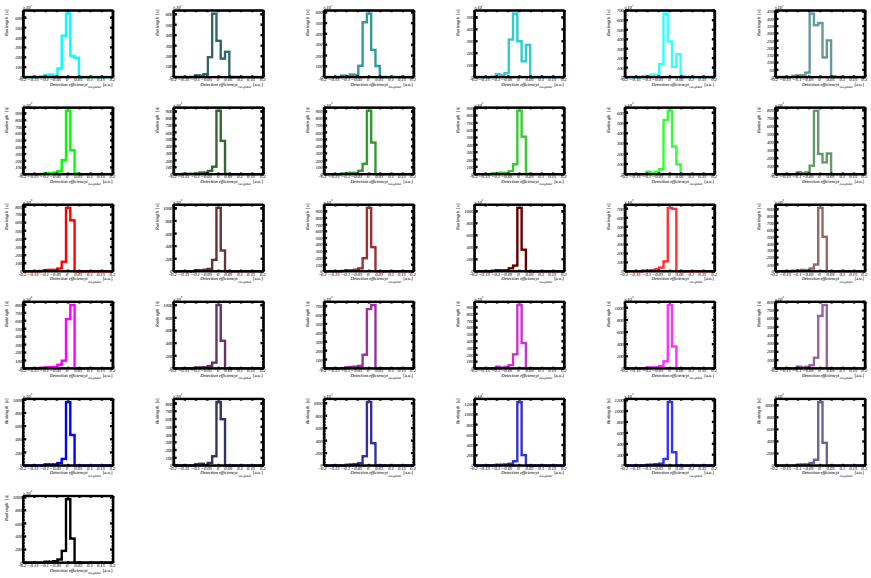

Figure 70: Fitted PMT relative detection efficiency distribution of each run with respect to the globally fitted PMT relative detection efficiency. Each row of plots gives the PMTs of one ring (upper row=ring F, lower ring=ring A) of DOM 808996420. The x-axis ranges from -0.2 to +0.2.

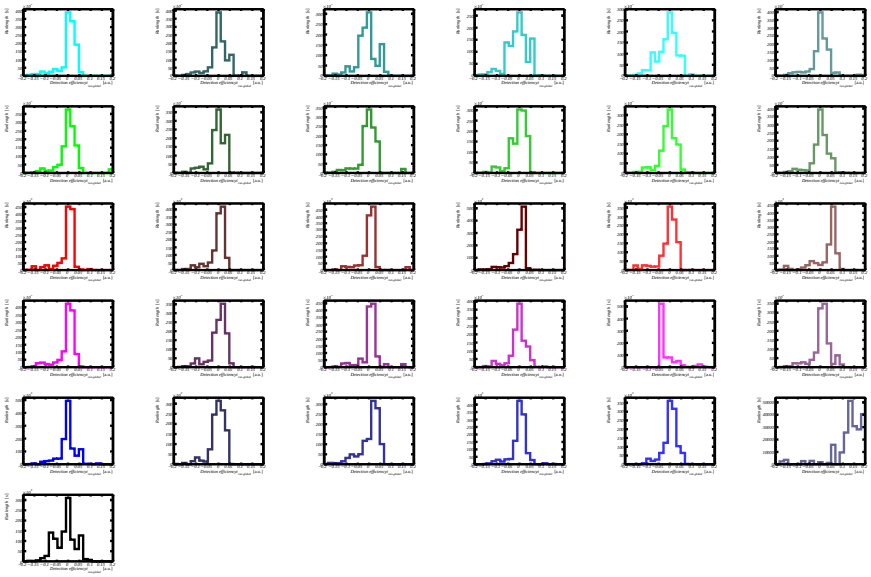

Figure 71: Fitted PMT relative detection efficiency distribution of each run with respect to the globally fitted PMT relative detection efficiency. Each row of plots gives the PMTs of one ring (upper row=ring F, lower ring=ring A) of DOM 809503299. The x-axis ranges from -0.2 to +0.2.

12 Appendix D: PMT time spread distributions

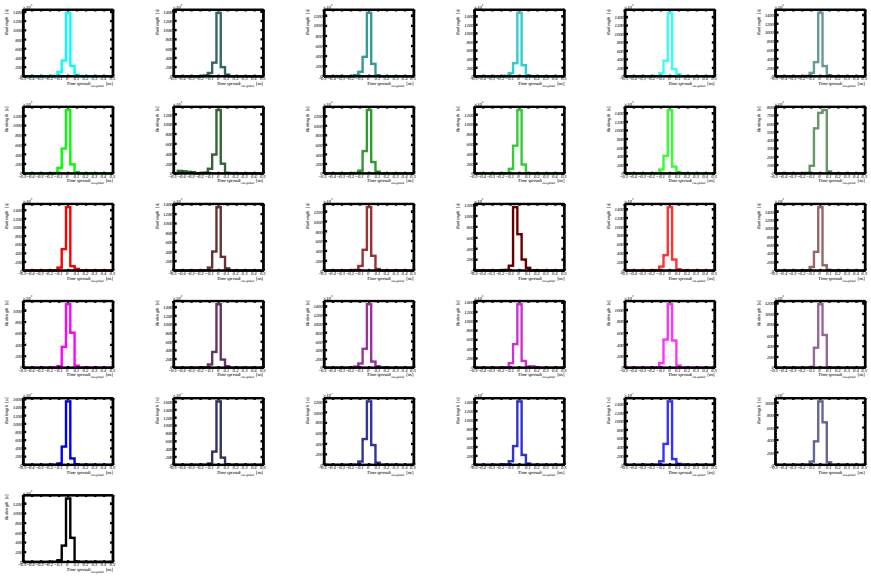

Figure 72: Fitted PMT time spread distribution of each run with respect to the globally fitted PMT time spread. Each row of plots gives the PMTs of one ring (upper row=ring F, lower ring=ring A) of DOM 808430036. The x-axis ranges from -0.5 to +0.5 ns.

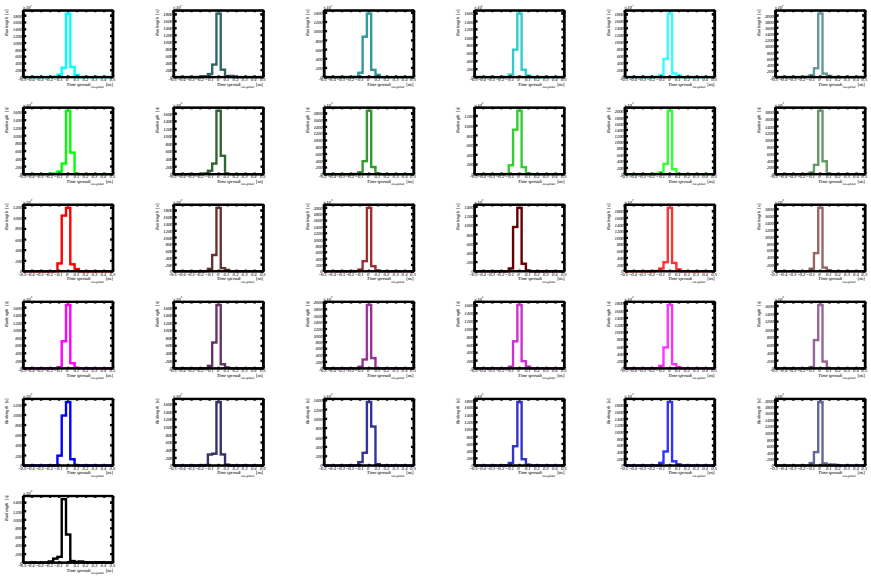

Figure 73: Fitted PMT time spread distribution of each run with respect to the globally fitted PMT time spread. Each row of plots gives the PMTs of one ring (upper row=ring F, lower ring=ring A) of DOM 808430449. The x-axis ranges from -0.5 to +0.5 ns.

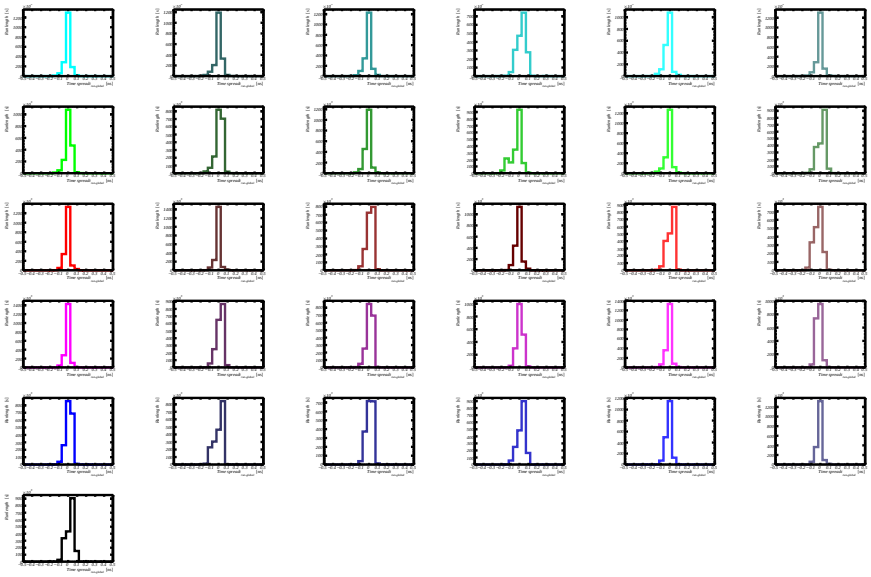

Figure 74: Fitted PMT time spread distribution of each run with respect to the globally fitted PMT time spread. Each row of plots gives the PMTs of one ring (upper row=ring F, lower ring=ring A) of DOM 808430571. The x-axis ranges from -0.5 to +0.5 ns.

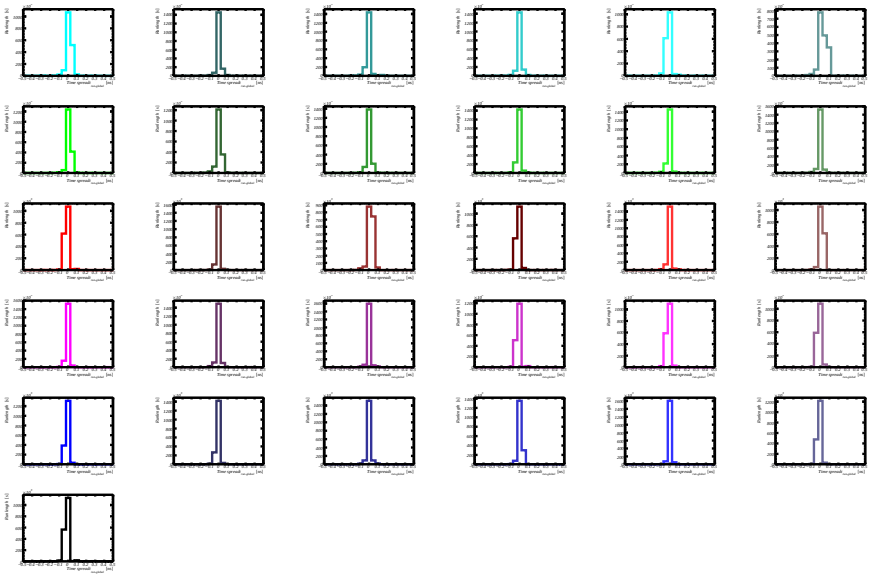

Figure 75: Fitted PMT time spread distribution of each run with respect to the globally fitted PMT time spread. Each row of plots gives the PMTs of one ring (upper row=ring F, lower ring=ring A) of DOM 808447091. The x-axis ranges from -0.5 to +0.5 ns.

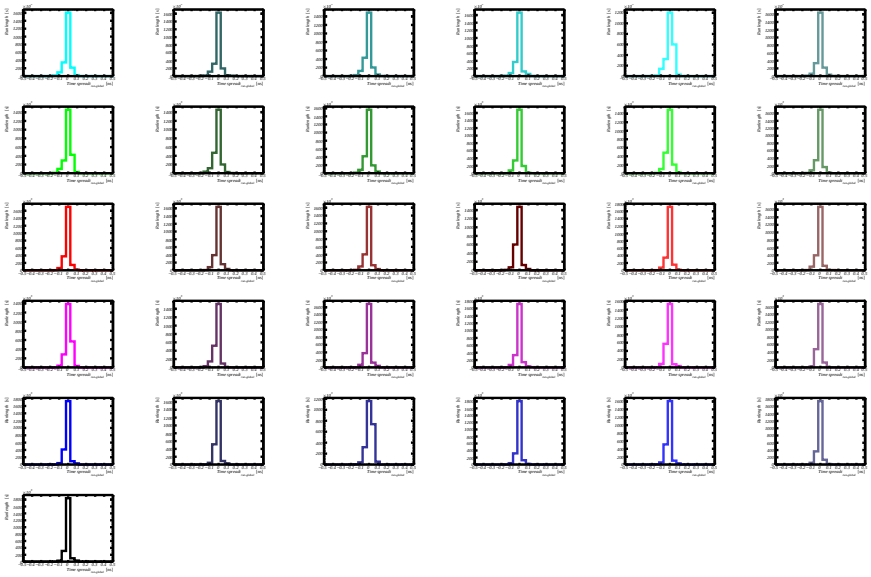

Figure 76: Fitted PMT time spread distribution of each run with respect to the globally fitted PMT time spread. Each row of plots gives the PMTs of one ring (upper row=ring F, lower ring=ring A) of DOM 808467569. The x-axis ranges from -0.5 to +0.5 ns.

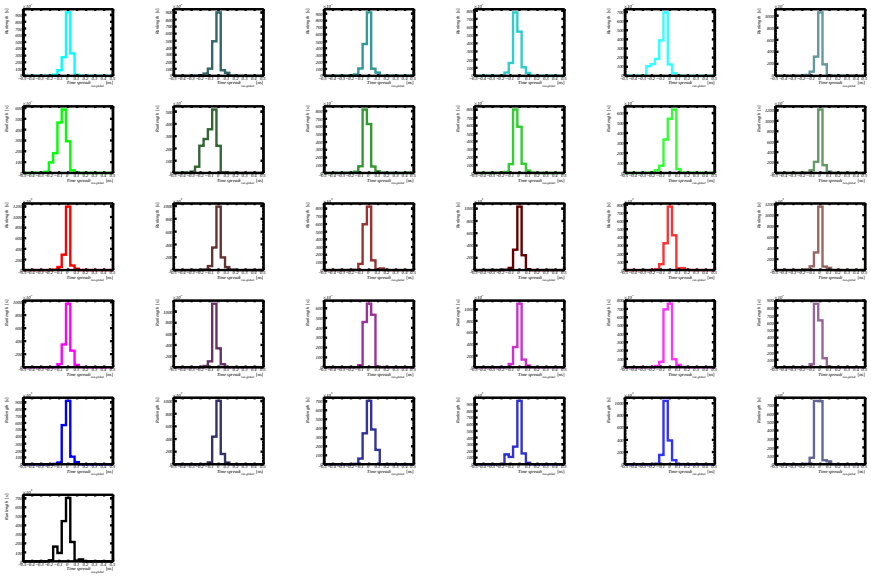

Figure 77: Fitted PMT time spread distribution of each run with respect to the globally fitted PMT time spread. Each row of plots gives the PMTs of one ring (upper row=ring F, lower ring=ring A) of DOM 808468365. The x-axis ranges from -0.5 to +0.5 ns.

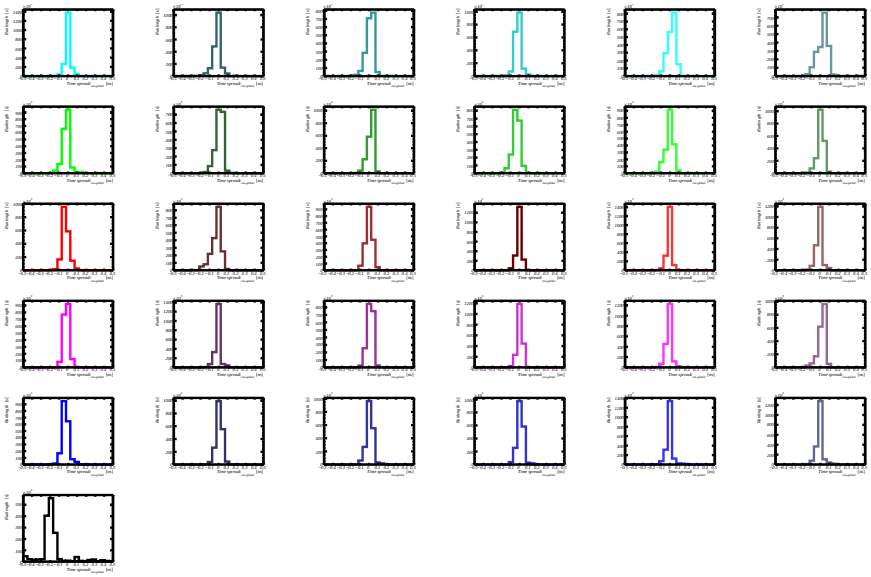

Figure 78: Fitted PMT time spread distribution of each run with respect to the globally fitted PMT time spread. Each row of plots gives the PMTs of one ring (upper row=ring F, lower ring=ring A) of DOM 808474231. The x-axis ranges from -0.5 to +0.5 ns.

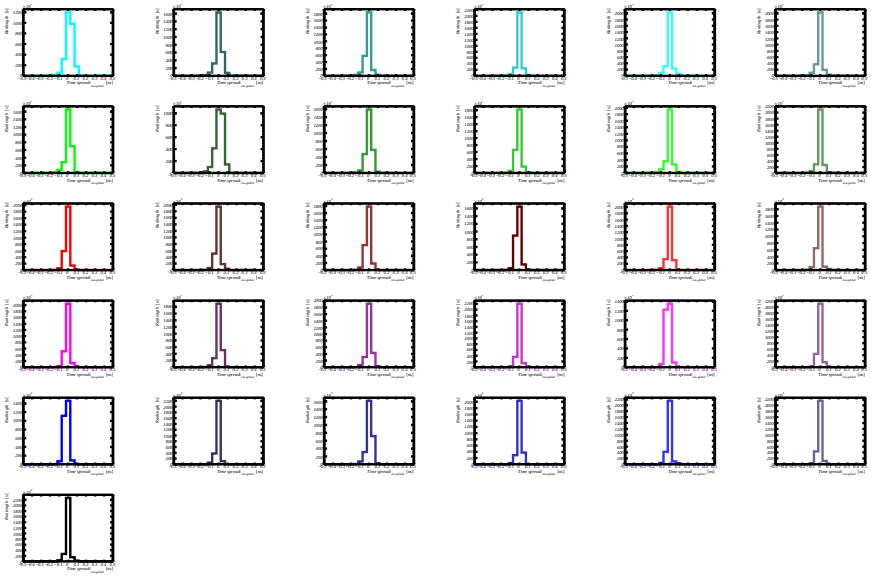

Figure 79: Fitted PMT time spread distribution of each run with respect to the globally fitted PMT time spread. Each row of plots gives the PMTs of one ring (upper row=ring F, lower ring=ring A) of DOM 808965918. The x-axis ranges from -0.5 to +0.5 ns.

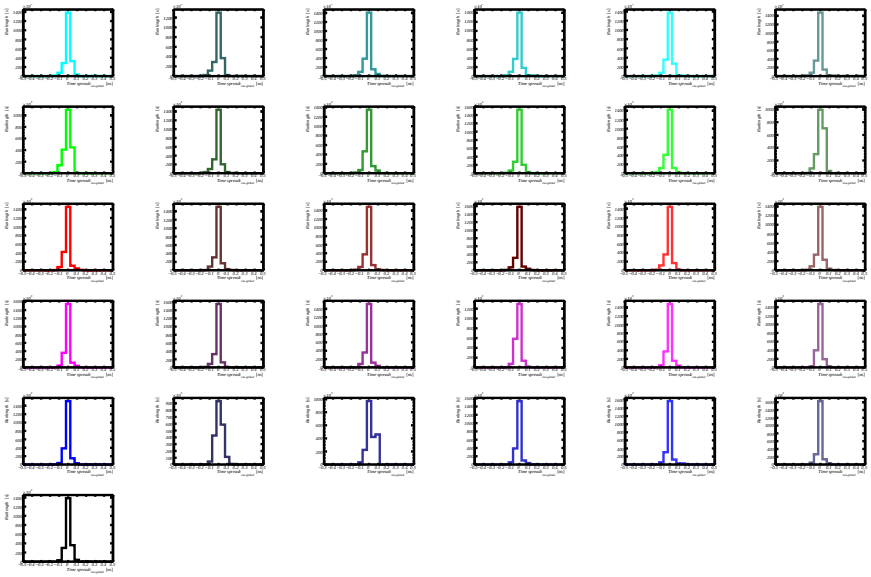

Figure 80: Fitted PMT time spread distribution of each run with respect to the globally fitted PMT time spread. Each row of plots gives the PMTs of one ring (upper row=ring F, lower ring=ring A) of DOM 808966287. The x-axis ranges from -0.5 to +0.5 ns.

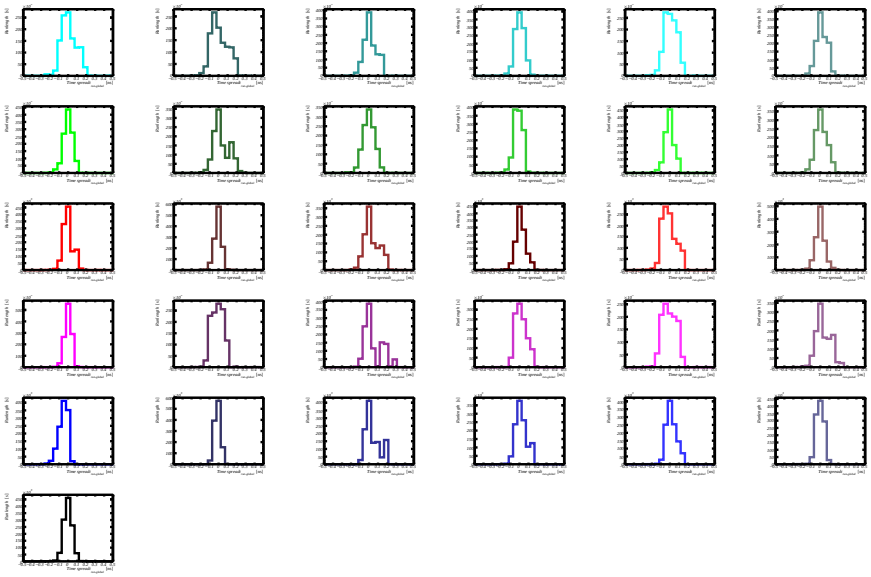

Figure 81: Fitted PMT time spread distribution of each run with respect to the globally fitted PMT time spread. Each row of plots gives the PMTs of one ring (upper row=ring F, lower ring=ring A) of DOM 808972586. The x-axis ranges from -0.5 to +0.5 ns.

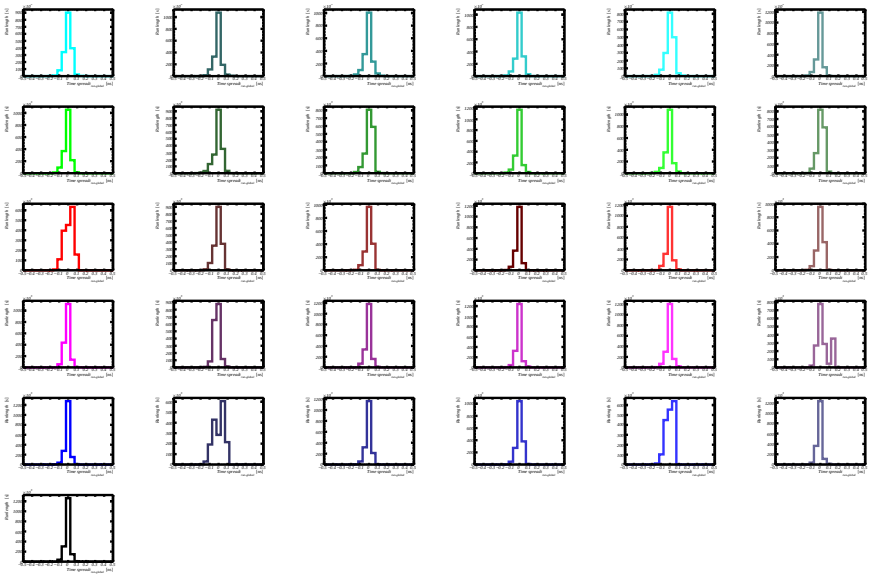

Figure 82: Fitted PMT time spread distribution of each run with respect to the globally fitted PMT time spread. Each row of plots gives the PMTs of one ring (upper row=ring F, lower ring=ring A) of DOM 808974928. The x-axis ranges from -0.5 to +0.5 ns.

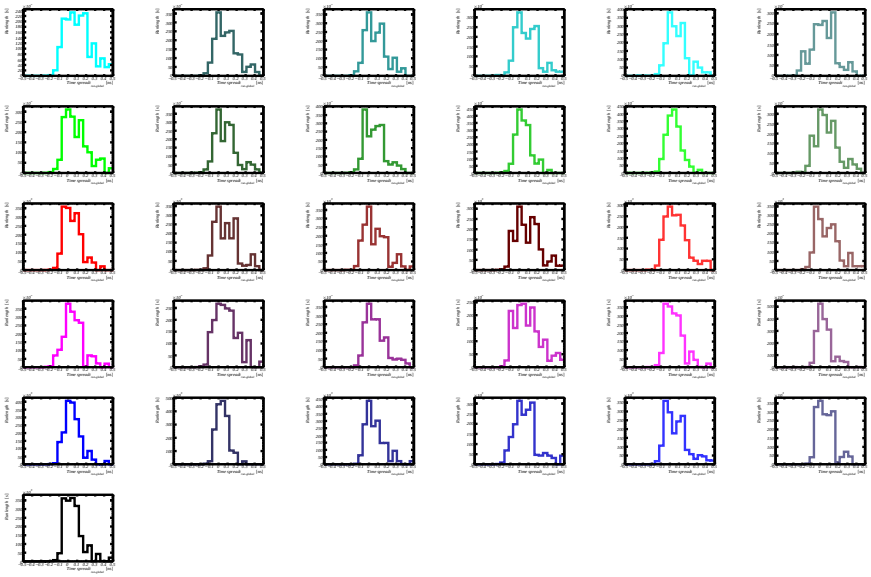

Figure 83: Fitted PMT time spread distribution of each run with respect to the globally fitted PMT time spread. Each row of plots gives the PMTs of one ring (upper row=ring F, lower ring=ring A) of DOM 808982574. The x-axis ranges from -0.5 to +0.5 ns.

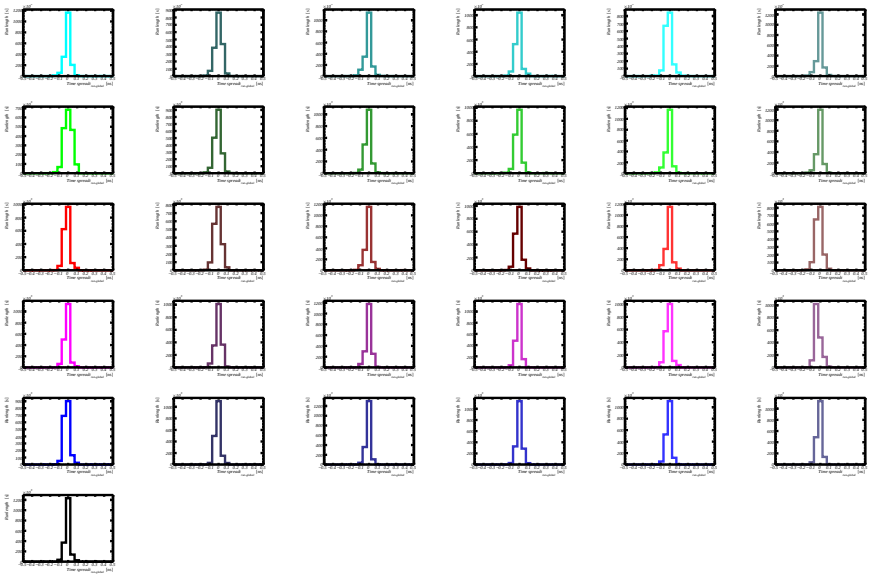

Figure 84: Fitted PMT time spread distribution of each run with respect to the globally fitted PMT time spread. Each row of plots gives the PMTs of one ring (upper row=ring F, lower ring=ring A) of DOM 808987051. The x-axis ranges from -0.5 to +0.5 ns.

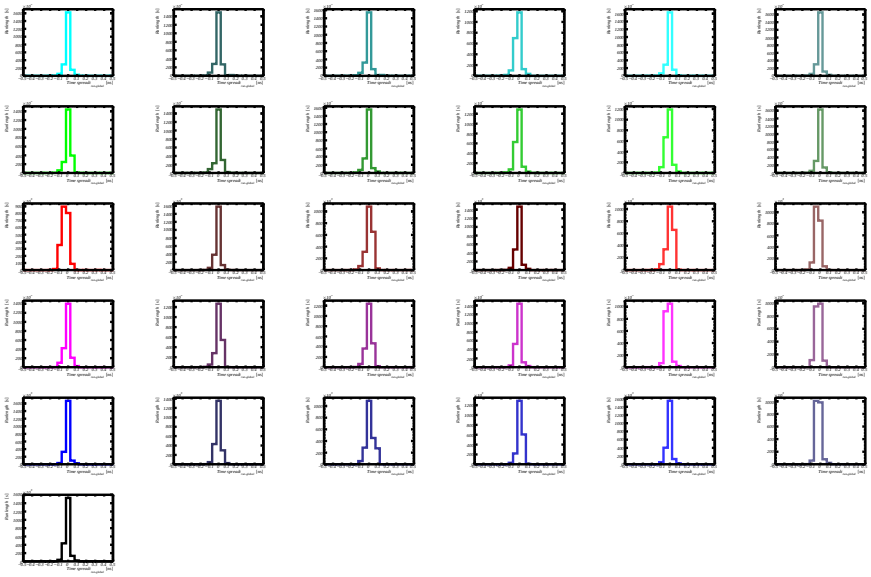

Figure 85: Fitted PMT time spread distribution of each run with respect to the globally fitted PMT time spread. Each row of plots gives the PMTs of one ring (upper row=ring F, lower ring=ring A) of DOM 808987121. The x-axis ranges from -0.5 to +0.5 ns.

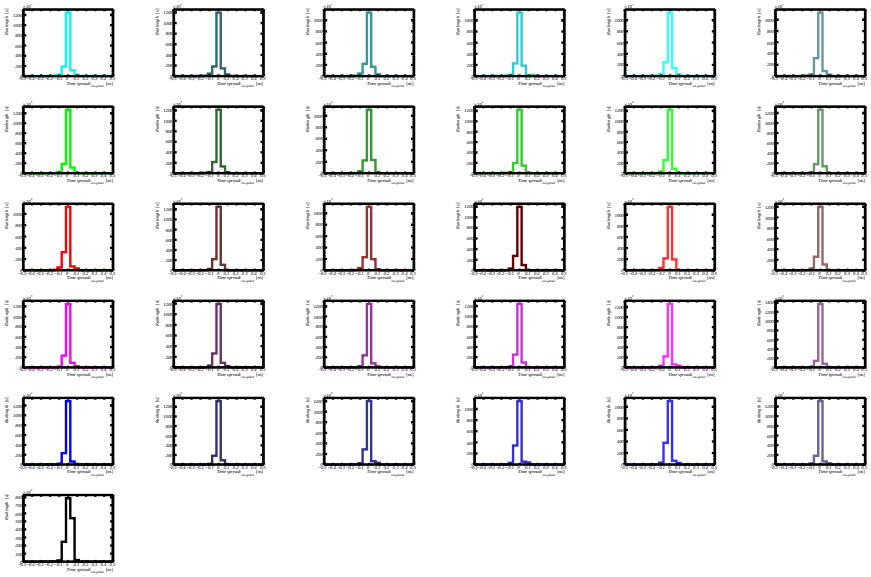

Figure 86: Fitted PMT time spread distribution of each run with respect to the globally fitted PMT time spread. Each row of plots gives the PMTs of one ring (upper row=ring F, lower ring=ring A) of DOM 808992603. The x-axis ranges from -0.5 to +0.5 ns.

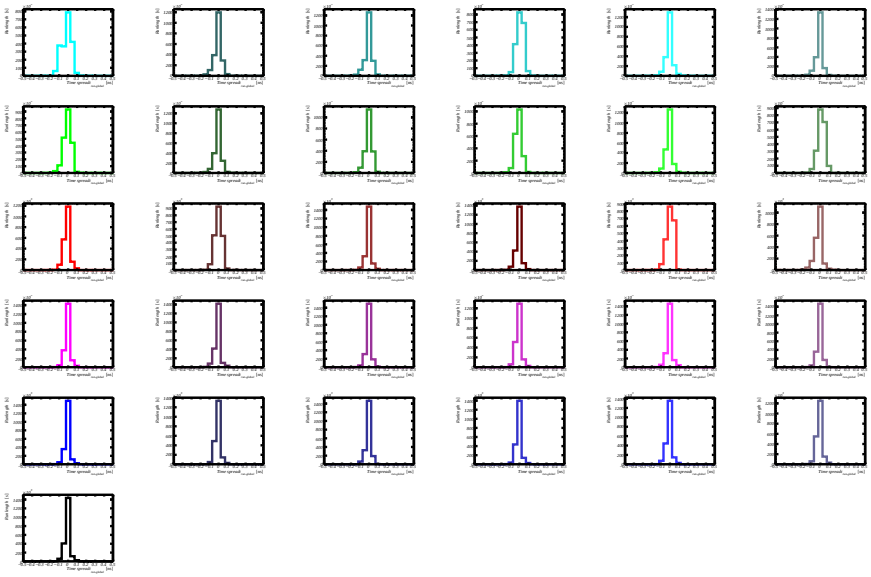

Figure 87: Fitted PMT time spread distribution of each run with respect to the globally fitted PMT time spread. Each row of plots gives the PMTs of one ring (upper row=ring F, lower ring=ring A) of DOM 808995481. The x-axis ranges from -0.5 to +0.5 ns.

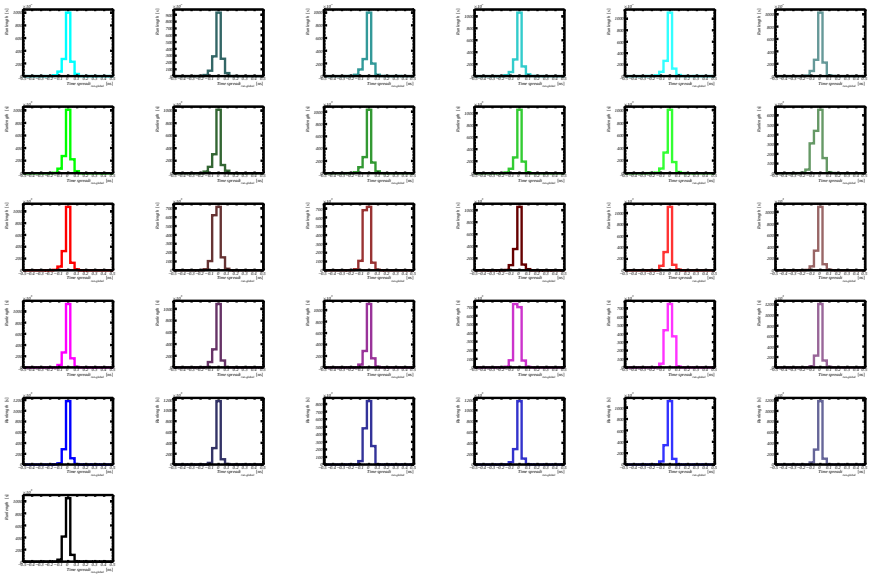

Figure 88: Fitted PMT time spread distribution of each run with respect to the globally fitted PMT time spread. Each row of plots gives the PMTs of one ring (upper row=ring F, lower ring=ring A) of DOM 808996420. The x-axis ranges from -0.5 to +0.5 ns.

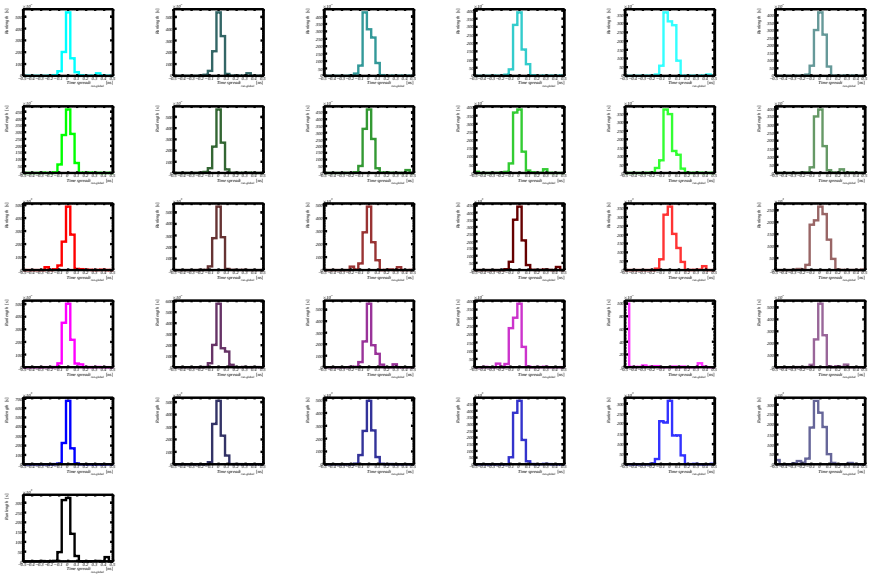

Figure 89: Fitted PMT time spread distribution of each run with respect to the globally fitted PMT time spread. Each row of plots gives the PMTs of one ring (upper row=ring F, lower ring=ring A) of DOM 809503299. The x-axis ranges from -0.5 to +0.5 ns.

13 Appendix B: Inter-PMT calibration values

PMT #	Time offset [ns]	Det. eff. [a.u.]	Time spread [ns]
F1	-0.435622	1.31083	2.43083
F2	4.0227	1.26624	2.27742
F3	3.4248	1.09679	2.17536
F4	0.55245	1.22215	2.20434
F5	0.627092	1.27048	2.53469
F6	0.456041	1.21239	2.24629
E1	0.61484	1.1348	2.53056
E2	0.164525	1.07283	2.41506
E3	0.7574	1.18011	2.30817
E4	-1.77427	1.12335	2.56116
E5	0.618862	1.09053	2.42839
E6	-0.841378	1.13291	2.51411
D1	-1.57548	1.16155	2.45094
D2	-0.329611	1.15086	2.41551
D3	-0.879294	1.05682	2.2917
D4	1.346	1.20377	2.35639
D5	3.16472	1.03029	2.04697
D6	0.742444	1.05621	2.32959
C1	-1.46173	1.20184	2.48458
C2	-0.379672	1.05325	2.41938
C3	-1.42416	1.12251	2.70478
C4	-2.10884	1.11268	2.8796
C5	0.544367	1.08029	2.56091
C6	-0.986132	1.21307	2.08348
B1	0.891906	1.04701	2.1414
B2	0.862679	1.10981	2.32392
B3	-1.36276	1.05139	2.51848
B4	-3.50288	1.02304	2.83145
B5	-1.11574	1.05925	2.59359
B6	0.741926	1.04656	2.35569
A1	-1.35518	1.07451	2.26591

Table 3: Calibrated PMT quantities of DOM 808430036.

PMT #	Time offset [ns]	Det. eff. [a.u.]	Time spread [ns]
F1	0.773175	1.33167	2.58741
F2	3.56587	1.20329	2.4995
F3	3.51289	1.229	2.43881
F4	2.67124	1.28949	2.37638
F5	-0.477587	1.28984	2.584
F6	0.570235	1.22689	2.40589
E1	-0.921342	1.13655	2.47874
E2	-1.26919	0.959543	2.62487
E3	2.65605	1.14521	2.2751
E4	0.187716	1.11836	2.51739
E5	-0.798927	1.08961	2.63616
E6	0.369785	1.18714	2.21542
D1	-0.659884	1.1748	2.58347
D2	-1.30105	1.13361	2.48472
D3	1.03702	1.10845	2.17987
D4	-0.432526	1.19212	2.34429
D5	0.0208545	1.12382	2.38764
D6	-0.393881	1.08182	2.18832
C1	-1.49368	1.21502	2.50595
C2	-1.92917	1.07138	2.57684
C3	-0.915517	1.18187	2.33311
C4	1.74745	1.1624	2.28608
C5	-0.522197	1.06986	2.45025
C6	-1.63496	1.24994	2.3807
B1	0.740733	1.05471	2.42121
B2	-3.33838	0.959761	2.84015
B3	-1.71258	1.02674	2.53391
B4	-1.06205	1.10315	2.50464
B5	0.982764	1.03695	2.38995
B6	-1.03066	1.04254	2.48213
A1	1.05778	0.66894	2.28461

Table 4: Calibrated PMT quantities of DOM 808430449.

PMT #	Time offset [ns]	Det. eff. [a.u.]	Time spread [ns]
F1	0.881196	1.29918	2.38689
F2	-0.338528	1.18795	2.37998
F3	0.969464	1.16654	2.34
F4	1.08986	1.29076	2.3987
F5	-0.0453767	1.21312	2.59957
F6	-2.59268	1.22132	2.53332
E1	0.298193	1.15632	2.40512
E2	-0.73704	1.03882	2.39887
E3	0.85871	1.21441	2.34819
E4	1.77682	1.20474	2.48996
E5	1.9552	1.00201	2.52055
E6	0.901585	1.20035	2.25911
D1	3.15109	1.17824	2.29172
D2	-0.751701	1.14701	2.45846
D3	-0.464296	1.06618	2.2352
D4	0.288148	1.01824	2.26884
D5	0.825409	1.12023	2.34842
D6	-0.170587	1.03362	2.34358
C1	2.00519	1.11976	2.12641
C2	0.274928	1.10092	2.36692
C3	-0.363821	1.19934	2.33793
C4	1.15837	1.22629	2.33098
C5	-1.51138	1.03627	2.25097
C6	-4.62469	1.18776	2.40714
B1	-2.20804	1.05752	2.55038
B2	-1.81253	1.06439	2.60708
B3	0.695954	1.04487	2.46227
B4	0.707106	1.07932	2.10018
B5	1.07299	0.900534	2.20436
B6	-1.50041	1.07931	2.62992
A1	-1.78914	1.08363	2.51247

Table 5: Calibrated PMT quantities of DOM 808430571.

PMT #	Time offset [ns]	Det. eff. [a.u.]	Time spread [ns]
F1	0.418222	1.37022	2.67711
F2	1.7627	1.2895	2.27412
F3	0.989708	1.19092	2.61362
F4	2.34418	1.35769	2.56781
F5	-1.34515	1.30718	2.47073
F6	-2.35579	1.15846	2.64582
E1	1.71008	1.17013	2.13444
E2	0.9563	1.0091	2.37158
E3	2.81813	1.2116	2.30596
E4	1.03763	1.22837	2.41463
E5	-0.960554	1.06389	2.6387
E6	0.0811976	1.1972	2.6013
D1	-1.02532	1.22482	2.5401
D2	-0.0699217	1.10397	2.28375
D3	0.446668	1.1006	2.09072
D4	-0.200754	1.17297	2.26048
D5	-1.45458	1.1454	2.54236
D6	2.72648	1.10771	2.09854
C1	0.180621	1.19072	2.20736
C2	-2.44472	1.00435	2.53354
C3	1.69283	1.25994	2.44973
C4	-0.664234	1.24505	2.47225
C5	-2.47804	1.00042	2.2381
C6	-1.49805	1.22977	2.08587
B1	0.279513	1.10014	2.19678
B2	-0.548474	1.08135	2.3075
B3	-1.36597	1.07887	2.5857
B4	1.36793	1.07753	2.20072
B5	1.80263	0.984153	2.09749
B6	-0.911333	1.11973	2.33544
A1	-3.29192	1.00674	2.4625

Table 6: Calibrated PMT quantities of DOM 808447091.

PMT #	Time offset [ns]	Det. eff. [a.u.]	Time spread [ns]
F1	-1.66832	1.29381	2.74937
F2	-0.0276811	1.20293	2.50246
F3	-1.22972	1.13853	2.47753
F4	0.181874	1.26349	2.52161
F5	1.44395	1.26165	2.54995
F6	0.64855	1.32441	2.54482
E1	-0.0538341	1.18843	2.46285
E2	-0.304135	0.986368	2.40968
E3	0.93206	1.17106	2.36716
E4	1.26806	1.18357	2.40232
E5	2.07496	1.09009	2.23034
E6	-2.54305	1.19608	2.54841
D1	-0.758242	1.17788	2.1731
D2	-1.52109	1.16189	2.64181
D3	-1.44335	1.06139	2.40535
D4	-0.664703	1.15733	2.30401
D5	-0.768205	1.11187	2.24916
D6	-0.89815	1.07139	2.35694
C1	1.66514	1.19898	2.38578
C2	1.24759	1.02413	2.23229
C3	0.965666	1.1305	2.34378
C4	1.48563	1.15438	2.34182
C5	-0.57592	1.04708	2.58037
C6	-0.123116	1.22141	2.28117
B1	-1.14061	1.07396	2.40423
B2	0.83514	1.08782	2.407
B3	1.07236	1.04026	2.17607
B4	1.81284	1.08061	2.2737
B5	0.487951	0.98549	2.23712
B6	-1.23226	1.05779	2.43111
A1	-1.16937	1.05909	2.22157

Table 7: Calibrated PMT quantities of DOM 808467569.

PMT #	Time offset [ns]	Det. eff. [a.u.]	Time spread [ns]
F1	0.733835	1.1006	2.46569
F2	1.84189	1.02247	2.41443
F3	1.61943	1.25532	2.2175
F4	1.71955	1.27348	2.52905
F5	0.883627	1.262	2.57963
F6	-0.544304	1.24072	2.6191
E1	-2.11506	1.12375	2.89245
E2	0.219066	0.747708	2.67937
E3	0.711234	1.16817	2.42821
E4	0.914609	1.19008	2.53371
E5	-2.10729	0.884236	2.82596
E6	0.839081	1.188	2.34483
D1	0.954279	1.11704	2.24332
D2	0.532169	1.07453	2.46241
D3	-1.48088	1.16121	2.42099
D4	-0.809567	1.17465	2.23412
D5	0.582442	1.08072	2.37706
D6	-0.209861	1.14679	2.45116
C1	0.402461	1.18603	2.44944
C2	1.04497	1.08603	2.31126
C3	-1.09737	1.23459	2.4547
C4	-1.74558	1.20325	2.55614
C5	-1.20748	1.06173	2.76635
C6	-1.72936	1.25392	2.32317
B1	-0.371697	1.08308	2.42726
B2	-1.56112	1.09378	2.2978
B3	-1.82949	1.06602	2.50155
B4	-0.436396	0.989062	2.38508
B5	2.55435	1.02511	2.22887
B6	-0.250165	1.05821	2.45243
A1	1.94263	1.02164	2.23246

Table 8: Calibrated PMT quantities of DOM 808468365.

PMT #	Time offset [ns]	Det. eff. [a.u.]	Time spread [ns]
F1	0.8579	1.31158	2.27375
F2	1.79023	1.13587	2.38539
F3	0.577292	1.16728	2.44749
F4	1.88148	1.28628	2.22619
F5	0.000430455	1.12825	2.43982
F6	-0.498083	1.23608	2.6777
E1	1.14609	0.907374	2.3961
E2	0.82641	0.954016	2.10121
E3	1.66194	1.17933	2.10264
E4	-1.75046	0.937392	2.7592
E5	-1.30979	1.00453	2.54079
E6	-1.08664	1.08793	2.47406
D1	-0.314623	1.1113	2.58449
D2	-3.14457	1.02064	2.66429
D3	-0.793554	1.06904	2.33557
D4	1.00197	1.13307	2.13315
D5	-1.34265	1.04995	2.35595
D6	0.591947	1.11491	2.38813
C1	-0.33232	1.21776	2.58604
C2	-1.08982	1.03041	2.69707
C3	1.11143	1.14154	2.16177
C4	-0.637639	1.10318	2.23985
C5	-0.686012	1.05421	2.37075
C6	0.578176	1.23549	2.45303
B1	0.131199	1.04543	2.49059
B2	0.460388	1.05363	2.3939
B3	-0.523578	1.09384	2.40902
B4	0.506728	1.09514	2.38961
B5	-0.91113	0.97233	2.32615
B6	0.923298	1.07861	2.56682
A1	0.373962	0.168455	2.64987

Table 9: Calibrated PMT quantities of DOM 808474231.

PMT #	Time offset [ns]	Det. eff. [a.u.]	Time spread [ns]
F1	1.3063	1.26426	2.2655
F2	1.09456	1.15046	2.34922
F3	0.00090331	1.12716	2.47055
F4	1.88392	1.31052	2.45834
F5	1.80183	1.25953	2.54888
F6	-0.0938183	1.27911	2.76769
E1	-0.430176	1.15036	2.44221
E2	1.69901	0.974838	2.35682
E3	3.39092	1.09085	2.15364
E4	-1.1572	1.17169	2.5817
E5	-0.663527	1.06802	2.68669
E6	0.605985	1.12702	2.35017
D1	0.063737	1.1564	2.19259
D2	0.195776	1.06627	2.14505
D3	0.0646421	1.05382	2.3347
D4	2.20863	1.1235	1.97993
D5	0.429028	1.08996	2.25951
D6	0.691437	1.07995	2.31087
C1	-1.70504	1.21778	2.40627
C2	0.228101	1.04573	2.30062
C3	-1.95142	1.16203	2.57356
C4	2.31879	1.19722	2.22308
C5	-1.996	1.03656	2.41634
C6	-1.02005	1.25834	2.22606
B1	-2.67236	1.01421	2.64501
B2	-3.09446	1.06785	2.64508
B3	-1.18336	0.926203	2.35612
B4	-1.05822	1.05809	2.36116
B5	0.503861	1.06592	2.11185
B6	-0.786836	1.03864	2.42047
A1	-0.674952	1.05253	2.38644

Table 10: Calibrated PMT quantities of DOM 808965918.

PMT #	Time offset [ns]	Det. eff. [a.u.]	Time spread [ns]
F1	0.441512	1.2867	2.53557
F2	-1.05814	1.20451	2.5839
F3	0.77084	1.2081	2.43608
F4	2.41605	1.25985	2.38576
F5	0.33084	1.22774	2.54592
F6	-0.832999	1.24774	2.49451
E1	2.37547	1.11077	2.4479
E2	0.241022	1.02755	2.34637
E3	3.22137	1.11621	2.35238
E4	3.53589	1.12525	2.33319
E5	-2.17516	1.00588	2.57899
E6	0.964747	1.17809	2.37787
D1	-0.0696585	1.13821	2.38316
D2	1.81752	1.13593	2.39631
D3	-1.51482	1.06016	2.37424
D4	0.202058	1.18493	2.324
D5	-2.985	1.08761	2.73097
D6	1.02887	1.08918	2.41407
C1	0.146856	1.22298	2.4117
C2	-1.01409	0.981549	2.71784
C3	-2.95956	1.18445	2.73978
C4	-1.75832	1.17386	2.42482
C5	1.19707	1.11649	2.28542
C6	-2.68116	1.21712	2.4206
B1	-0.482218	1.06739	2.42857
B2	-2.96818	1.10718	2.75903
B3	2.02988	1.07614	2.20638
B4	-1.06533	1.07722	2.57285
B5	-0.0586403	1.04312	2.36359
B6	0.322548	1.05726	2.2856
A1	0.580717	1.08486	2.30751

Table 11: Calibrated PMT quantities of DOM 808966287.

PMT #	Time offset [ns]	Det. eff. [a.u.]	Time spread [ns]
F1	-0.884936	1.04048	2.71688
F2	1.43409	1.01434	2.44057
F3	-0.448449	1.21357	2.59467
F4	-0.125288	1.35196	2.46398
F5	0.267789	1.02724	2.36739
F6	0.10931	1.23424	2.446
E1	1.69475	0.869188	2.20906
E2	0.848813	1.01702	2.29118
E3	0.468293	0.879964	2.64034
E4	-0.784432	0.933436	2.90447
E5	1.44982	0.993194	2.44823
E6	0.81607	0.992635	2.51306
D1	-0.3602	1.15863	2.60921
D2	2.86085	1.10887	2.28494
D3	0.281739	1.0477	2.18001
D4	-0.220037	1.1335	2.33645
D5	1.52174	0.991653	2.58508
D6	2.45778	1.07089	2.13091
C1	2.48233	1.16703	2.29482
C2	-1.79966	1.05015	2.46538
C3	-1.50331	1.12871	2.37403
C4	0.826619	1.22143	2.36798
C5	-0.660272	1.044	2.41344
C6	-3.0301	1.16371	2.32201
B1	-3.07234	1.02064	2.7861
B2	-0.567337	1.00816	2.47114
B3	0.685912	1.02671	2.22587
B4	-0.169659	1.07322	2.33075
B5	-1.79897	0.99299	2.36507
B6	-2.16683	1.0472	2.56987
A1	-0.614086	0.90441	2.24565

Table 12: Calibrated PMT quantities of DOM 808972586.

PMT #	Time offset [ns]	Det. eff. [a.u.]	Time spread [ns]
F1	1.63492	1.29424	2.57778
F2	2.20326	1.25866	2.45515
F3	0.148446	1.19644	2.62063
F4	1.53639	1.23769	2.39981
F5	-0.367809	1.25788	2.59994
F6	-1.19764	1.20034	2.69743
E1	-1.60623	1.10564	2.84728
E2	2.95877	1.00598	2.38491
E3	0.105995	1.25433	2.64992
E4	-1.02725	1.19252	2.65675
E5	-0.172763	1.06237	2.57668
E6	1.57423	1.19927	2.3208
D1	1.32585	1.18312	2.31876
D2	-0.506345	1.04916	2.58341
D3	-1.12208	1.02036	2.36526
D4	-1.5245	1.11352	2.42871
D5	-0.0267776	1.11876	2.40209
D6	2.39625	1.05759	2.10054
C1	1.33527	1.19929	2.42511
C2	1.45972	1.09428	2.58848
C3	-0.657221	1.18877	2.65381
C4	0.223765	1.09417	2.46895
C5	0.942405	1.05908	2.20486
C6	-0.552433	1.17053	2.47001
B1	-0.027085	1.07115	2.39254
B2	-0.837757	1.09746	2.62742
B3	-1.40732	1.03057	2.56975
B4	-0.91212	1.03055	2.38668
B5	-1.59983	1.02469	2.73458
B6	-2.42806	1.05162	2.61121
A1	-1.87204	1.09885	2.45924

Table 13: Calibrated PMT quantities of DOM 808974928.

PMT #	Time offset [ns]	Det. eff. [a.u.]	Time spread [ns]
F1	0.106255	1.11984	2.60955
F2	2.26141	1.20406	2.39816
F3	-0.23259	1.10779	2.36288
F4	0.710051	1.29894	2.70781
F5	2.71327	1.16747	2.38644
F6	-1.85184	0.998935	2.76667
E1	0.884704	1.16355	2.317
E2	1.74474	0.982182	2.08367
E3	0.264785	1.08447	2.72474
E4	2.84087	1.17323	2.33642
E5	1.91841	0.969791	2.1365
E6	-1.80835	1.04033	2.64651
D1	1.49325	1.17278	2.4704
D2	0.10989	1.10078	2.60291
D3	-1.57702	1.05842	2.61164
D4	-0.528554	1.10992	2.53859
D5	3.23367	0.94608	2.1793
D6	-1.12988	1.07202	2.45099
C1	-0.890156	1.17372	2.50523
C2	-0.24274	1.01409	2.43324
C3	0.551941	1.10917	2.39403
C4	-1.71183	1.12148	2.7876
C5	-2.48706	1.02189	2.53452
C6	-2.58799	1.20561	2.43988
B1	0.633192	1.04462	2.38964
B2	2.50954	1.06191	2.2458
B3	-1.54286	1.09274	2.35183
B4	-3.15488	1.06849	2.69879
B5	-1.31859	0.944228	2.58035
B6	0.0239641	1.04543	2.48412
A1	-0.935605	1.01447	2.36467

Table 14: Calibrated PMT quantities of DOM 808982574.

PMT #	Time offset [ns]	Det. eff. [a.u.]	Time spread [ns]
F1	0.981002	1.27154	2.49612
F2	4.02922	1.24509	2.32398
F3	2.14799	1.19841	2.28851
F4	-0.537945	1.32746	2.85579
F5	-1.15167	1.23876	2.64291
F6	-0.00803478	1.32023	2.33759
E1	1.52676	1.09105	2.26632
E2	2.53913	0.962605	2.12093
E3	0.139807	1.22361	2.55363
E4	-0.152712	1.23862	2.46554
E5	-0.707251	0.985295	2.66229
E6	-0.722492	1.20518	2.59383
D1	-1.22464	1.12493	2.62361
D2	-1.46695	1.07987	2.70615
D3	-0.669449	1.09329	2.37482
D4	1.31775	1.17806	1.93298
D5	-0.792908	1.11315	2.64496
D6	-1.81782	1.11432	2.57785
C1	0.1117	1.22926	2.58982
C2	-0.489657	1.09955	2.48862
C3	0.286289	1.16959	2.39111
C4	0.962225	1.15026	2.32622
C5	1.25368	1.08156	2.50976
C6	-1.30784	1.17627	2.09125
B1	-0.992607	1.07766	2.46011
B2	-2.11815	1.10954	2.47283
B3	-1.86467	1.06583	2.44431
B4	-1.32089	1.13817	2.44278
B5	-0.663309	1.02599	2.22556
B6	1.85281	1.06222	2.31107
A1	0.860643	1.0387	2.22654

Table 15: Calibrated PMT quantities of DOM 808987051.

PMT #	Time offset [ns]	Det. eff. [a.u.]	Time spread [ns]
F1	-1.50971	1.31105	2.44797
F2	0.14746	1.22844	2.55729
F3	-1.36098	1.2037	2.39496
F4	1.93301	1.28978	2.42045
F5	-0.0337954	1.25691	2.42386
F6	0.872985	1.22922	2.12534
E1	1.52627	1.07869	2.06814
E2	3.62785	1.05568	2.08006
E3	-0.41652	1.169	2.57366
E4	3.06722	1.17502	2.37234
E5	0.651741	1.01334	2.24643
E6	0.399998	1.16204	2.42225
D1	-0.0389683	1.10389	2.3855
D2	1.38378	1.08583	2.16532
D3	-0.232679	1.09629	2.36303
D4	-1.12644	1.24192	2.2202
D5	-2.29772	1.05255	2.52959
D6	0.926994	1.07594	2.24014
C1	-1.43346	1.21334	2.59741
C2	1.11821	1.08406	2.438
C3	-1.8088	1.16957	2.581
C4	1.42472	1.20474	2.35916
C5	-1.30855	1.10157	2.39165
C6	-1.44321	1.28555	2.46063
B1	1.57698	1.06642	2.1063
B2	-4.37934	1.05692	2.63067
B3	-0.926759	1.06579	2.5871
B4	2.23681	1.10913	1.94794
B5	-0.326133	1.03351	2.34233
B6	-0.746774	1.08175	2.55845
A1	-1.50419	1.10952	2.65377

Table 16: Calibrated PMT quantities of DOM 808987121.

PMT #	Time offset [ns]	Det. eff. [a.u.]	Time spread [ns]
F1	-0.982421	1.28465	2.71485
F2	1.03271	1.16324	2.41154
F3	2.01585	1.18261	2.3787
F4	-0.0269351	1.25748	2.64391
F5	-1.33582	1.31954	2.68887
F6	-0.794196	1.26865	2.60171
E1	1.19718	1.14375	2.25862
E2	2.94213	1.01671	2.15411
E3	-0.588027	1.0987	2.44339
E4	1.99698	1.20195	2.50423
E5	-1.82849	1.0354	2.72267
E6	-0.342703	1.1753	2.36374
D1	-1.83594	1.12416	2.81811
D2	2.08824	1.07421	2.46925
D3	0.143255	1.07396	2.3976
D4	-0.188208	1.14958	2.38054
D5	1.79347	1.05456	2.16951
D6	0.237329	1.09363	2.17679
C1	1.28199	1.19298	2.233
C2	-0.236029	1.08245	2.44197
C3	1.40336	1.19959	2.46209
C4	0.92881	1.18724	2.24691
C5	-1.28413	1.06326	2.55199
C6	-3.41687	1.29438	2.30485
B1	-3.40561	1.0475	2.66215
B2	2.39965	0.988261	2.07606
B3	-1.18063	1.09173	2.5177
B4	-2.11654	1.09278	2.74364
B5	-0.0912861	1.01393	2.53805
B6	0.0247612	0.996492	2.49139
A1	0.16812	1.04294	2.12346

Table 17: Calibrated PMT quantities of DOM 808992603.

PMT #	Time offset [ns]	Det. eff. [a.u.]	Time spread [ns]
F1	0.924093	1.28898	2.41693
F2	1.58906	1.19523	2.4542
F3	0.57154	1.19754	2.58679
F4	0.881679	1.29157	2.45993
F5	0.559946	1.17358	2.48818
F6	-0.643205	1.25799	2.55319
E1	-1.28294	1.1196	2.55927
E2	1.82805	0.957122	2.07203
E3	1.45429	1.1576	2.37263
E4	1.85019	1.17867	2.35643
E5	2.67162	1.00385	2.25251
E6	2.49319	1.19363	2.18567
D1	1.22008	1.18884	2.47825
D2	-2.92324	1.10754	2.62305
D3	-0.269538	1.10883	2.34781
D4	-0.954157	1.14981	2.50106
D5	-1.14173	1.09525	2.54169
D6	0.0954289	1.04873	2.53386
C1	-0.966753	1.19974	2.45433
C2	-1.28337	1.01212	2.62932
C3	2.21266	1.22481	2.08167
C4	0.461594	1.1279	2.35824
C5	-0.636039	1.04432	2.25196
C6	-3.92841	1.21052	2.58207
B1	-2.96018	1.04767	2.6288
B2	-0.67501	1.07071	2.54764
B3	-0.997441	0.970726	2.31186
B4	0.842744	1.10105	2.37003
B5	1.37906	1.01497	2.43564
B6	0.978299	1.06881	2.48515
A1	-3.3515	1.00246	2.66985

Table 18: Calibrated PMT quantities of DOM 808995481.

PMT #	Time offset [ns]	Det. eff. [a.u.]	Time spread [ns]
F1	0.82829	1.33901	2.51283
F2	4.08118	1.19586	2.29421
F3	-0.0162585	1.18741	2.3888
F4	-0.552165	1.31044	2.52342
F5	-1.92374	1.29259	2.7575
F6	0.535535	1.26084	2.50139
E1	-0.0622835	1.19886	2.19918
E2	1.49392	1.007	2.31211
E3	1.63962	1.14145	2.279
E4	1.41575	1.16695	2.41986
E5	-1.11698	1.03643	2.42801
E6	1.40281	1.1991	2.3518
D1	0.636429	1.1511	2.44051
D2	-2.58593	1.11626	2.76779
D3	-0.557696	1.07491	2.30668
D4	-3.07886	1.17221	2.63455
D5	0.199743	1.08179	2.4236
D6	-1.63353	1.04001	2.28286
C1	2.26461	1.19003	2.22614
C2	-0.969517	0.942644	2.45445
C3	-0.2545	1.21448	2.27691
C4	-0.24256	1.15728	2.42598
C5	1.80527	1.07037	2.10888
C6	-0.947922	1.21527	2.42437
B1	0.117201	1.0716	2.30397
B2	-0.324087	1.09187	2.33806
B3	-0.377805	1.03157	2.31255
B4	-1.02663	1.08575	2.35269
B5	-1.14034	1.02743	2.37144
B6	-0.144296	1.05106	2.35833
A1	0.534749	1.05305	2.07961

Table 19: Calibrated PMT quantities of DOM 808996420.

PMT #	Time offset [ns]	Det. eff. [a.u.]	Time spread [ns]
F1	2.22493	1.39037	2.4248
F2	2.34883	1.22606	2.16323
F3	2.77503	1.13727	2.38471
F4	0.301023	1.32633	2.46888
F5	-1.19524	1.23384	2.62662
F6	-0.584835	1.26973	2.53989
E1	1.72595	1.1721	2.47231
E2	0.960547	1.03452	2.08007
E3	-0.00808578	1.14175	2.43742
E4	1.03672	1.17471	2.37189
E5	-2.56509	1.07471	2.63587
E6	0.976553	1.20476	2.19403
D1	-1.09338	1.15675	2.3852
D2	0.425544	1.15496	2.2443
D3	-2.9861	1.10627	2.35461
D4	-0.0845747	1.15756	2.3269
D5	2.88985	1.07497	2.01709
D6	0.370795	1.10014	2.33124
C1	-2.18371	1.21692	2.65474
C2	0.793916	1.10331	2.3661
C3	-0.643943	1.11388	2.40505
C4	-1.8127	1.15548	2.36357
C5	-1.03045	0.0348199	2.67317
C6	1.19385	1.21609	2.11093
B1	-0.0973523	1.01643	2.12839
B2	-1.42921	1.04441	2.29675
B3	-0.271551	1.00197	2.44648
B4	-2.75032	1.03881	2.48592
B5	1.09636	1.00127	2.25695
B6	0.0457657	0.804157	2.30236
A1	-0.429127	1.0034	2.08571

Table 20: Calibrated PMT quantities of DOM 809503299.

14 Appendix C: Inter-DOM L1 hit time difference plots

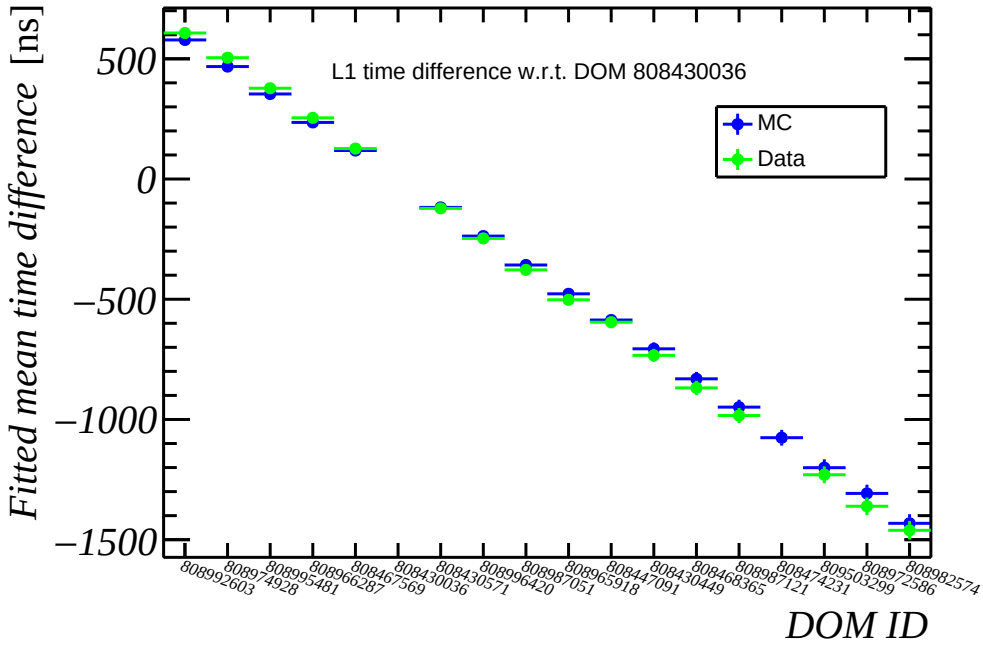

Figure 90: Mean time difference between L1-hits on a DOM i and DOM 808430036.

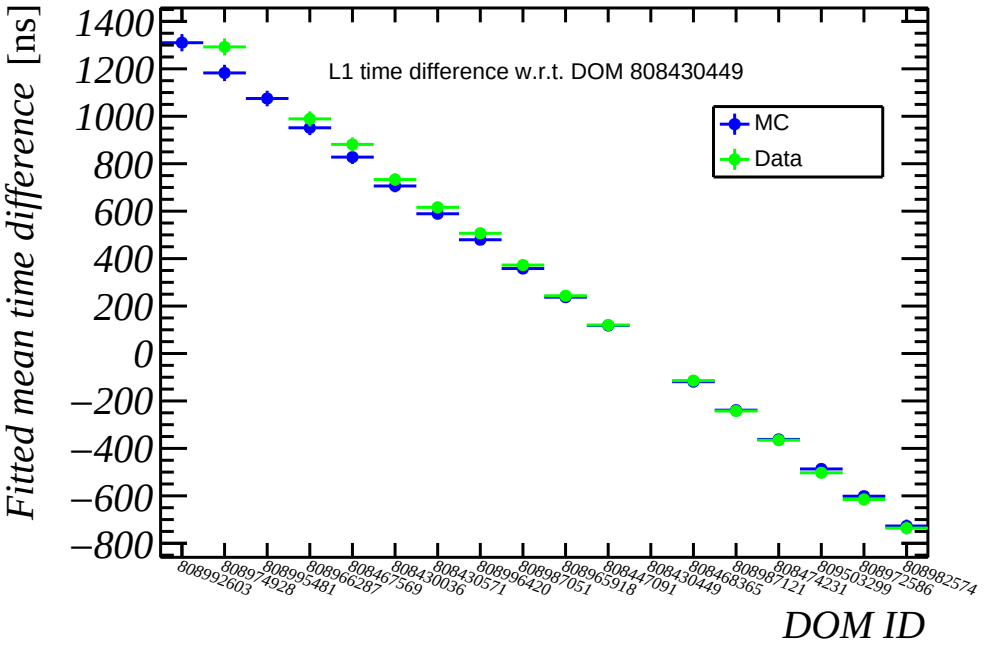

Figure 91: Mean time difference between L1-hits on a DOM i and DOM 808430449.

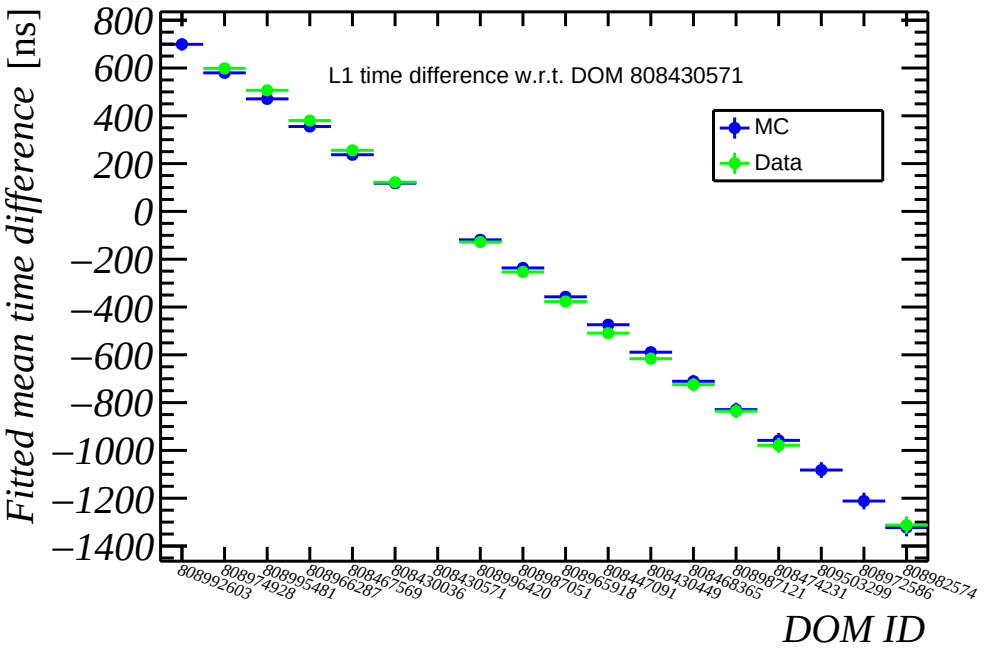

Figure 92: Mean time difference between L1-hits on a DOM i and DOM 808430571.

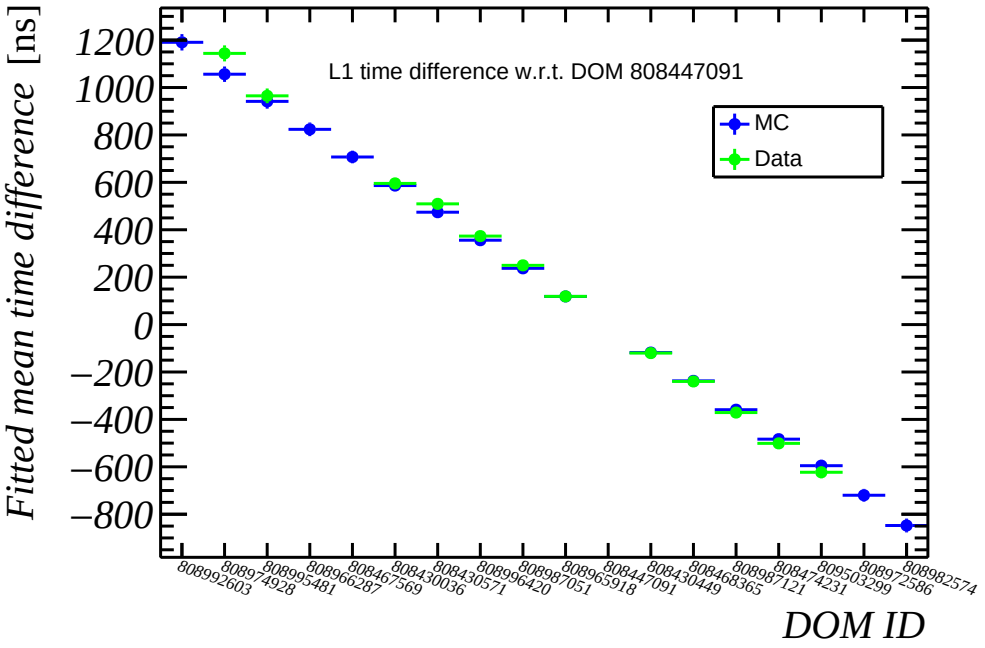

Figure 93: Mean time difference between L1-hits on a DOM i and DOM 808447091.

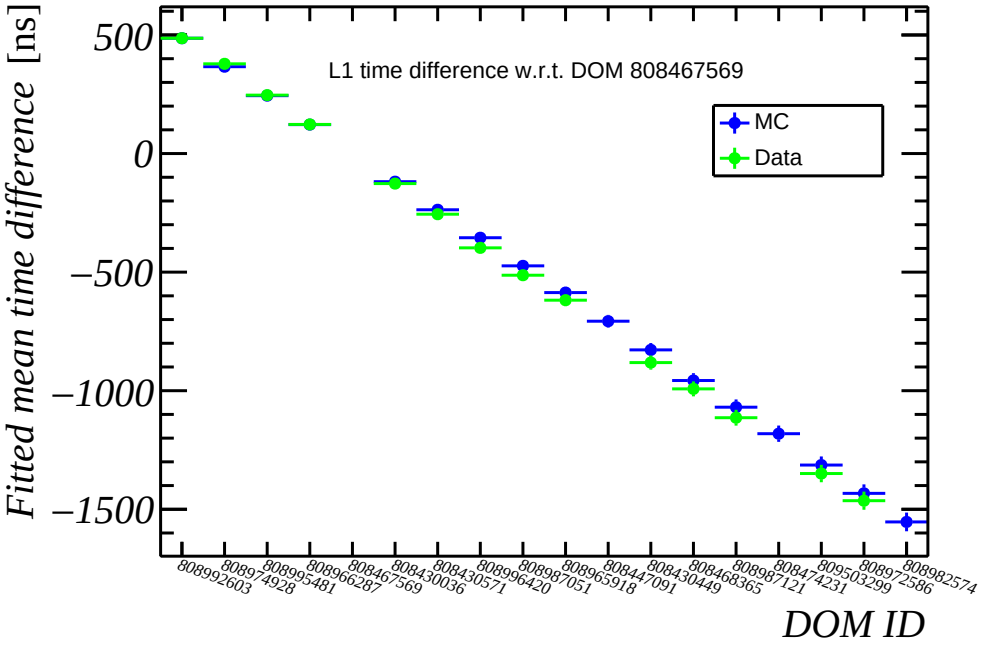

Figure 94: Mean time difference between L1-hits on a DOM i and DOM 808467569.

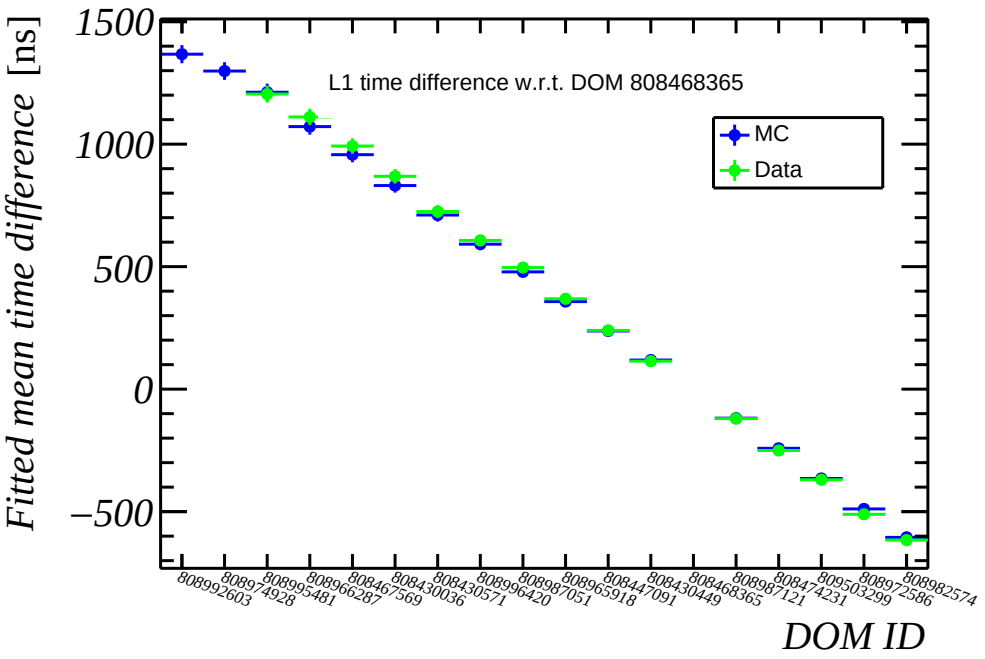

Figure 95: Mean time difference between L1-hits on a DOM i and DOM 808468365.

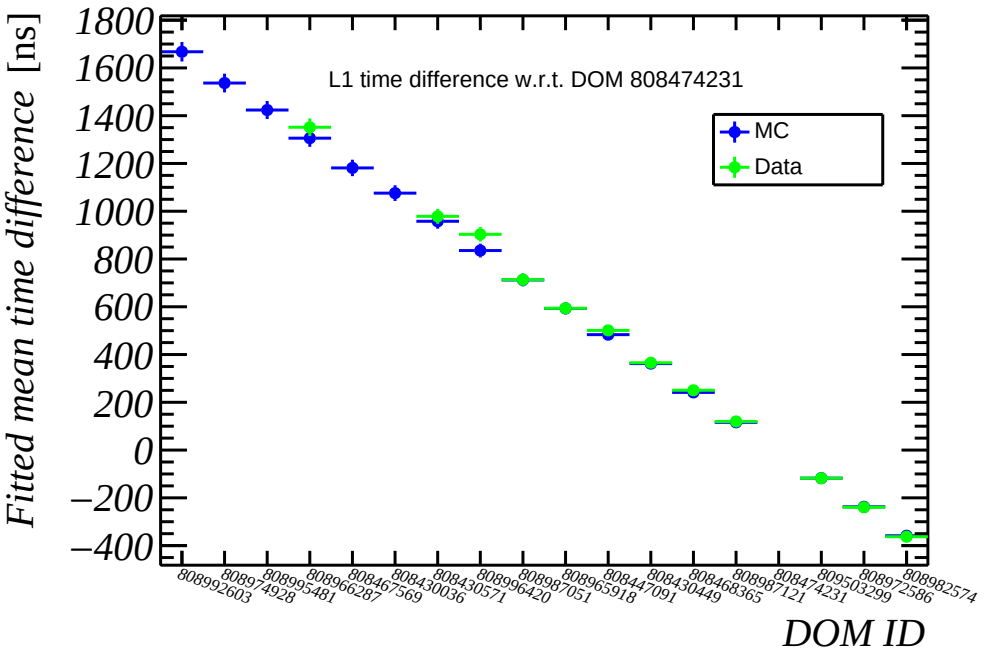

Figure 96: Mean time difference between L1-hits on a DOM i and DOM 808474231.

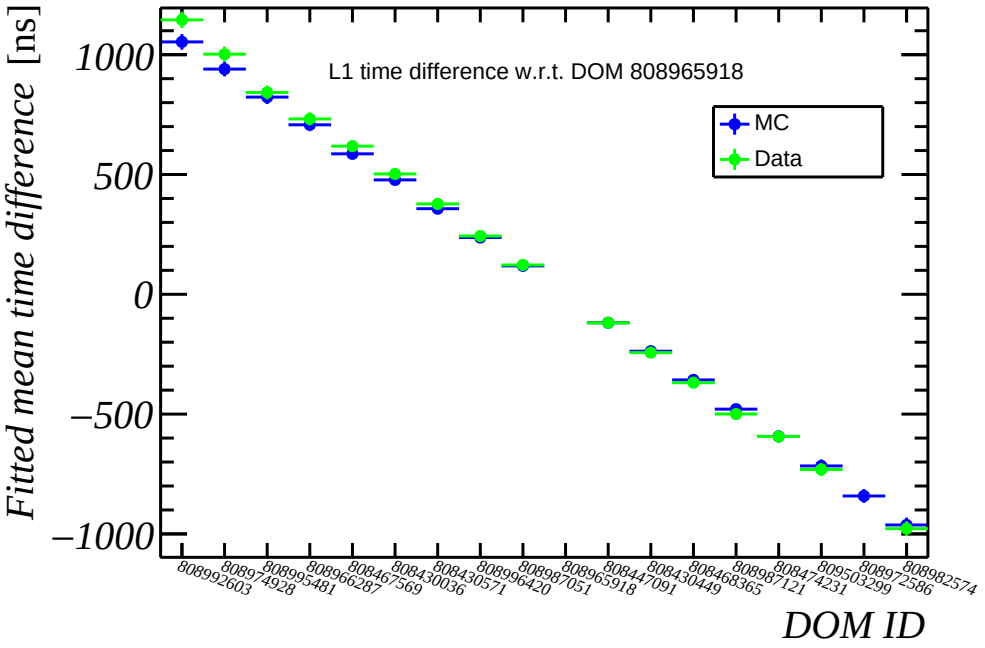

Figure 97: Mean time difference between L1-hits on a DOM i and DOM 808965918.

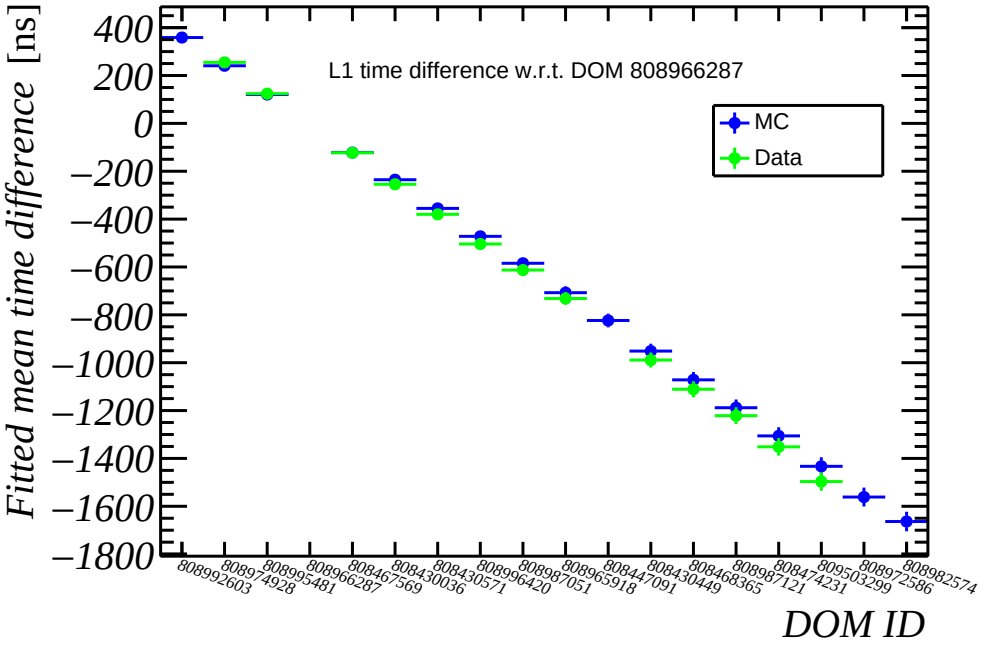

Figure 98: Mean time difference between L1-hits on a DOM i and DOM 808966287.

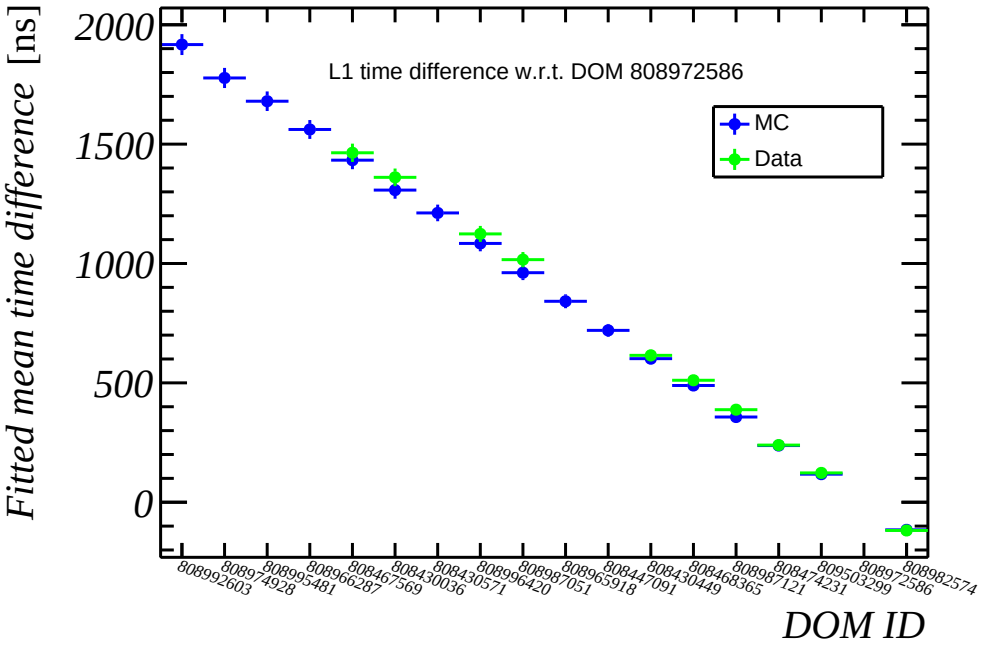

Figure 99: Mean time difference between L1-hits on a DOM i and DOM 808972586.

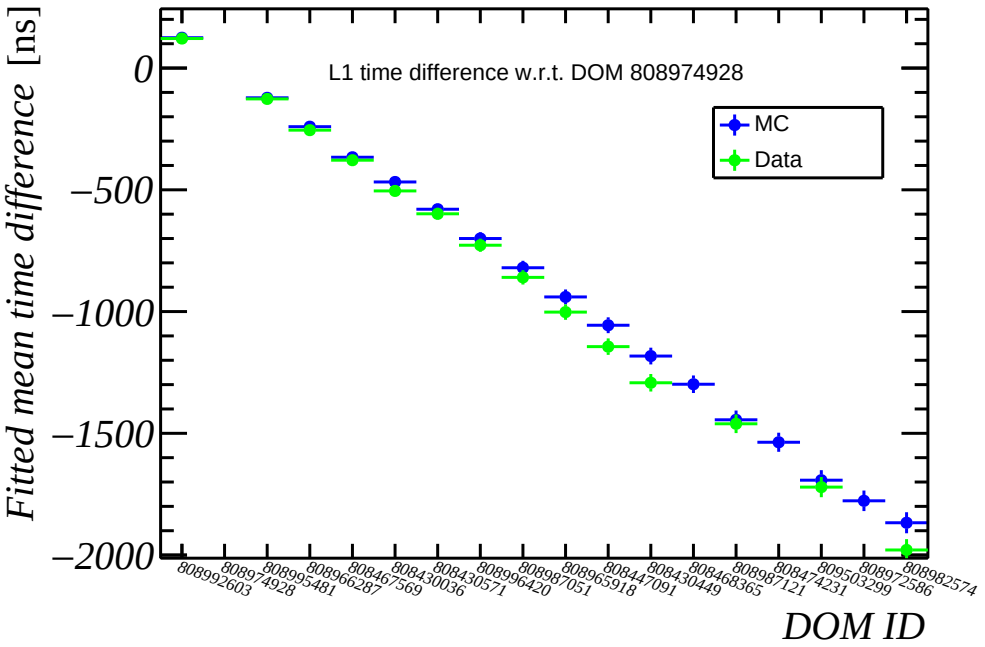

Figure 100: Mean time difference between L1-hits on a DOM i and DOM 808974928.

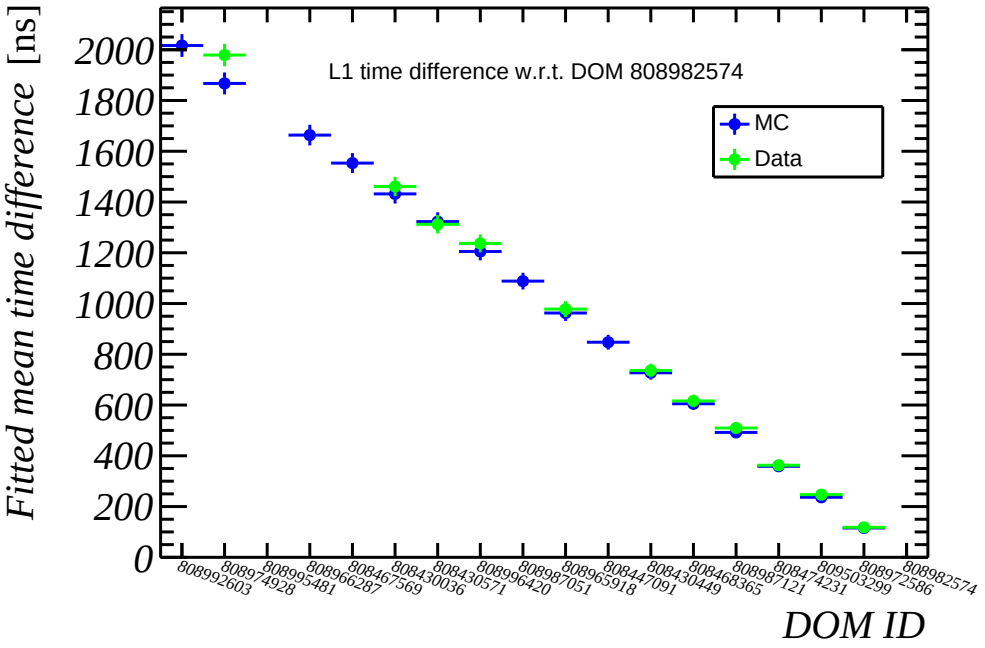

Figure 101: Mean time difference between L1-hits on a DOM i and DOM 808982574.

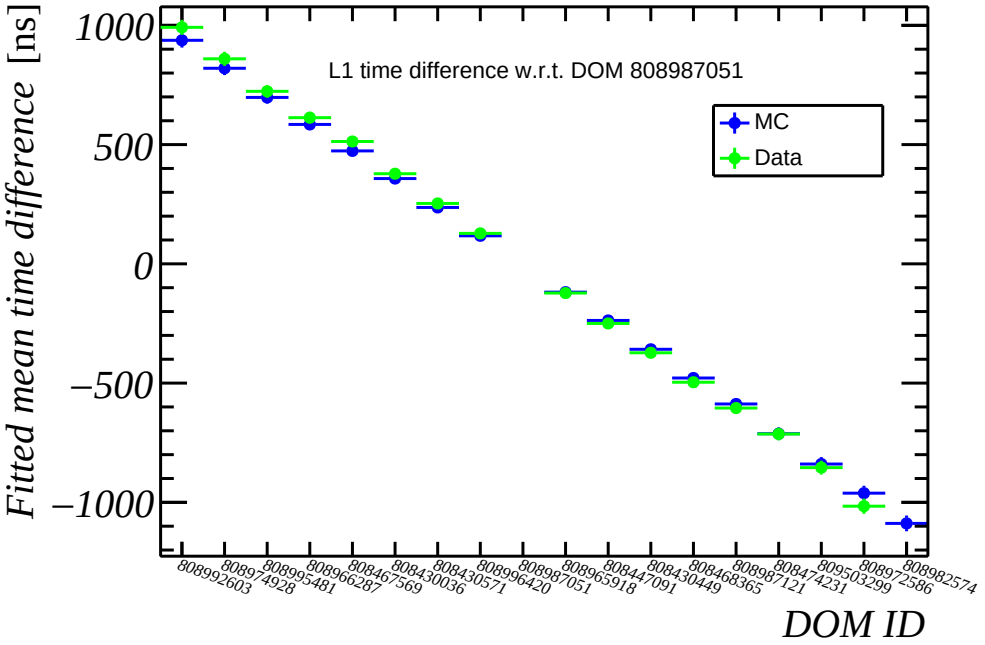

Figure 102: Mean time difference between L1-hits on a DOM i and DOM 808987051.

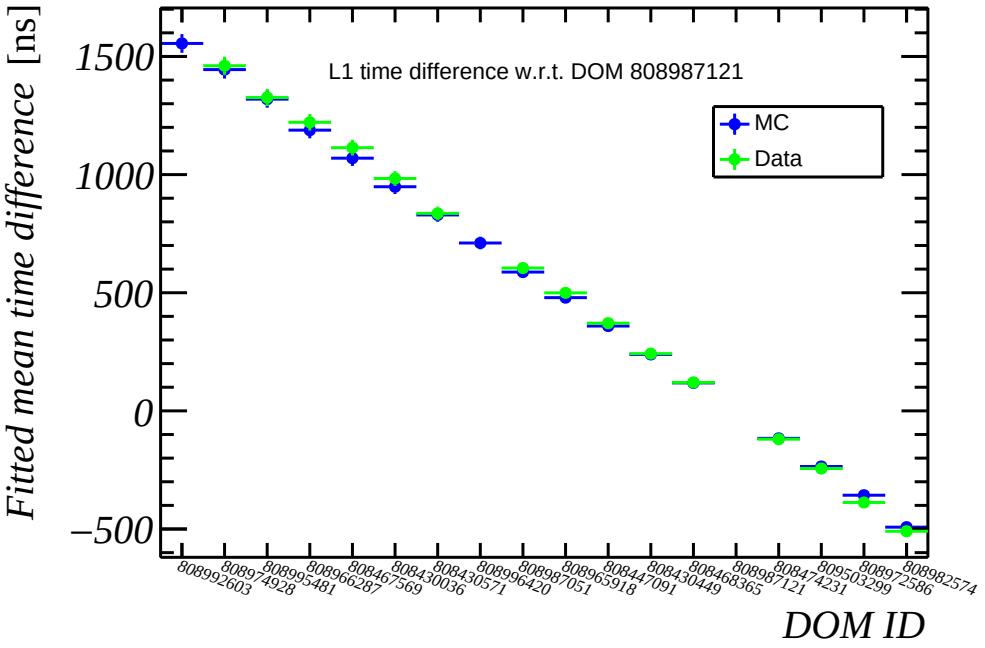

Figure 103: Mean time difference between L1-hits on a DOM i and DOM 808987121.

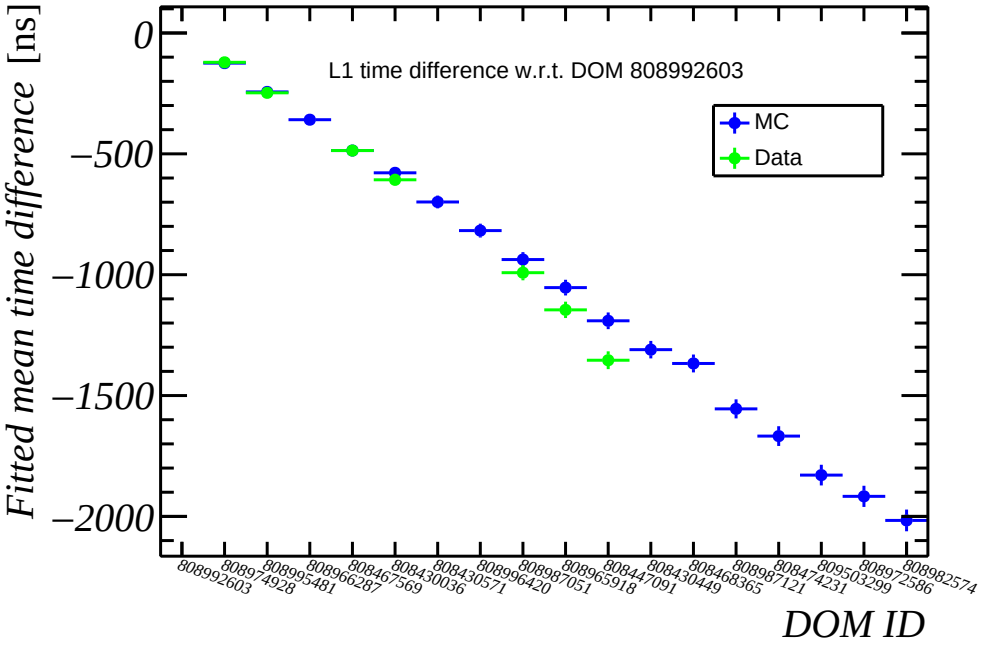

Figure 104: Mean time difference between L1-hits on a DOM i and DOM 808992603.

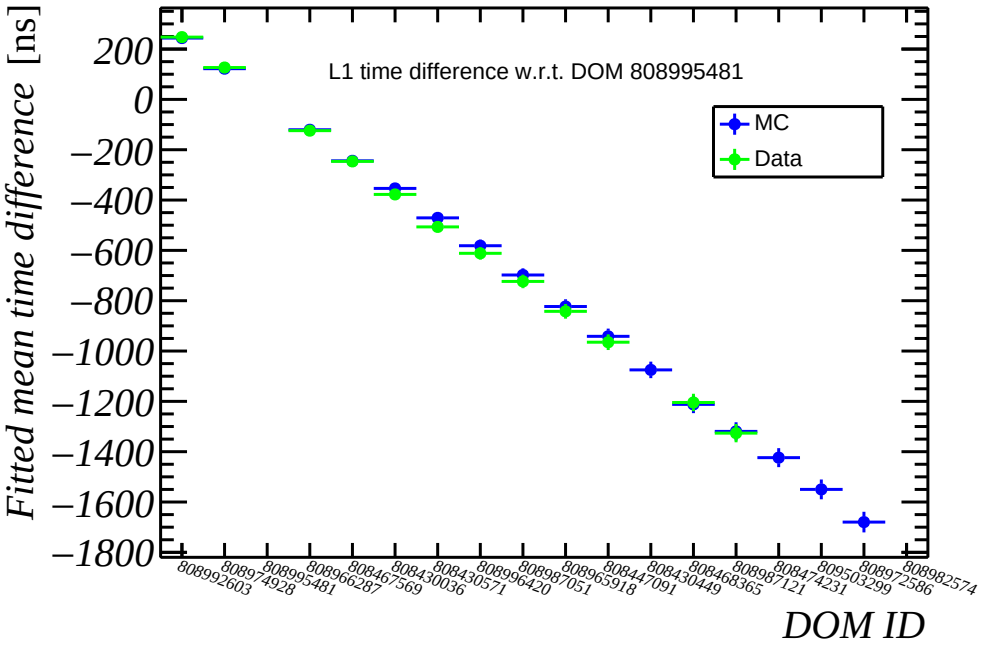

Figure 105: Mean time difference between L1-hits on a DOM i and DOM 808995481.

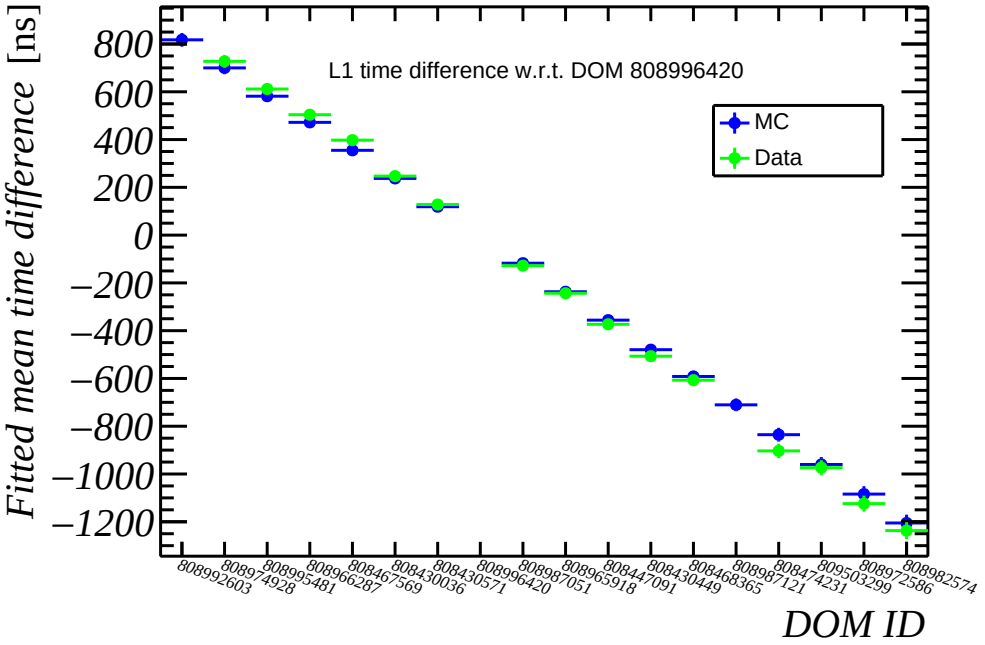

Figure 106: Mean time difference between L1-hits on a DOM i and DOM 808996420.

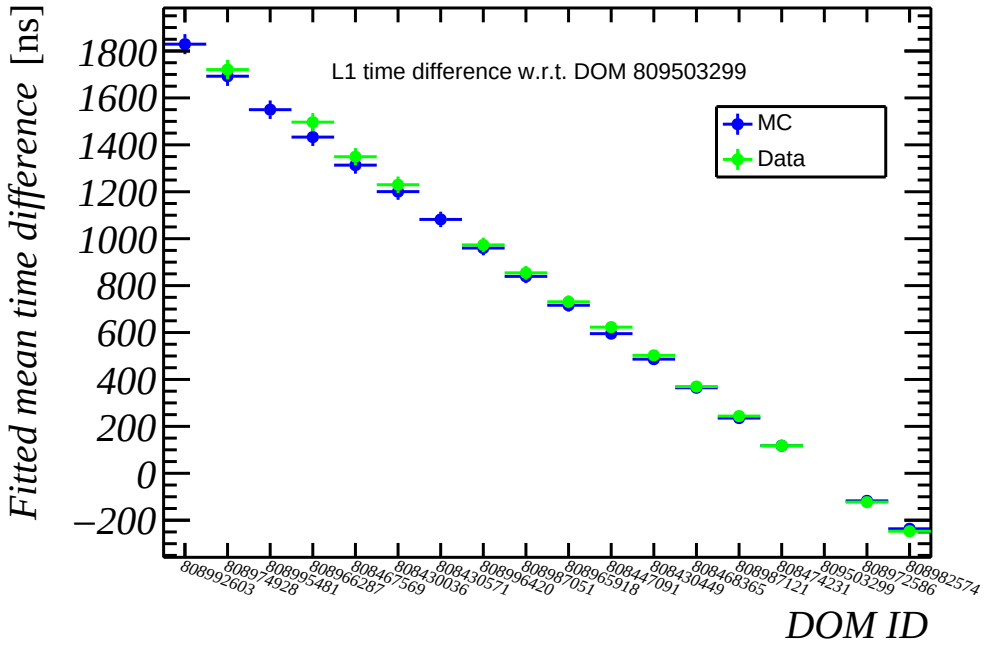

Figure 107: Mean time difference between L1-hits on a DOM i and DOM 809503299.